DESIGN ANALYSIS FOR CHANNEL RECTIFICATION OF GANDAK RIVER IN BIHAR

A DISSERTATION

Submitted in partial fulfillment of the
requirements for the award of the degree
of
MASTER OF TECHNOLOGY
in
WATER RESOURCES DEVELOPMENT & MANAGEMENT

By

ANIRBAN DATTA

DEPARTMENT OF WATER RESOURCES DEVELOPMENT & MANAGEMENT
INDIAN INSTITUTE OF TECHNOLOGY ROORKEE
ROORKEE - 247 667 (INDIA)

JUNE, 2011

INDIAN INSTITUTE OF TECHNOLOGY ROORKEE
ROORKEE

CANDIDATE'S DECLARATION

I hereby certify that the work which is being presented in the thesis entitled "**Design Analysis For Channel Rectification of Gandak River In Bihar**" in partial fulfilment of the requirement for the award of degree of Master of Technology with specialization in Water Resources Development (Civil), submitted in the Department of Water Resources Development and Management, Indian Institute of Technology Roorkee, Roorkee, India, is an authentic record of my own work carried out during a period from August2010 to June 2011 under the supervision of Dr. Nayan Sharma, Professor and HOD, Department of Water Resources Development & Management, Indian Institute of Technology Roorkee, Roorkee.

The matter presented in this thesis has not been submitted by me for the award of any other degree of this or any other institute.

Anirban Datta
(ANIRBAN DATTA)

This is to certify that the above statement made by the candidate is correct to the best of my knowledge.

Supervisor
(Dr. NAYAN SHARMA)
Professor and HOD,
Department of Water Resources Development & Management
Indian Institute of Technology, Roorkee – 247667
INDIA

Date : June ,2011
Place : Roorkee

ABSTRACT

River morphology is one of the most complex natural phenomena, not only because the flow and flow patterns vary in temporal and spatial dimensions, but also because the coupling to the river valley and channel, in which the flow is contained, varies. This complex morphological nature of alluvial rivers and their effect on the well being of the human race settled along and around the system has necessitated a wide range of research interest. These interests are driven by a desire to solve and harness the erratic and sometimes destructive nature of these rivers. To understand the physical processes occurring in rivers, the development of physical and mathematical modeling methods have proven to be instrumental. The concept of numerical modeling for flow simulation has found large acceptance over the past decades as a means to simplify and solve these problem.

In this present study a hybrid modeling is attempted in the Gandak River around Gopalgunj Area. One dimensional HECRAS 4.1 model is used to study the general sediment flow along the reach. PHYSICAL MODEL study is used to simulate the area adjacent to the bridge site. The study is supplemented by the application of satellite based spatio-temporal variation of channel migration in the vicinity of study area.

Major channel migration occurred between the year 1988 to 2010 .The channel has shifted its course erratically, resulting in subsequent shifting and bifurcation.

The physical model is run for two scenarios, one with clear water condition and the other for sediment concentration of 2000ppm. Model dimension on the ground is 25m by 12m. Geometric scale of Lr =400 and Zr= 50. With clear water simulation the model is verified against observed stage and discharge.

The Numerical Model study shows extreme aggradation and degradation all along the study reach. The Physical Model study shows from that deposition has occurred in the middle of the channel between the abutments and erosion while scouring occurred at the toe of the guide bank. And it is also evident that the left guide bank is under more attack due to the secondary flow generated at the upstream section of the guide bank. To prevent the damage that may occur on the guide bank and to channelize the flow to the centre of the river, submerged vanes are proposed.

ACKNOWLEDGEMENT

I wish to record my sincere thanks with profound sense of respect and gratitude for my supervisor, **Prof. Nayan Sharma.** The words prove to be insufficient to express my deep feelings for his benevolence and elaborative guidance throughout the study period.

I express my heartfelt thanks and gratitude to all the Professors of this department, WRD&M ; Prof. Gopal Chauhan, Prof U. C. Choube, Prof. Ram Pal Singh, Prof. G.C Mishra, Dr. M.L. Kansal, Dr. D.Khare, Dr. S.K. Mishra, Dr. Ashish Pandey. I also wish to convey my gratitude to Dr. Manoj Arora of Civil Engineering Department and professors from other Departments for their salient contribution during the course to fill the capacity in me in meeting the inputs required by this dissertation work. I am also thankful to the staff members of WRD&M for their help and gentleness in other formalities.

I express my deep sense of gratitude towards Bihar Rajya Pul Nigam, Government of Bihar, Patna for assisting me in my dissertation work through prompt correspondence all the time during the study.

I would like to thank my fellow student of my batch for their constant support specially Himanshu Arora and Belay Zeleke Desta, both of whom has helped and enriched me through our mutual discussions regarding our studies.

I also gratefully acknowledge the various authors and publications from where relevant references have been drawn in this dissertation.

Finally, I offer my hearty respect to my parents for their blessings on me and throughout the study.

June, 2011 **(ANIRBAN DATTA)**

TABLE OF CONTENTS

LIST OF FIGURES

LIST OF TABLES

NOTATIONS

Symbol Description

γ_w = specific weight of water;

γ = unit weight of fluid ;

g = acceleration due to gravity;

q = water discharge per unit width;

Q = water discharge;

Q_b = bank full discharge;

R =correlation co-efficient;

S = longitudinal bed slope;

Ω = unit stream power;

w = water surface width of stream / channel;

Y_o = observed value;

Y_p = predicted value;

ABBREVIATIONS

CWC	:	Central Water Commission
E	:	Determinant Coefficient (Nash Sutcliffe-Coeff)
WAPCOS	:	Water and Power Consultancy Services
HEC	:	Hydrological Engineering Center
RAS	:	River Analysis System
R	:	Correlation coefficient
HEC	:	Hydrologic Engineering Center
RMSE	:	Root Mean Square Error
DHI	:	Delft Hydraulics Institute
WRD&M	:	Water Resources Development And Management
USCE	:	United States Corps of Engineers
ASCE	:	American Society of Civil Engineering

Chapter -1

INTRODUCTION

1.1 GENERAL

River morphology is one of the most complex natural phenomena, not only because the flow and flow patterns vary in temporal and spatial dimensions, but also because the coupling to the river valley and channel, in which the flow is contained, varies. This complex morphological nature of alluvial rivers and their effect on the well being of the human race settled along and around the system has necessitated a wide range of research interest. These interests are driven by a desire to solve and harness the erratic and sometimes destructive nature of these rivers. To understand the physical processes occurring in rivers, the development of physical and mathematical modeling methods have proven to be instrumental. The concept of numerical modeling for flow simulation has found large acceptance over the past decades as a means to simplify and solve these problem.

Alluvial rivers carry the sediment with the flow. The hydraulic parameter of the channel decides the sediment transport capacity. When the sediment quantity becomes more or less than the transport capacity, deposition or scour occurs causing morphological changes in the course affecting the structure made across or along the river channel, as well as flow pattern of the river. The morphological changes of river is also interrelated with the hydraulic parameters of the channel changes such as bed deformation and bank erosion because of mutual relationship between water flow and sediment transport. Better understanding of these process and mechanism is very important for river engineering purposes to manage hydraulic structures and prevent disaster from flood, and environmental engineering purposes to maintain river ecosystem and landscape.

The morphology of alluvial river channels is a consequence of complex interaction between a number of constituent physical processes, such as flow, sediment transport and bed deformation.

The major driving forces governing the behaviour of alluvial river channels are: sediment supply, flow regime (from upstream), channel topography, and the nature and volume of sediment being locally eroded and transported by the stream (from the bed and the riverbanks, and eventually deposited further downstream). It turns out that all alluvial river channels are subject from time to time to disturbances in their immediate environment caused by natural or artificial effects, namely variable inflow, sediment supply, and various human activities, such as reservoir construction, channel regulation, and water diversion.

Flows are primary driving forces governing the behaviour of alluvial river morphology. An increase in flow magnitude may initiate bed surface movements and bank erosion, once the force exerted by the flood event has passed some threshold for movement or erosion. The timing and frequency of flood may also have profound effects on a population; a flood can cause catastrophic damage to civil infrastructure located on or nearby the river.

Reliable and quantitative estimate of the bed aggradations or degradation are very important in alluvial river for developing durable fairway to get sufficient water depth in low flow as well as accurately predicting the water surface elevations during floods in estimating flood to protect the bank from erosion. Thus, engineers are greatly interested in accurately predicting the behavior of river under various flows and sediment loads so that better information can be obtained for the planning and design of river control structures, flood protection measures and other water diversion structures.

In recent years, the improved understanding of physical processes involved in the study of river hydraulics has led to the development of physical-mathematical formulations to explain the natural phenomena and to forecast changes due to, for example, human interference. There remain important knowledge gaps, however, which concern not only the complex nature of water and sediment movements, changes in bed configuration and their dynamic interactions, but also the utilization of reasonably accurate results by water managers, policy makers and engineers in real-life situations. (Tassi, 2007)

Furthermore the dynamics of flow is even more complicated in alluvial rivers due to wide

differences in hydraulic properties and resistances of flow in the main channel and the subsidiary channels.

Thus studying the river morphology, from these numerical and physical models, engineers try to design certain control mechanisms and structures to ensure the morphological changes are managed or contained for some certain purposes. These purposes may range from bank protection, navigation, safety of water control structures etc. River Channel Rectification is a process involving construction of structures across or along the stream for achieving these specific aims. These structures include levees built along river bank to control floods, spus, guide banks, jack jetties, submerged vanes constructed for altering the local flow conditions or for guiding the flow. The main purpose of river channel rectification includes protecting the bank, induce bed erosion for navigational purposes, guiding the flow through a designated c/s etc.

In the present study for our designated study area along the river Gandak in Bihar the stream channel needs to be stabilized for keeping the river confined in a certain domain for the purpose of construction of a bridge across the river inside the perimeter of the study area. For the safety of the structure, as well as for the safety of the human settlement nearby, it is important that the river remain stable morphologically for the upstream and downstream stretch mentioned here in this work. To achieve this end, study of river morphology and suitable design of river channel rectification is adopted to address the problem. For the study of river morphology one dimensional numerical model and physical model is used. Numerical models HEC-RAS 4.1 is used for one dimensional river flow simulation. Satellite images of the study area from 1988 to 2010 have been taken into consideration to observe and understand the dynamics of the river in this specific timeframe.

1.2 OBJECTIVE OF STUDY

- To analyze the satellite images of the river section for observing the spatial and temporal changes in morphology of the river.
- To create a one dimensional mathematical model of the river for flow simulation studies to understand the fluvial dynamics and water surface profile in the study reach.
- To carry out physical model test to investigate and assess the impact of reducing the river channel flow from two channels into one river channel.
- Based on the studies conducted on river morphology, suitable river channel rectification is suggested for the proposed site for guiding the flow through the designated channel.

1.3 GANDAK RIVER SYSTEM

The Kali Gandaki or Gandaki River (also known as the Narayani in southern Nepal and the Gandak in India) is one of the major rivers of Nepal and a left bank tributary of the Ganges in India It is also called Krishna Gandaki in Nepal. In Nepal the river is notable for its deep gorge through the Himalayas and its enormous hydroelectric potential. It has a total catchment area of 46,300 square kilometers, most of it in Nepal. It lies between the similar Kosi system to the east and the Karnali (Ghaghara) system to the west.

The entry point of the river at the Indo-Nepal border is also the confluence called Triveni with rivers Pachnad and Sonha descending from Nepal. Pandai river flows into Bihar from Nepal in the eastern end of the Valmiki Sanctuary and meets Masan. The Gandak flows southeast 300 km across the Gangetic plain of Bihar state through Champaran, Gopalganj, Saran and Muzaffarpur districts. It joins the Ganges near Patna just downstream of Hajipur at Sonepur (also known as Harihar Kshetra).

Gandak River is part of the Indo-Gangetic Plains. The Indo-Gangetic plains are one of the most extensive tracts of Quaternary alluvial sedimentation in the world, characterized by two mega fans, formed by the Gandak and Kosi river systems and an interfan area between them drained by the channels of the Burhi Gandak, Baghmati and Kamla-Balan River systems. The main

feature of the river systems of northern Bihar is the recognition of three different classes based on their source areas:

- The mountain-fed river systems (e.g. Kosi and Gandak) probably first developed here antecedent rivers in the early evolution of the mountain front eroded back preferentially, at points of structural weakness and captured the evolving drainage of the high mountain terrain to the north.
- The foothills-fed river systems (e.g. Baghmati), which have developed by localized valley erosion on the uplifting foothills and is probably much younger.
- The plains-fed rivers (e.g.Burhi Gandak) have clearly developed because without them the other river systems are not able to receive the runoff from monsoonal rains.

The drainage pattern is typically dendritic with high angles of tributary convergence in the high mountains and foothills (north of the mountain front; see Fig 1.1). On the alluvial plains, south of the mountain front, the Gandak and Kosi rivers are characterized by their divergent patterns. The other river systems with gently converging pattern in the upstream region and are more sinuous in the downstream region.

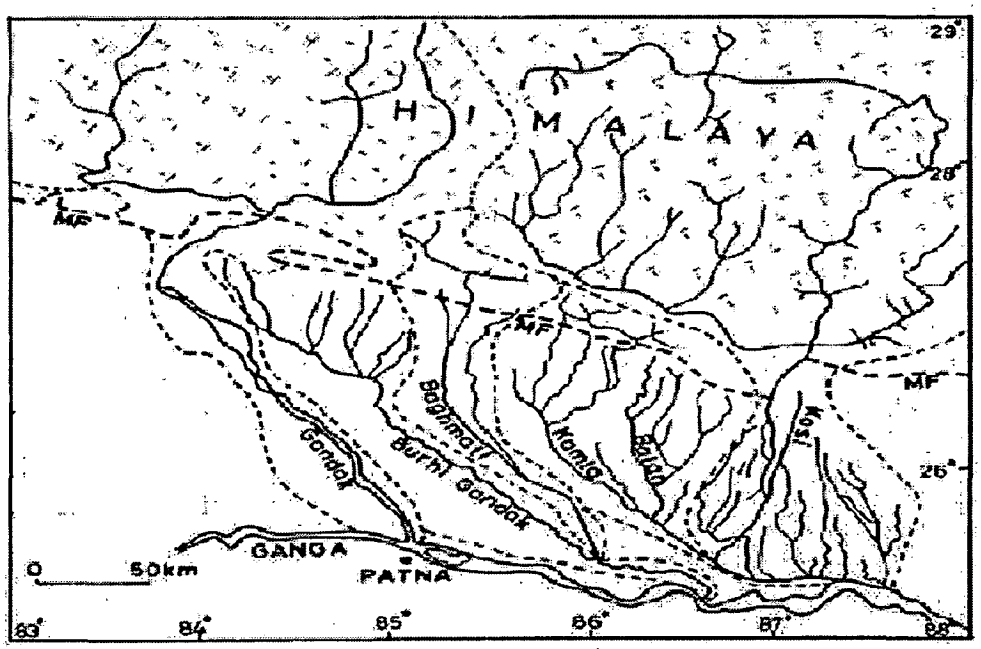

Fig 1.1 Gandak River Systems (Sinha, 1998)

The plains of north Bihar experience monsoonal rainfall, preceded by pre-monsoon showers. The average annual rainfall in the plains is 100-160cm where as the foothills above the plains experience a higher annual rainfall (>200cm). The main monsoon usually arrives in mid-June in the plains and ceases in September contributing over 85% of the annual rainfall. In the foothills, the main rain starts a little earlier, usually in late May, and may continue longer, into late October.

1.4 STUDY AREA

The study area is located in between 26°30'00''N 84°24'00''E and 26°40'00''N 84°30'00''E at around Gopalganj and its perimeter contains River Gandak on the East and River Basi on the West. The area extends from the confluence of both the Rivers in the South towards North for about 8.5 Km. The study area is in Gopalgunj district of Bihar, between Gopalgunj and Bethia. A bridge is being constructed at the confluence to connect the two townships.

Fig 1.2 IRS IMAGE OF THE STUDY AREA (2010)

1.6 METHODOLOGY

- Extensive study of satellite images from different times ranging from 1988 to 2010 are performed to detect geo-spatial and temporal changes in river morphology in this time frame using ERDAS Imagine 9.1 and ARCGIS 9.3 software.
- Manning's n is assed in all segments of the whole study area through simulating the flow using 1-D hydraulic model namely HEC-RAS 4.1.
- One dimensional steady flow is used to determine water surface profile and supplement physical model study. For this purpose we have used HEC-RAS 4.1, which is one of the robust and extensively used one dimensional numerical model.
- Study of physical model is done to understand the flow pattern around the bridge site, the aggradations or degradations of bed level, scouring around the guide banks etc.
- We design the suitable river channel rectification/ control structures for serving the pre-defined purpose of the stream to reach our objective goal

1.7 ORGANIZATION OF THESIS

Chapter -1- Introduction to the thesis

Chapter -2- Review of literature

Chapter -3- Numerical Modeling and Flow Simulation Studies

Chapter - 4- Physical Model Study

Chapter - 5-Results and Observations of Flow Simulation Studies

Chapter - 6-Design of River Channel Rectification Works and Conclusion

Reference

Appendices

Chapter -2

LITERATURE REVIEW

2.1 SEDIMENT TRANSPORT IN ALLUVIAL RIVERS

An essential and well-known feature of alluvial channels is that their morphology, flow-resistance, and sediment-transport characteristics adjust in response to prevailing flow and alluvial conditions. Alluvial streams carry extremely varying discharge and sediment loads. The ratio of maximum to minimum discharge can attain values as high as 1000 or more in many streams (Garde& Raju, 2000). Hence sediment transport problems for alluvial rivers (mobile bed streams) are current and critical concern of engineers. In particular, estimating the length and maximum depth of deposition or erosion that occurs during a flow event when there is a change in the longitudinal slope of the channel is an important problem. Deposition occurs when the slope changes from steep to mild and erosion occurs when the slope changes from mild to steep. Once, a flood is over, or in a gradual time span, large changes on the river bed are observed with banks or piers eroded, while other locations get covered or aggraded. It might be impacted that when extremely large floods with limited sediment supplies and high sediment carrying capacities occur in rivers with erodible bed and bank materials, scour will continue to take place within the erosive capacity of the stream till it approaches the minimum/optimum value required to transport the available material.

Traditional approaches have investigated the ways in which stream flows, sediment loads and channel forms vary along a river from headwaters to mouth and with time over periods ranging from hours to years. Represented in their most simple form, rivers have been viewed as a unidirectional system that changes progressively from headwaters to mouth. The river continuum concept takes the physical structure of a stream, coupled with the hydrological regime and energy inputs to produce a series of responses.

2.2 MORPHOLOGY AT DIFFERENT STAGES OF A RIVER

An exemplary representation of history of river channel evolution may be envisioned through Fig: 2.1 (Schumm 2000).

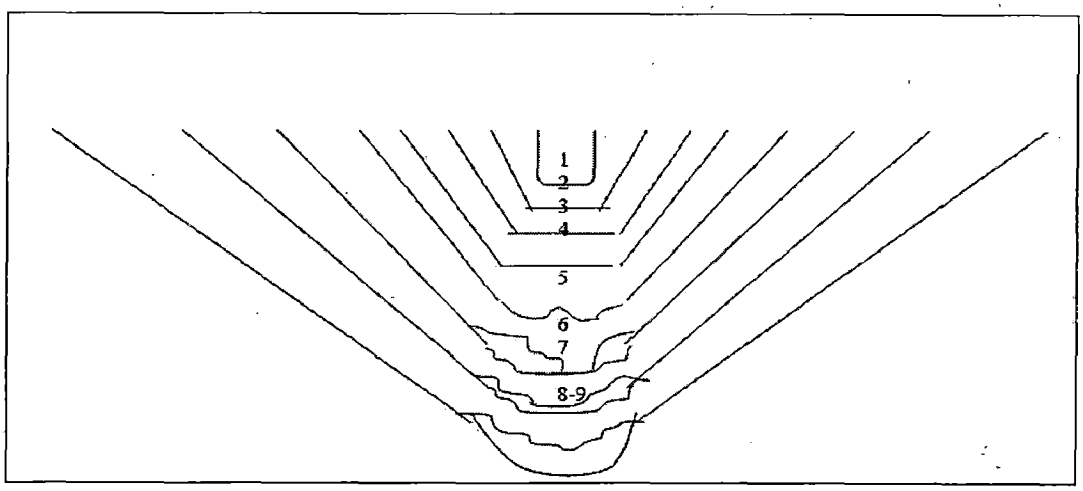

Fig: 2.1 *Cross Section of Valley and Incising Stream at time*

The historical background of a river is based on how the channel evolved through the passage of time, adapting to change in fluvial and alluvial conditions. In the Fig: 2.1, the evolutionary transient phases of a channel in the vertical plane are presented. From 1-4 the channel is confined by the bed rock valley walls. During stages 5-7 the channel is constrained by bedrock valley wall and terraces of older alluvium. Finally, at the stage of 8-9 the channel has reached to regime (Schumm; 2000).

High floods are usually accompanied by high sediment charge, it could be speculated that the oldest streams were wide, shallow, steep, braided bed-load channel (Fig: 2.2a)The decrease in the sediment load perhaps were more rapid than the discharge a meander-braided transition pattern developed with a well defined single thalweg (Fig: 2.2b). The thalweg, in turn, became the channel as a new floodplain formed and the channel further narrowed with further reduction of sediment load (Fig: 2.2c). Finally, as bed load became a fraction of its former volume, a meandering mixed load channel with large meanders formed (Fig: 2.2 d).

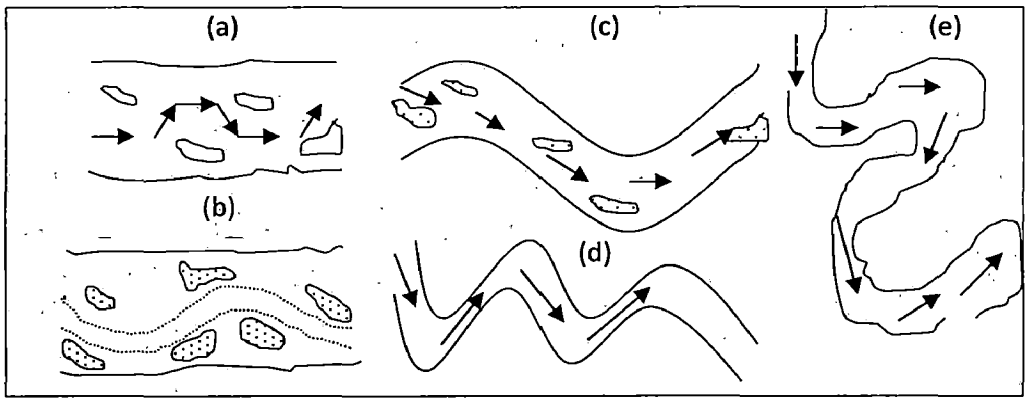

Fig: 2.2 Sequence of Channel Changes with Decrease in Discharge

Primarily concerning to the Longitudinal bed profile it is found customary to mention the hydraulic characteristics of river flow dynamics with sediment discharge which constitutes and imparts dynamism to river streambed and other river morphological parameters. It is spontaneous to understand that a river originates from its watershed at higher altitudes of mountainous slopes which relatively receive high intensity rainfalls. Mainly, large river streams all around the world starts its voyages from higher mountainous elevation towards the sea. In the beginning the path of the flow is so steep that it has enormous potential to erode the bed in the vertical direction by virtue of which it develops V-shaped river section deep gorge or canyons. It has no flood plains and covers full width of its valley at all stages. A river at its young stage is characterized by presence of rapids, water falls, steep and varying gradients and presence of lakes.

At this stage the river is said to become mature after its youth stage. The slope at this stage is so reduced that it can no more cut the bed but starts widening. The sediment transportation capacity is just adequate to transport the sediments in the flow from upstream and the sediment material is derived from bank widening.

If the sediment content in the flow is above the transporting capacity heavier sediments are settled on the bed upstream the profile slope. Conversely, if the transporting rate capacity is yet to be satisfied, the bed material picked up and the stream slope is reduced. Hence, matured streams adjust its profile slope delicately. It is in the stage of maturity that the stream flows sinusoidal or meandering path in plan.

2.3. FLOW RESISTANCE IN ALLUVIAL RIVERS

The major feature of alluvial and other sediment-laden channels concerning flow resistance is a boundary consisting of movable particles, and hence, the formation of mobile bed forms and permission of water to flow through the voids between the particles. Accordingly, the velocity distribution and boundary shear near the bed are modified from those of similar rigid-boundary channels.

The problem of predicting the resistance to flow and velocity distribution in alluvial streams is complicated by two factors (Rouse, 1965). Firstly, *the configuration of the bed changes with changes in flow conditions*. This changing bed condition makes it extremely difficult to describe the resistance due to these bed forms by a constant resistance coefficient. Secondly, under certain conditions, *a part of the sediment load is transported in a state of suspension*. The material that gets into suspension changes the flow and fluid characteristics and this has significant influence on the velocity distribution and hence on the mean velocity.

The channel bed forms can be loosely classified as plane bed, ripples, dunes, and antidunes. From the view point of resistance, the plane-bed channel is similar to plane rigid-wall channel in that the source of resistance is surface resistance. The major differences between the two are: **(1)** for a rigid impervious boundary, no water will penetrate the boundary, whereas for the sediment bed, water moves through the voids between the bed particles, and **(2)** for a sediment plane bed, some energy and momentum are spent on picking up, transporting and depositing the bed sediment. This is true even in the case of flow with equilibrium sediment transport for which the plane bed remains constant with respect to time.

For ripple-bed channels, the sources of resistance are from the form resistance as well as the surface resistance. For channels with dunes and antidunes, there is wave resistance in addition to the form and surface resistances. For antidunes, the water surface wave is in phase with the antidunes and the flow Froude number is high, around unity or greater, and hence, the relative contribution of wave resistance is more significant than for the case of dunes.

Bed form geometry is always three dimensional. The bed configurations migrate with sediment particles moving on their surface. For channels with finite width, the bed forms change across the channel, especially for compound channels and rivers with floodplains. Large bed forms behave similar to large wall roughness elements, and can be regarded as macro-roughness. The

nature of the roughness effects is best represented by the size, shape, and spatial distribution of the roughness elements (Rouse 1965).

Expressing the roughness parameter **K** in terms of contributing nondimensional parameters of relative sediment size ***ds/h***, size gradation ***G***, relative density **Δρs /ρ**, sediment shape **ξ**, and suspended sediment concentration parameter ***Cs*** , where **ds**=representative size measure of sediment, ***h***=flow depth, **ρ** =density of fluid; where **ρs** =density of sediment. Thus, for a steady flow in a straight, prismatic, simple geometry, sediment-laden channel, the cross sectional flow resistance for either energy or momentum concept is

$$f, \frac{n}{d_s^{1/6}}, or\, S = F\left(R, F, S_w, S_o, \eta, N, \frac{d_s}{h}, \frac{\Delta\rho_s}{\rho}, \xi, G, C_s\right)$$

Where Sw is water surface profile, So channel bed slope, η cross sectional geometric shape, R Reynolds number, F Froude number and N non uniformity of the channel in both profile and plan. A discussion of the physical implication of the 11 independent contributing parameters in the right-hand side of Eq. (2.1) is given in Yen (1991) Eq. (2.1) represents a complicated relationship between the 11 dimensionless independent parameters and the resistance coefficient. Rigorous studies on the relative importance of these parameters have yet to be performed. Such studies would require an extensive amount of new field and laboratory data for numerous flow and sediment conditions. Special measuring devices and consistent measuring techniques would be required for the collection of such data. The symbolic form of the independent parameters in Eq. (2.1) is only meant to be indicative. Many alternative forms of the non-dimensional independent parameters have been proposed to replace those in Eq. (2.1). for example, the particle Froude number, particle Reynolds number, shear velocity to mean velocity ratio, and Shields' number have appeared in the literature. The selection and use of these alternative parameters depends partly on the specific conditions and partly on personal preference (Yen, 2002). These alternative forms of parameters can be obtained through cross multiplication and combination of the basic parameters given in Eq. (2.1) and these basic parameters can be replaced by the derived parameters on a one-by-one basis.

The most frequently used formulas relating open-channel flow velocity, V, to resistance coefficient are

$$V = \frac{K_n}{n} R^{2/3} S^{1/2} \qquad \text{(Manning's)}$$

$$V = \sqrt{\frac{8g}{f}} \sqrt{RS} \qquad \text{(Darcy-Weisbach)}$$

$$V = C\sqrt{RS} \qquad \text{(Chezy)}$$

in which ***n***, ***f***, and ***C*** are the Manning, Weisbach, and Chezy resistance coefficients, respectively; ***R***=hydraulic radius, ***S***=slope; ***g***=gravitational acceleration; and ***Kn*** **=1 m1/2/s** for ***V*** and ***R*** in SI units, **1.486 ft1/3-m1/6/s** for English units, and for dimensionally homogeneous Manning formula (Yen 1992). From Eq. (2.2) – (2.4), the resistance coefficients can be related as

$$\sqrt{\frac{f}{8}} = \frac{n}{R^{1/6}} \frac{\sqrt{g}}{K_n} = \frac{\sqrt{g}}{C} = \frac{\sqrt{gRS}}{V}$$

Thus, knowing the value of one resistance coefficient, the corresponding values of the other resistance coefficients can be computed.

2.4 STREAM SLOPE

In general the longitudinal slope of a stream shows a continual decrease along its length. Examination of stream profiles would show that the slope is greatest near the source, decreasing more or less regularly as the river follows its course. Such reduction in slopes corresponds to a longitudinal profile which is concave upwards (Garde and Raju 2000). Several factors are responsible for this. The reasons put forward by different scientists and engineers have been summarized in the following lines.

Firstly, size of bed material being transported decreases in downstream direction due to abrasion (Garde and Raju 2000). Hack (1962) found slope varied as $d^{0.60}$ for stream in Verginia and Meryland (USA). Shulits (1941) assumed that the stream slope is proportional to the size of the bed material and accordingly proposed a slope reduction equation (Eq: 2.1)

$$S = S_o e^{-\alpha x} \qquad (2.1)$$

S_o and S are the slopes at x=0 and at any distance x being measured in downstream direction and α a slope reduction coefficient. Brush (1961) and Hack (1962) have shown that the stream slope

is proportional to a negative power of the length of the stream up to that point indicating there by a decrease in slope along the length in conformity with the equation.

Low water profiles of the river Mississippi between Fort Jackson and Cairo of the Ohio between Cairo- Pittsburg (USA) and of several rivers in Europe are found to confirm the Eq: (2.1) (Garde and Raju 2000).

Secondly, in humid regions, the discharge in a stream increases in the downstream direction due to inflow from the tributaries. Unless there is a corresponding increase in the sediment inflow, the stream would necessarily flatten to the extent required by the increased sediment and water discharge (Garde and Raju 2000).

Thirdly, the sediment contribution of the upper region of a drainage basin is large compared to the run-off contribution to the stream flow. Which mean higher sediment contribution necessitating higher slope. While the lower region of the same drainage basin contributes smaller sediment quantity compared to its run-off discharge contribution signifying flatter slope requirement (Garde and Raju 2000).

Fourthly, on lower part of river sediments are usually finer and the streams are narrow with greater depth to width ratio leading to higher hydraulic efficiency requiring flatter slope (Garde and Raju 2000).

Garde (1982) presented an analysis considering the change in the bed material size, discharge and sediment load in the direction of flow.

He gave following relationships.

$d = d_0 e^{\alpha_1 x}$ [Variation in sediment size in the downstream direction] (2.2)

$Q = Q_0 e^{\alpha_2 x}$ [Variation in discharge α_2 between 0.001 to 0.0078/ km For Indian rivers] (2.3)

$Q_T = Q_{T0} e^{\alpha_3 x}$ [Variation in Total sediment load discharge α_3 between 0.0006 to 0.002/ km for Indian rivers] (2.4)

Where d=sediment size; d_0 =Sediment size at x=0; x=Distance measured in flow direction; Q=Discharge; Q_0 =Discharge at x=0; Q_T =Total sediment load discharge; Q_{T0} = Q_T at x=0; α_1, α_2, α_3 are coefficients.

Combining the Eqs. 2.2), (2.3) and (2.4) with Kondap's relation for width & depth and a sediment transport law,Garde (1982) showed that;

$$S = S_0 e^{(0.178\ \alpha_3 - 0.426\ \alpha_2 - 0.713\ \alpha_1)\,x} \qquad (2.5)$$

Where So and S are slopes at x equal to zero and at any value x.

Thus, depending on the relatives values of α_1, α_2 and α_3 it is possible to get a decreasing, increasing, or constant slope in a long reach. The fact has been observed by investigators such as Hack (1962).

2.5 STREAM BED CHANGES DURING THE FLOODS

On several alluvial streams, the stream bed elevation was seen to rise during flood while the bed was lower after the flood receded. On few other streams exactly opposite happenings have been recorded. These changes can be very rapid for example on the Missouri river at Omaha, Nebraska (USA), the bed was found to be scouring at a rate of 0.3 m per minute during a flood. (Garde and Raju 2000).

In the simplest form to understand the process of bed profile variation one has to assess the inflow out flow of sediment discharge in the reach under the consideration.

a) If the incoming amount or the rate of the sediment upstream of the reach is higher than outgoing from the reach downstream it is obvious that the difference of the two quantities must have been dropped within the length of the reach. This process of rising of the bed level is called Aggradation.

b) Conversely, if the incoming amount or the rate of the sediment upstream of the reach is lower than outgoing from the reach downstream then the difference of the two quantities must have been fulfilled by picking up the bed materials from within the length of the reach.This process of lowering of the bed level is called Degradation.

2.6 OCCURRENCES OF AGGERADATIONS AND DEGRADATION

2.6.1 AGGRADATION

2.6.1.1 OCCURRENCE OF AGGRADATION

Occurrence of aggradation is the most often observed phenomena on the upstream side of Dams, Barrages and any other disturbances caused by man made features or natural activities like barricade due to land slide. Because of disturbance in the equilibrium state of sediment flow in the stream causing reduction in the bed profile slope the sediment carrying capacity of the flow is weakened, which leads to settling of the sediment contained in the flow (Basically bed load) is retained in the zone upstream to such features.

Other instance of aggradation of river bed is rising of the water level in the Lake or the sea which causes to reduce the slope of the water surface of river leading to a drop in the sediment transporting capacity and the result is aggradation.The situation of aggradation involves lower rate of sediment outflow than the inflow so that temporal gradient of bed level is positive.

In the sediment continuity equation

$$\frac{\partial z}{\partial t}+\frac{1}{(1-\lambda)}\frac{\partial q_t}{\partial x}=0 \qquad (2.6)$$

Where λ = Porosity of the bed; q_t= Rate of sediment inflow per unit width; z= Bed elevation.

The consequences of aggradation more often reduce the conveyance capacity of the channel due to reduction in the flow area.

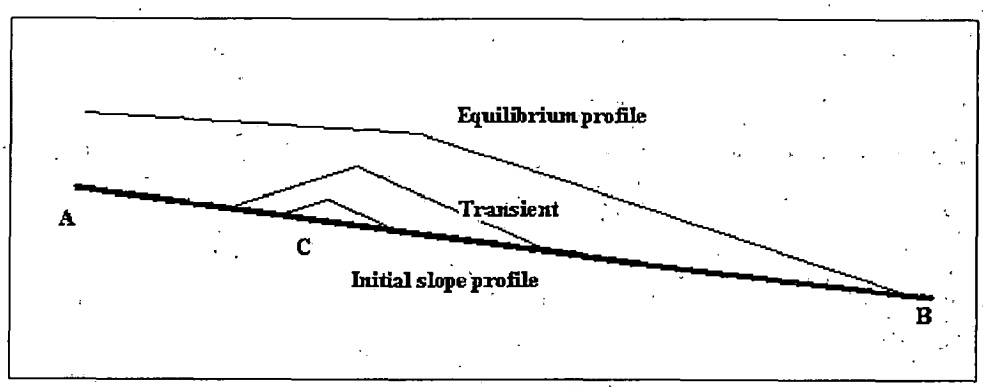

Fig: 2.3 Aggradation and Equilibrium L-Profile

Figure: 2.3 shows how the process of aggradation reaches to final equilibrium condition. Where the aggradation takes place because of increase in the sediment load in the flow above its transport capacity part of the sediment of the bed load is disposed on the bed of the channel which gradually extends upstream and downstream (as shown in the figure continues) till new profile is attained. This new profile is the equilibrium state of the profile adequate to transport the incoming sediment discharge.

2.6.1.2 EFFECTS OF AGGRADATION

a) Firstly, aggradation shrinks the active flow area of the river. Consequently, the flow is pushed to spread to wider coverage extending the flood affected area.

b) In the reservoirs behind the storage dams, the filling up of the reservoir leads to decrease in the depth of the usable water. This necessitates fixing a dead level in the design of such structures.

c) Bank erosion and river migration problems are more pronounced in the aggrading rivers like lower reaches of the river Brahmaputra.

d) Aggradation of the river bed restricts the navigational opportunities of the river courses.

e) The effect of aggradation extends the flood detention period over the flood plain during wet season causing water table to raise causing water logging (Garde and Raju 2000).

2.6.2 DEGRADATION

2.6.2.1 OCCURRENCE OF DEGRADATION

Most often degradation of streambed is observed to be lowered downstream of Large Capacity Reservoirs and Pools. Such degradation was observed in Cherry Creek USA where the extent of lowering being measured was 4.9m. But wherever sound rock exposures are encountered the process of degradation have found retarded (Garde and Raju 2000).

Another prominent location of occurrence of degradation is confluence of two or more rivers. Tributaries, generally steeper than the main stream but carry less run-off cause to lower the bed. At the instances, where the water discharges in the stream increases due to mixing of tributaries

with relatively sediment free water discharge enhances the sediment transport capacity degradation occurs subsequently. And one another cause of degradation is because of increase in water surface profile slope as the result of fall in level of a lake. This type of degradation was noted in White river in California USA (Garde and Raju 2000).

Another location of degradation is where river has been started to flow along the cut-off developed in the meandered river (Fig: 2.4). The cut-off shortens the length of the river. In the beginning the cut-off has narrow width which gradually opens to accommodate the discharge through the channel.

In the meandered rivers, the meandering process advances to a stage that the river no more can negotiate a long serpentine path which impose more resistance and take a shortest channel route at an incidence of high flow.

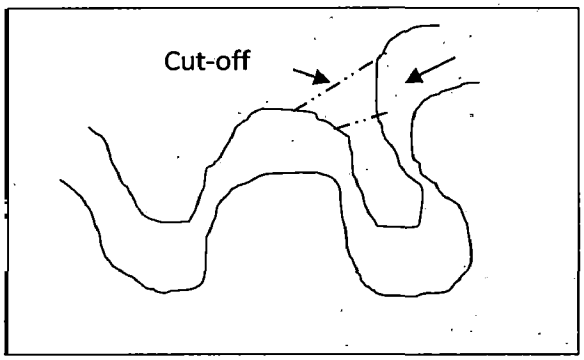

Fig: 2.4 Shortening of the River Flow Path due to Cut-off Development

2.6.2.2 EFFECT OF DEGRADATION

Followings are some of the much pronounced effects both harmful as well as beneficial in the study of River Engineering.

a) Formation of Hydraulic Jump is apparently pushed downstream in spillways and Barrages due to downstream bed level lowering jeopardizing the stability of the structure. This situation was faced in the Wisconsin River at downstream of Praire Du San Dam (USA).

b) Dams constructed in pervious strata exhibit increase seepage head due to increase in level difference between upstream and downstream water. The effect of this could be more uplift and seepage.

c) While in case of lowering of tail water level downstream of a Power Generation point due to degradation leads to increase in available effective heads for more power

generation. This has occurred at Paraire Du Sac Dam in the Wisconsin river USA. And also at Upperborn power house at Munich on the Saalach River.

d) Lowering of river bed by degradation process increases the capacity of the river channel to carry the flood flow, by lowering the high flood level of the river. Creating an artificial degradation by construction of a big reservoir was a method that had been suggested as a possible solution to the flood problem of the Yellow river in China and Kosi River in the Indian Territory. Lowering of water level due to degradation reduces the height of the ground water table in the adjoining areas.

e) Lowering of water level may expose pile foundation of bridges abutments and other structures to air and this may lead to deterioration of piling & stability endangering the whole structure. This problem has also been observed in many of the river bridges around on their downstream due to increased flow intensities aggravated by the construction of the bridges.

f) Degradation also causes lowering of water level at the existing irrigation intakes and thus makes the diversion of water for irrigation more difficult.

g) Degradation may cause substantial lowering of bed in navigable rivers and in extreme cases locks may become inoperative. Such difficulties have been encountered on a lock at the Wisconsin River (USA) and on the Mausa River (Holland) (Garde and Raju 2000).

2.7 MATHEMATICAL MODELLING OF ALLUVIAL RIVERS

Mathematical modelling of fluvial flow, sediment transport and morphological evolution started half a century ago and, to date, a variety of mathematical models have been developed and are in widespread use. However, the quality of mathematical river modelling remains uncertain because of: (a) poor assumptions in model formulations; (b) simplified numerical solution procedure; (c) the implementation of sediment relationships of questionable validity; and (d) the problematic use of model calibration and verification as assertions of model veracity.

The ability to make accurate calculations of fluvial flow, sediment transport, the associated morphological evolution processes and water quality is vital in a period when the concern over the river environment and the influence of human intervention is increasing. The interaction between sediment and turbulent flow is of fundamental interest in the field of two-phase flow, and modelling the strongly coupled flow– sediment–morphology system provides a problem of considerable interest in computational fluid dynamics. Fluvial sediment transport process has been an increasingly important subject in the fields of water resources engineering, hydrology, geographical, geological, and environmental sciences, and more fundamentally fluid dynamics.

Fluvial sediment transport poses great challenges for river scientists and engineers. The essence of the discipline is the interaction between the fluid (water) and the solid (dispersed sediment particles) phases. The exposure of the fluvial systems to the natural and variable environment (climatic, geological, ecological and social, etc.) adds to the complexity of the process of sediment transport and the resulting morphological evolution of rivers.

The earlier efforts in mathematical river modelling were almost exclusively built on traditional fluvial hydraulics—that is, one-dimensional (1D) and two-dimensional (2D) Saint-Venant equations. The 1D and 2D models are at present widely used in engineering practice; yet the future of mathematical river modelling will undoubtedly be the more advanced full 3D computational fluid dynamics (Cao and Carling 2002).

2.7.1 MAJOR ISSUES OF MATHEMATICAL MODELS FORALLUVIAL RIVERS

Mathematical models of alluvial rivers can be categorized into two types: academic and applied. Academic models often deal with 'how and why' problems, being devoted to the conceptualization, mathematical formulation, solution (analytical or numerical) and interpretation of the flow, sediment transport, and morphological reaction. Improving the understanding of the mechanism of interaction among water, sediment and morphology is the major purpose of academic models. On the other hand, applied models are entirely concerned with quantitative modelling of the river systems in response to natural changes and human activities (e.g. construction of dams, bridges and flood control works). Currently, the most extensively used fluvial models are either 1D or depth-averaged (shallow) 2D, which are built upon traditional hydraulics principles—that is, Saint-Venant equations (Cao and Carling 2002).

2.7.2 1D AND 2D COMPUTATIONAL HYDRAULICS MODELS

This section mainly focuses on 1D hydraulic model, while most aspects examined here are pertinent to depth-averaged 2D cases. Based on cross-section-averaged variables, 1D numerical modelling of alluvial rivers has been most widely used in the fields of river training, hydropower generation, flood control and disaster alleviation, water supply, navigation improvement, as well as environment enhancement. HEC-6, ISIS-Sediment, GSTAR3D, CCHED, HEC-RAS and Mike11 are examples of a number of mathematical river models developed for fluvial water–sediment–morphology systems. The outputs of these models usually include sediment transport rates, changes in bed elevation and amounts of erosion and deposition throughout the river system considered. It has been recognized that 1D models are appropriate primarily for long-term and long-reach situations, whereas these models have been less successful for local flow–sediment–morphology problems as can be anticipated. Prior studies in this connection have focused on such aspects as flow resistance relations (including parameter identification and optimization), grain sorting, non-equilibrium modules, numerical techniques, and effects of vertical distributions. In the present state of the art, it is a common practice to tune the friction factor and sediment transport formulae to reconcile the computational results with measurements. In this section the fundamental components of 1D model are examined. In particular the effects of simplified continuity equations and the asynchronous solution procedure

are addressed, which have rarely been studied before except for a formative comparison by Krishnappan (Cao and Carling 2002).

2.7.3 SIMPLIFIED CONTINUITY EQUATION FOR WATER-SEDIMENT MIXURE

Alluvial flows over erodible beds can be distinguished from those over fixed beds in that the flow may entrain sediment from the bed or in contrast render the sediment carried by the flow to be deposited on the bed, which usually causes riverbed degradation or aggradation. This aspect is referred to as the bottom mobile (free) boundary problem. At the same time, the water–sediment mixture may have properties (density, etc.) different from clear water. In spite of these apparently known features of erodible-bed alluvial flows, it is often assumed that the rate of bed morphological evolution is of a lower order of magnitude than flow changes with adequately low sediment concentration. Accordingly, in existing 1D and 2D models, the water–sediment mixture continuity equation is almost exclusively assumed to be identical to that for a clear-water flow over a fixed bed without considering the alluvial riverbed mobility. This simplified mixture continuity equation is, in its form, the same as that in the traditional Saint-Venant equations. The effect of this treatment appears to have been quantitatively addressed only by Correia et al(1992) and discussed by Rahuel(1993) Stevens(1988) claimed that bed mobility is important for complete coupling of water and sediment in discussing Lyn's(1987) analysis. Worm leaton and Ghumman(1994) compared the performance of several simplified models, but exclusive of a fully coupled model on a rigorous basis. Therefore the effect of bed mobility on model performance has not been apparent (Cao and Carling 2002).

2.7.4 SIMPLIFIED EQUATIONS IN ANALYTICAL MODELS

It is interesting to note that there have been several analytical models for channel aggradation and degradation. Whereas providing an easy-to-use approach to evaluating the response of channels to the changing of a simple water and sediment hydrograph or base lowering, these models are based heavily on assumptions. First, the flow is assumed to be quasi-steady, leading to the elimination of local derivatives in the water–sediment mixture continuity and momentum

equations. Second, in the momentum equation the nonlinear convective acceleration term is ignored, yielding a diffusion model for bed elevation evolution. A slightly modified type of models, namely hyperbolic models have been developed by partly including the non-linear convective effect using a perturbation technique. Finally in the sediment continuity equation the temporal concentration term is almost exclusively not taken into account in order to make the analytical solution tractable. One of the major difficulties in using these analytical models is the determination of the model coefficients involved. Additionally, it appears not encouraging to use these analytical models with highly variable hydrographs (complicated boundary conditions). More comments on these analytical models can be found in Zanre and Needham (1996). It is necessary to recognize that the momentum equation for the mixture flow over erodible bed differs from that of fixed-bed clear water flow. However, it seems a common practice to reduce it to a clear water flow momentum equation, recognizing the uncertainty inherent in the resistance relationship that must be incorporated to close the momentum equation (Cao and Carling, 2002).

2.7.5 SEDIMENT TRANSPORT FUNCTIONS

A function is necessary to determine sediment transport rate and, for heterogeneous sediments, the size distribution of bed material being transported. A large number of functions have been developed. However, most, if not all, of these functions have been confirmed using specific laboratory and/or field measurement datasets, and none has been proved to be universally correct. Also it cannot be stated which function is the 'best' to use for a given situation. Distinct sediment transport functions will yield different answers, and normally the sediment rates/discharges are more sensitive to the choice of sediment function than the changes of river morphology. The latter concurs with the known feature that the time-scale of changes in flow variables (velocity, depth and sediment discharge, etc.) is normally significantly less than that of bed evolution. This aspect will be recalled later with respect to the asynchronous solution procedure commonly used in current mathematical river modeling practice. Therefore model developers and end-users have to judge the computational results based on their experience and their understanding of the basis on which existing sediment transport functions were derived and validated. Undoubtedly the modelling output is still subject to model developers and end-users—the lack of objectiveness is apparent. Using both laboratory and river datasets, Yang and

Wan(1991) compared the performance of several sediment transport functions that are popularly used, and showed that, for river datasets considered, the accuracy in ascending order was Engelund–Hansen(1967), Laursen(1958), Colby(1964), Ackers–White(1973), Einstein(1950), Toffaletti(1969), and Yang(1973). At the same time Yang and Wan (1991) claimed that the rating does not guarantee that any specific function is better than others under all hydraulic and sediment cases. For gravel-bed rivers, the formulae of Einstein, Parker, and Ackers– White were shown to perform reasonably well(Gomez and Church,1989).To measure the applicability of sand transport functions, an 'applicability index' was proposed by Williams and Julien(1989) on the basis of river characteristics. These authors argue that developing a universal (at least to a certain extent) procedure to help choose the 'optimum' sediment transport function among the large pool of candidates will be one of the most realistic strategies to cope with the uncertainty due to sediment transport functions (Cao and Carling ,2002).

2.6.6 MODEL CALIBRATION AND VERIFICATION/VALIDATION

2.6.6.1 Model calibration

A mathematical river model encompasses a number of parameters to be determined. One primary question is whether there is a unique combination of these parameters. From time to time the same (or similar) results are produced using different sets or combinations of model parameters. Usually there is no way to choose between these sets of parameters, other than to invoke extra-evidential considerations such as symmetry, simplicity, flexibility, personal, political or metaphysical preferences as well as prejudices and financial considerations. A secondary question arises as to how the overall performance of modeling can be objectively judged in comparison with measurement. This is especially critical for 3D modeling as normally there are many megabytes of numbers (typically with over 50 000 nodes for a real river problem), and it is almost impossible for model developers and end-users to view, assimilate, interpret and present even a small fraction of the output. That way, the judgment of acceptable agreement with measured data is virtually on a basis of a limited portion of information, for example some selected verticals and cross-sections, etc. Known too many model developers and end-users is the fact that it is fairly feasible to reconcile the computed results to measurements within a local

area by tuning the various parameters. Thirdly, it is hard to specify the initial conditions, whereas the computation can be sensitively influenced by the initial status in the non-linear systems; therefore the agreement between computed and measured results in general is largely not unbiased but subjective (Cao and Carling, 2002).

2.6.6.2 Model verification and validation

A verified model is useful as a prediction tool because of its demonstrated truth, and implies its reliability as a basis for decision-making. Equally correct is the term 'validation', which usually connotes legitimacy. It can, but does not necessarily denote an establishment of truth. Instead, it indicates the establishment of legitimacy, generally in terms of contracts, arguments, and methods. Validation means making legally valid, granting official sanction to or confirming the validity of something. A valid model contains no known errors or detectable flaws and is internally consistent. Verification is only possible in closed, rather than open systems, in which all components of the system are established independently, and are correct. Its application to natural systems is misleading. Alluvial river models are never closed systems, and therefore it is incorrect to use the term 'verification' for such models. Below are two specific reasons that make alluvial river models open. First, the model requires a number of input parameters that are not completely known. These input parameters are often embedded in turbulent closure modules, boundary conditions, sediment transport and entrainment functions as well as numerical discretization schemes, etc. Second, the observation and measurement of both independent and dependent quantities are laden with inferences and assumptions. Although many inferences and assumptions can, in some cases, be justified with experience, the degree to which the assumptions hold in new and complicated studies can never be established a priori. Alluvial river systems are complicated in that turbulence is one of the last problems in classic physics, which remains to be solved, and this is further aggravated due to the presence of sediments. It is essential to recognize the restricted sense of the term 'validation'. Legitimacy, official sanction, or being free of apparent errors and inconsistency does not necessarily mean truth or correctness, although truth or correctness is not precluded. It is misleading if the term validation is used to refer to actual modeling results in any particular realization. It is fairly popular for river modelers to use interchangeably the terms verification and validation. Thus they misleadingly imply that

validation establishes model veracity. Even more critically, the term validation is used to suggest that the physical river phenomenon is accurately represented by numerical models. As stated above, there exist a lot of critical problems with the model calibration–verification/validation phases, both logically and practically. The most significant problem comes with the verification/validation phase, where the model is claimed a success. This is, as a matter of fact, committing the basic logic error of affirming the model output. Oreskes et al.describe this as follows 'To claim that a proposition (or model) is verified because empirical data match a predicted outcome is to commit the fallacy of affirming the consequent. If a model fails to reproduce observed data, then we know that the model is faulty in some way, but the reverse is never the case. Confirming observations do not demonstrate the veracity of a model or a hypothesis, they only support its probability.' The misuse of the terms verification and validation in mathematical river modeling can be risky with respect to public interests. Often the decision-makers may not be experts in river hydraulics. It is the responsibility of model developers and end-users to correctly inform the decision-makers of what mathematical Models can realistically reflect, and more essentially the degree to which the modeling results can be relied upon (Cao and Carling, 2002).

2.8 REVIEW OF THE EXISTING MODELS PERTAINING TO ALLUVIAL STREAMS

2.8.1 DELFT HYDRAULIC LABORATORY MODEL

DE Varies (1973) developed a mathematical model combining continuity and momentum equations along with Chezy's equations for alluvial streams. In this model, the two dependent variables U(x, t) and Z(x, t) are computed in two separate steps. In this model, Cunge et al (1980) commented that computational time step cannot be chosen arbitrarily. This model is true for coarse sediment only.

2.8.2 CHEN'S MODEL

Chen (1973) formulated a model based on Saint Venant's continuity and momentum equations of unsteady flow of sediment-laden water. This model is capable of flood and sediment routing in a gradually varied flow channel. He used sediment load functions from Einstein's Bed load function as well as Toffaleti's function. Chen for the first time formulated a mathematical model that included sediment transport for generalized use. His works have proved to be a landmark in the field of open channel modeling for sediment-laden flow (Chen, 1973).

2.8.3 DASS MODEL

Dass (1975) developed multi-stream flow and compound stream flow models by adopting the uncoupled solution procedure to rout water and sediment in non-uniform channels with the capability to simulate bed level changes. The governing equations adopted by Dass are:

$$\frac{\partial Q}{\partial x}+\frac{\partial A}{\partial t}+\frac{\partial A_d}{\partial t}-q_l=0 \qquad (2.7)$$

$$\frac{\partial Q_s}{\partial x}+p\frac{\partial A_d}{\partial t}+\frac{\partial A_s}{\partial t}-q_s=0 \qquad (2.8)$$

$$\frac{\partial Q}{\partial t}+\frac{\partial(\rho QV)}{\partial x}+gA\frac{\partial y}{\partial x}+gAS_f-M_c=0 \qquad (2.9)$$

Where; x=Horizontal distance along the channel; t= Time; Q=Total discharge of sediment laden water; A= Area of available flow; Ad = Area of deposit; q*l* = lateral inflow; As =Volume of sediment concentration in flow; ρ = Density of sediment laden water; p= Porosity of bed material; qs = Lateral inflow of sediment; Qs = Sediment Discharge. Sf = Energy slope; Mc=Factor dependent on bed slope; V= Mean velocity of flow;

However, the validation of the model has been done in a hypothetical channel case (Dass, 1975).

2.8.4 FLUVIAL MODELS (1978 and 1984)

Chang and Hill (1976) developed this model in 1976.The same equations of St. Venant are solved. In the case of aggradation, the deposition is made starting from the lowest point in horizontal layers. A four point implicit finite difference schemes with uncoupled solution procedure is used to solve the equations. Channel width adjustments are used to reflect lateral migration. Manning's equation is used to represent resistance to flow.

He also developed FLUVIAL 11 Model in 1984 which employs a space-time domain in which space domain is represented by the discrete cross-sections along the river reach and the time domain is represented by discrete time steps. The model uses the concept enunciated by Langbein and Leopold that the equilibrium channel represents a state of balance with a minimum rate of energy expenditure along the channel. Chang has considered the bank erodibility or coefficient of bank erosion to predict the bank changes. Fluvial 11 is undoubtedly a promising model for channel changes prediction. However the adoption of empirical bank erodibility factor appears to have constrained its universal applicability and may require considerable calibration efforts. This model cannot be applicable for a river of multi-channel configuration.

2.8.5 HEC-6 MODEL

This model has been developed by W.A.Thomas at Hydrologic Engineering Centre, U.S.A. in 1977. There are five different options provided for the transport of sediment, viz Lausen's equation, Toffaleti's equation, Yang's stream power function, Duboy's equation and $Q_t = f(Q,S)$. The flow equation is the Manning's equation. For numerical solution, uncoupled explicit finite difference scheme is used. Simulation of reservoir sedimentation using HEC-6 was reported to be successful (HEC 2004).

2.8.6 WATER RESOURCES MODELLING FROM DHI WATER AND ENVIRONMENT

MIKE 11 - River and Channel Hydraulics

MIKE 11 is a one-dimensional hydrodynamic software package including a full solution of the St. Venant equations, plus many process modules for advection-dispersion, water quality and ecology, sediment transport, rainfall-runoff, flood forecasting, real-time operations, and dam break modelling.

The software can simulate flow and water level, water quality and sediment transport in rivers, irrigation canals, reservoirs and other inland water bodies. It is an engineering tool with capabilities provided in a modular framework. It can be applied on numerous applications - from simple design tasks to large forecasting projects including complex structure operation policies. It allows you to integrate your river and floodplain modelling with watershed processes, detailed floodplain representation, sewer systems and coastal processes. MIKE 11 offers links to groundwater codes (Mike 11 User Guide, 1993).

2.8.7 HEC-RAS - (Version-4.0, 2006)

This is the latest version developed by US Army Corps of Engineers at Hydrologic Engineering Center. This is Next Generation of hydrologic engineering software which encompasses several aspects of hydrologic engineering including; river hydraulics; reservoir system simulation; flood damage analysis; and real time river forecasting for reservoir operations. The system is comprised of a graphical user interface (GUI), separate hydraulic analysis components, data storage and management capabilities, graphics and reporting facilities. The HEC-RAS system will ultimately contain three one dimensional hydraulic analysis components (i) Steady flow water surface profile (ii) Unsteady flow simulations (iii) movable boundary sediment transport computations. Apart from this software contains several hydraulic design features. This is capable of importing GIS data or HEC-2 data (Brunner, 2002; HEC-RAS Manual, 2006).

It is an integrated system of software, designed for interactive use in a multi-tasking environment. The system is comprised of a graphical user interface, separate hydraulic analysis components, data storage and management capabilities, graphics and reporting facilities.

The HEC-RAS system will ultimately contain three one-dimensional hydraulic analysis components for:

- Steady flow water surface profile computations
- Unsteady flow simulation
- Movable boundary sediment transport computations

A key element is that all three components will use a common geometric data representation and common geometric and hydraulic computation routines. In addition to the three hydraulic analysis components, the system contains several hydraulic design features that can be invoked once the basic water surface profiles are computed (HEC-RAS Manual, 2006).

The review of existing models indicates that several models are available with different features. All the models use St. Venant's equations and have different sediment predictors, energy slope relations and distribution of aggradation/degradation equations. A natural river has many complexities due to its size, flow variations, concentration of sediment and its properties, engineering works carried out on the river and other geographical, meteorological, social factors. Due to these reasons, no model can claim to have considered all the factors. Therefore, the models cannot have universal applicability. Hence, for modelling a particular river one should be very careful to choose a model, which is applicable according to the characteristics of that river.

Hec-Ras (version 4.0) is latest in the family of the existing models for sediment transport & mobile bed modeling, so in this dissertation it has been envisaged to initiate work on this model to figure out the suitability for the specific purpose as well for specific applicability.

2.9 GENERAL PHILOSOPHY OF THE MODELLING SYSTEMS IN HEC-RAS

HEC-RAS is an integrated system of software, designed for interactive use in a multi-tasking, multi-user network environment. The system is comprised of a graphical user interface (GUI), separate hydraulic analysis components, data storage and management capabilities, graphics and reporting facilities. The system contains three one-dimensional hydraulic analysis components for: (1) steady flow water surface profile computations; (2) unsteady flow simulation; and (3) movable boundary sediment transport computations. A key element is that all three components use a common geometric data representation and common geometric and hydraulic computation routines. In addition to the three hydraulic analysis components, the system contains several hydraulic design features that can be invoked once the basic water surface profiles are computed (Brunner, 2002; Warner, 2002).

2.9.1 OVERVIEW OF HYDRAULIC CAPABILITIES

HEC-RAS is designed to perform one-dimensional hydraulic calculations for a full network of natural and constructed channels. The following is a description of the major hydraulic capabilities of HEC-RAS.

Steady Flow Water Surface Profiles: This component of the modeling system is intended for calculating water surface profiles for steady gradually varied flow. The system can handle a single river reach, a dendritic system, or a full network of channels. The steady flow component is capable of modeling subcritical, supercritical, and mixed flow regime water surface profiles.

The basic computational procedure is based on the solution of the one-dimensional energy equation. Energy losses are evaluated by friction (Manning's equation) and contraction/expansion (coefficient multiplied by the change in velocity head). The momentum equation is utilized in situations where the water surface profile is rapidly varied. These situations include mixed flow regime calculations (i.e., hydraulic jumps), hydraulics of bridges, and evaluating profiles at river confluences (stream junctions).

The effects of various obstructions such as bridges, culverts, weirs, spillways and other structures in the flood plain may be considered in the computations. The steady flow system is designed for

application in flood plain management and flood insurance studies to evaluate floodway encroachments. Also, capabilities are available for assessing the change in water surface profiles due to channel improvements, and levees.

Unsteady Flow Simulation: This component of the HEC-RAS modelling system is capable of simulating one-dimensional unsteady flow through a full network of open channels. The unsteady flow equation solver was adapted from Dr. Robert L. Barkau's UNET model (HEC, 2004). This unsteady flow component was developed primarily for subcritical flow regime calculations.

The hydraulic calculations for cross-sections, bridges, culverts, and other hydraulic structures that were developed for the steady flow component were incorporated into the unsteady flow module. Additionally, the unsteady flow component has the ability to model storage areas and hydraulic connections between storage areas, as well as between stream reaches.

Sediment Transport/Movable Boundary Computations: This component of the modeling system is intended for the simulation of one-dimensional sediment transport/movable boundary calculations resulting from scour and deposition over moderate time periods (typically years, although applications to single flood events will be possible).

The sediment transport potential is computed by grain size fraction, thereby allowing the simulation of hydraulic sorting and armoring. Major features include the ability to model a full network of streams, channel dredging, various levee and encroachment alternatives, and the use of several different equations for the computation of sediment transport.

The model will be designed to simulate long-term trends of scour and deposition in a stream channel that might result from modifying the frequency and duration of the water discharge and stage, or modifying the channel geometry. This system can be used to evaluate deposition in reservoirs, design channel contractions required to maintain navigation depths, predict the influence of dredging on the rate of deposition, estimate maximum possible scour during large flood events, and evaluate sedimentation in fixed channels (Brunner, 2002 ; Warner 2002; Manual HEC-RAS,2006).

2.9.2 THEORITICAL BASIS FOR ONE- DIMENTIONAL FLOW CALCULATION

HEC-RAS is currently capable of performing one-dimensional water surface profile calculations for steady gradually varied flow in natural or constructed channels. Subcritical, supercritical, and mixed flow regime water surface profiles can be calculated.

2.9.2.1 Equations for Basic Profile Calculations

Water surface profiles are computed from one cross section to the next by solving the Energy equation with an iterative procedure called the standard step method. The Energy equation is written as follows:

$$Y_2 + Z_2 + \frac{\alpha_2 V_2^2}{2g} = Y_1 + Z_1 + \frac{\alpha_1 V_1^2}{2g} + h_e \qquad (2.10)$$

Where: Y1, Y2 = depth of water at cross sections; Z1, Z2 = elevation of the main channel inverts; V1, V2 = average velocities (total discharge/ total flow area); $\alpha 1$, $\alpha 2$ = velocity weighting coefficients; g = gravitational acceleration; he = energy head loss; a diagram showing the terms of the energy equation is shown in Fig: 2.5.

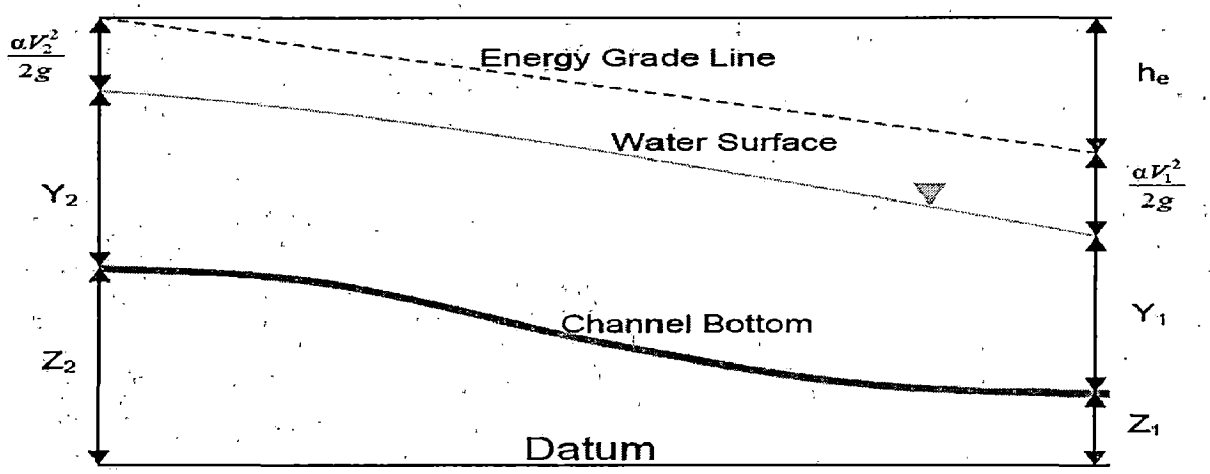

Fig: 2.5 Representations of Terms in the Energy Equation

The energy head loss (he) between two cross sections is comprised of friction losses and contraction or expansion losses. The equation for the energy head loss is as follows:

$$h_e = L\overline{S_f} + C\left|\frac{\alpha_2 V_2^2}{2g} - \frac{\alpha_1 V_1^2}{2g}\right| \quad (2.11)$$

The distance weighted reach length, L, is calculated as:

$$L = \frac{L_{lob}\overline{Q_{lob}} + L_{ch}\overline{Q_{ch}} + L_{rob}\overline{Q_{rob}}}{\overline{Q_{lob}} + \overline{Q_{ch}} + \overline{Q_{rob}}} \quad (2.12)$$

Where: Llob, Lch, Lrob = cross section reach lengths specified for flow in the left overbank, main channel, and right overbank, respectively ; Qlob ,Qch ,Qrob = arithmetic average of the flows between sections for the left overbank, main channel, and right overbank, respectively

2.9.2.2 Cross Section Subdivision for Conveyance Calculations

The determination of total conveyance and the velocity coefficient for a cross section requires that flow be subdivided into units for which the velocity is uniformly distributed. The approach used in HEC-RAS is to subdivide flow in the overbank areas using the input cross section n-value break points (locations where n-values change) as the basis for subdivision. Conveyance is calculated within each subdivision from the following form of Manning's equation (based on English units):

$$Q = KS_f^{1/2} \quad (2.13)$$

$$K = \frac{1.486}{n} AR^{2/3} \quad (2.14)$$

Where: K = conveyance for subdivision; n = Manning's roughness coefficient for subdivision

A = flow area for subdivision; R = hydraulic radius for subdivision (area / wetted perimeter)

The program sums up all the incremental conveyances in the overbanks to obtain a conveyance for the left overbank and the right overbank. The main channel conveyance is normally computed as a single conveyance element. The total conveyance for the cross section is obtained by summing the three subdivision conveyances (left, channel, and right).

In general, it is felt that the HECRAS default method is more commensurate with the Manning equation and the concept of separate flow elements (Brunner, 2002).

2.9.2.3 Composite Manning's n for the Main Channel

Flow in the main channel is not subdivided, except when the roughness coefficient is changed within the channel area. HEC-RAS tests the applicability of subdivision of roughness within the main channel portion of a cross section, and if it is not applicable, the program will compute a single composite n value for the entire main channel. The program determines if the main channel portion of the cross section can be subdivided or if a composite main channel n value is utilized.

The computed composite nc should be checked for reasonableness. The computed value is the composite main channel n value in the output and summary tables.

Evaluation of the Mean Kinetic Energy Head

Because the HEC-RAS software is a one-dimensional water surface profiles program, only a single water surface and therefore a single mean energy are computed at each cross section. For a given water surface elevation, the mean energy is obtained by computing a flow weighted energy from the three subsections of a cross section (left overbank, main channel, and right overbank). Figure 2.6 below shows how the mean energy would be obtained for a cross section with a main channel and a right overbank (no left overbank area).

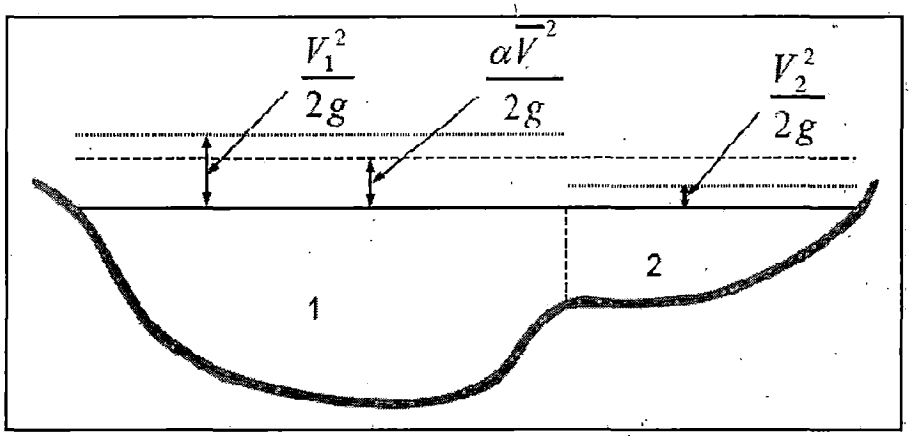

V1 = mean velocity for sub area 1, V2 = mean velocity for sub area 2

Fig: 2.6 Example of How Mean Energy is Obtained

To compute the mean kinetic energy it is necessary to obtain the velocity head weighting coefficient alpha. Alpha is calculated as follows:

Mean Kinetic Energy Head = Discharge-Weighted Velocity Head

$$\alpha\frac{\overline{V^2}}{2g} = \frac{Q_1\frac{V_1^2}{2g} + Q_2\frac{V_2^2}{2g}}{Q_1+Q_2} \quad = \quad \alpha = \frac{2g\left[Q_1\frac{V_1^2}{2g} + Q_2\frac{V_2^2}{2g}\right]}{(Q_1+Q_2)\overline{V^2}}$$

$$\alpha = \frac{\left[Q_1V_1^2 + Q_2V_2^2\right]}{(Q_1+Q_2)\overline{V^2}}$$

In general:

$$\alpha = \frac{\left[Q_1V_1^2 + Q_2V_2^2 + \ldots\ldots + Q_NV_N^2\right]}{Q\overline{V^2}} \qquad (2.15)$$

The velocity coefficient, α, is computed based on the conveyance in the three flow elements: left overbank, right overbank, and channel. It can also be written in terms of conveyance and area as in the following equation:

$$\alpha = \frac{(A_t)^2\left[\frac{K_{lob}^3}{A_{lob}^2} + \frac{K_{ch}^3}{A_{ch}^2} + \frac{K_{rob}^3}{A_{rob}^2}\right]}{K_t^3} \tag{2.16}$$

Where: At = total flow area of cross section; Alob, Ach, Arob = flow areas of left overbank, main channel and right overbank, respectively; Kt = total conveyance of cross section; Klob, Kch, Krob = conveyances of left overbank, main channel and right overbank, respectively.

Friction Loss Evaluation

Friction loss is evaluated in HEC-RAS as the product of Sf and L (Eq: 2.11), where Sf is the representative friction slope for a reach and L is defined by Eq: (2.12). The friction slope (Slope of the energy grade line) at each cross section is computed from Manning's equation as follows:

$$S_f = \left[\frac{Q}{K}\right]^2 \tag{2.17}$$

Alternative expressions for the representative reach friction slope (Sf) in HEC-RAS are as follows:

Average Conveyance Equation

$$\overline{S_f} = \left[\frac{Q_1 + Q_2}{K_1 + K_2}\right]^2 \tag{2.18}$$

Average Friction Slope Equation

$$\overline{S_f} = \frac{S_{f1} + S_{f2}}{2} \tag{2.19}$$

Geometric Mean Friction Slope Equation

$$\overline{S_f} = \sqrt{S_{f1} \times S_{f2}} \tag{2.20}$$

Harmonic Mean Friction Slope Equation

$$\overline{S_f} = \frac{2(S_{f1} \times S_{f2})}{S_{f1} + S_{f2}} \tag{2.21}$$

Equation (2.21) is the "default" equation used by the program; that is, it is used automatically unless a different equation is requested by input. The program also contains an option to select equations, depending on flow regime and profile type (e.g., S1, M1, etc)

Contraction and Expansion Loss Evaluation

Contraction and expansion losses in HEC-RAS are evaluated by the following equation:

$$h_{ce} = C\left|\frac{\alpha_1 V_1^2}{2g} + \frac{\alpha_2 V_2^2}{2g}\right| \tag{2.22}$$

Where: C = the contraction or expansion coefficient

The program assumes that a contraction is occurring whenever the velocity head downstream is greater than the velocity head upstream. Likewise, when the velocity head upstream is greater than the velocity head downstream, the program assumes that a flow expansion is occurring.

Steady Flow Program Limitations

The following assumptions are implicit in the analytical expressions used in the current version of the program:

1. Flow is steady.
2. Flow is gradually varied. (Except at hydraulic structures such as: bridges; culverts; and weirs. At these locations, where the flow can be rapidly varied, the momentum equation or other empirical equations are used.)

3. Flow is one dimensional (i.e., velocity components in directions other than the direction of flow are not accounted for).
4. River channels have "small" slopes; say less than 1:10.

Flow is assumed to be steady because time-dependent terms are not included in the energy equation (Eq: 2.10). Flow is assumed to be gradually varied because Eq: (2.10) is based on the premise that a hydrostatic pressure distribution exists at each cross section. At locations where the flow is rapidly varied, the program switches to the momentum equation or other empirical equations. Flow is assumed to be one-dimensional because Eq: (2.11) is based on the premise that the total energy head is the same for all points in a cross section. Small channel slopes are assumed because the pressure head, which is a component of Y in Eq: (2.10), is represented by the water depth measured vertically.

The program has the capability to deal with movable boundaries (i.e., sediment transport) and requires that energy losses be definable with the terms contained in Eq: (2.11).

Uniform Flow Computations

For preliminary channel sizing and analysis for a given cross section, a uniform flow editor is available in HEC-RAS. The uniform flow editor solves the steady-state, Manning's equation for uniform flow. The five parameters that make up the Manning's equation are channel depth, width, slope, discharge, and roughness.

$$Q = f(A, R, S, n) \quad (2.23)$$

Where: Q = Discharge; A = Cross sectional area; R = Hydraulic radius; S = Energy slope

n = Manning's n value

When an irregularly shaped cross section is subdivided into a number of sub areas, a unique solution for depth can be found. And further, when a regular trapezoidal shaped section is used, a unique solution for the bottom width of the channel can be found if the channel side slopes are provided. The dependant variables A, and R, can then be expressed in the Manning equation in terms of depth, width and side slope as follows:

$$Q = f(Y, W, z, S, n) \quad (2.24)$$

Where: Y = Depth; W= Bottom width; z = Channel side slope

By providing four of the five parameters, HEC-RAS will solve the fifth for a given cross section. When solving for width, some normalization must be applied to a cross section to obtain a unique solution, therefore a trapezoidal or compound trapezoidal section with up to three templates must be used for this situation.

Cross Section Subdivision for Conveyance Calculations

In the uniform flow computations, the HEC-RAS default Conveyance Subdivision Method is used to determine total conveyance. Sub areas are broken up by roughness value break points and then each sub area's conveyance is calculated using Manning's equation. Conveyances are then combined for the left overbank, the right overbank, and the main channel and then further summed to obtain the total cross section conveyance.

Bed Roughness Functions

Because Manning's n values are typically used in HEC-RAS, the uniform flow feature allows for the use of a number of different roughness equations to solve for n. HEC-RAS allows the user to apply any of these equations at any area within a cross section; however, the applicability of each equation should be noted prior to selection. Manning equation method, one n value or a range of n values is prescribed across the cross section and then the Manning's equation is used to solve for the desired parameter.

Sediment Transport Capacity

The sediment transport capacity function in HEC-RAS has the capability of predicting transport capacity for non-cohesive sediment at one or more cross sections based on existing hydraulic parameters and known bed sediment properties. It does not take into account sediment inflow, erosion, or deposition in the computations. Classically, the sediment transport capacity is comprised of both bed load and suspended load, both of which can be accounted for in the various sediment transport predictors available in HEC-RAS. Results can be used to develop sediment discharge rating curves, which help to understand and predict the fluvial processes found in natural rivers and streams.

Sediment Gradation

Sediment transport rates are computed for the prescribed hydraulic and sediment parameters for each representative grain size. Transport capacity is determined for each grain size as if that particular grain size made up 100% of the bed material. The transport capacity for that size group is then multiplied by the fraction of the total sediment that that size represents. The fractional transport capacities for all sizes are summed for the total sediment transport capacity.

$$g_s = \sum_{i=1}^{n} g_{si} p_i \qquad (2.25)$$

Where: gs = Total sediment transport; gsi = Sediment transport for size class i; Pi = Fraction of size class i in the sediment; n = Number of size classes represented in the gradation.

Because different sediment transport functions were developed differently with a wide range of independent variables, HEC-RAS gives the user the option to select how depth and width are to be computed. The HEC-6 method converts everything to an effective depth and width. However, many of the sediment transport functions were developed using hydraulic radius and top width, or an average depth and top width. For this reason, HEC-RAS allows the user to designate which depth/width method to use. If the default selection is chosen, then the method consistent with the development of the chosen function will be used. For irregular cross section shapes, HEC-RAS uses the effective depth/effective width or hydraulic radius/top width as the default. Also available for use is the hydraulic depth, which is used to represent the average depth and is simply the total area of the section divided by the top width.

Sediment Transport Functions

Because different sediment transport functions were developed under different conditions, a wide range of results can be expected from one function to the other. Therefore it is important to verify the accuracy of sediment prediction to an appreciable amount of measured data from either the study stream or a stream with similar characteristics. It is very important to understand the processes used in the development of the functions in order to be confident of its applicability to a given stream.

Typically, sediment transport functions predict rates of sediment transport from a given set of steady-state hydraulic parameters and sediment properties. Some functions compute bed-load transport, and some compute bed-material load, which is the total load minus the wash load (total transport of particles found in the bed). In sand-bed streams with high transport rates, it is common for the suspended load to be orders of magnitude higher than that found in gravel-bed or cobbled streams. It is therefore important to use a transport predictor that includes suspended sediment for such a case.

The following sediment transport functions which are also available in HEC-RAS:

- Ackers-White (1973)
- Engelund-Hansen (1967)
- Laursen (1958)
- Meyer-Peter Müller (1948)
- Toffaleti (1969)
- Yang (1973)

These functions were selected based on their validity and collective range of applicability. All of these functions, except for Meyer-Peter Müller(1948), are compared extensively by Yang and Wan (1991) over a wide range of sediment and hydraulic conditions. Results varied, depending on the conditions applied. The Meyer-Peter Müller(1948) and the bed-load portion of the Toffaleti(1969) function were compared with each other by Amin and Murphy (1981). They concluded that Toffaleti(1969) bed-load procedure was sufficiently accurate for their test stream, whereby, Meyer-Peter Müller(1948) was not useful for sand-bed channels at or near incipient. A short description three main sediment predictors is summarized below. (Brunner, 2002; Karamisheva(2006).

Ackers-White(1973): The Ackers-White transport function is a total load function developed under the assumption that fine sediment transport is best related to the turbulent fluctuations in the water column and coarse sediment transport is best related to the net grain shear with the mean velocity used as the representative variable. The transport function was developed in terms of particle size, mobility, and transport.

A dimensionless size parameter is used to distinguish between the fine, transitionary, and coarse sediment sizes. Under typical conditions, fine sediments are silts less than 0.04 mm, and coarse sediments are sands greater than 2.5 mm. Since the relationships developed by Ackers-White are applicable only to non-cohesive sands greater than 0.04 mm, only transitionary and coarse sediments apply. Original experiments were conducted with coarse grains up to 4 mm; however the applicability range was extended to 7 mm.

This function is based on over 1000 flume experiments using uniform or near-uniform sediments with flume depths up to 0.4 m. A range of bed configurations was used, including plane, rippled, and dune forms, however the equations do not apply to upper phase transport (e.g. anti-dunes) with Froude numbers in excess of 0.8. The general transport equation for the Ackers-White function for a single grain size is represented by:

$$X = \frac{G_{gr} s d_s}{D\left(\frac{u^*}{V}\right)^n} \qquad \text{and} \qquad G_{gr} = C\left(\frac{F_{gr}}{A} - 1\right) \tag{2.26}$$

Where: X = Sediment concentration, in parts per part; Ggr = Sediment transport parameter ; s = Specific gravity of sediments ; ds = Mean particle diameter ; D = Effective depth ; u* = Shear velocity ; V = Average channel velocity ; n = Transition exponent, depending on sediment size ; C = Coefficient ; Fgr = Sediment mobility parameter ; A = Critical sediment mobility parameter

A hiding adjustment factor was developed for the Ackers-White method by Profitt and Sutherland (1983), and is included in RAS as an option. The hiding factor is an adjustment to include the effects of a masking of the fluid properties felt by smaller particles due to shielding by larger particles. This is typically a factor when the gradation has a relatively large range of particle sizes and would tend to reduce the rate of sediment transport in the smaller grade classes (Brunner, 2002).

Engelund-Hansen(1967): The Engelund-Hansen function is a total load predictor which gives adequate results for sandy rivers with substantial suspended load. It is based on flume data with sediment sizes between 0.19 and 0.93 mm. It has been extensively tested, and found to be fairly consistent with field data.

The general transport equation for the Engelund-Hansen function is represented by:

$$g_s = 0.05\gamma_s V^2 \sqrt{\frac{d_{50}}{g\left(\frac{\gamma_s}{\gamma}-1\right)}}\left[\frac{\tau_0}{(\gamma_s-\gamma)d_{50}}\right]^{3/2} \qquad (2.27)$$

Where: gs = Unit sediment transport; γ = Unit wt of water; γs = Unit wt of solid particles; V = Average channel velocity; τo = Bed level shear stress; d50 = Particle size of which 50% is smaller

Yang(1973): Yang's method (1973) is developed under the premise that unit stream power is the dominant factor in the determination of total sediment concentration. The research is supported by data obtained in both flume experiments and field data under a wide range conditions found in alluvial channels. Principally, the sediment size range is between 0.062 and 7.0 mm with total sediment concentration ranging from 10 ppm to 585,000 ppm. Channel widths range from 0.44 to1746 ft, depths from 0.037 to 49.4 ft, water temperature from 0o to 34.3°Celsius, average channel velocity from 0.75 to 6.45 fps, and slopes from 0.000043 to 0.029 (Yang and Wan ,1991).

Yang (1984) expanded the applicability of his function to include gravel-sized sediments. The general transport equations for sand and gravel using the Yang function for a single grain size is represented by: (Garde and Raju, 2000; Brunner, 2002)

$$\log C_t = 5.435 - 0.286\log\frac{\omega d_m}{\nu} - 0.457\log\frac{u^*}{\omega} + \left(1.799 - 0.409\log\frac{\omega d_m}{\nu} - 0.314\log\frac{u^*}{\omega}\right)\log\left(\frac{VS}{\omega}-\frac{V_{cr}}{\omega}\right) \qquad (2.28)$$

For sand $d_m < 2mm$

$$\log C_t = 6.681 - 0.633\log\frac{\omega d_m}{\nu} - 4.816\log\frac{u^*}{\omega} + \left(2.784 - 0.305\log\frac{\omega d_m}{\nu} - 0.282\log\frac{u^*}{\omega}\right)\log\left(\frac{VS}{\omega} - \frac{V_{cr}S}{\omega}\right) \quad (2.29)$$

For gravel $d_m \geq 2mm$

Where: *Ct* = Total sediment concentration, ω = Particle fall velocity, *dm* =Med. particle diameter ν = Kinematic viscosity, *u** = Shear velocity, V = Average channel velocity, S = Energy gradient

2.9.3 THEORETICAL BASIS FOR SEDIMENT CALCULATIONS (HEC, 1981)

Sediment transport rates are calculated for each flow in the hydrograph for each grain size. The transport potential is calculated for each grain size class in the bed as though that size comprised 100% of the bed material. Transport potential is then multiplied by the fraction of each size class present in the bed at that time to yield the transport capacity for that size class. These fractions often change significantly during a time step; therefore an iteration technique is used to permit these changes to affect the transport capacity. The basis for adjusting bed elevations for scour or deposition is the Exner equation.

2.9.3.1 Equation for Continuity of Sediment Material Control Volume

Each cross section represents a control volume. The control volume width is usually equal to the movable bed width and its depth extends from the water surface to the top of bedrock or other geological control beneath the bed surface. In areas where no bedrock exists, an arbitrary limit (called the "model bottom") is assigned (Fig: 2.7). The control volume for cross section 2 is represented by the heavy dashed lines. The control volumes for cross sections 1 and 3 join that for cross section 2, etc.

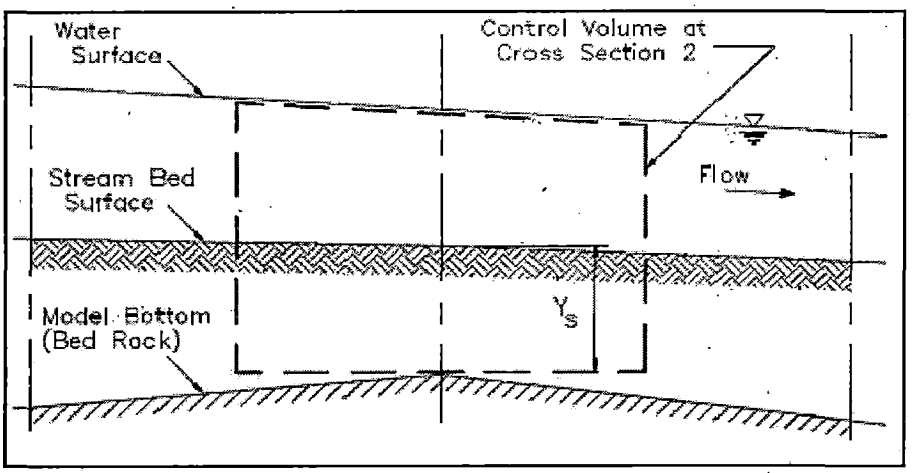

Fig: 2.7 Control Volume for Bed Material

2.9.3.2 Exner Equation

The above description of the processes of scour and deposition must be converted into numerical algorithms for computer simulation. The basis for simulating vertical movement of the bed is the continuity equation for sediment material (Eq: 2.30)

$$\frac{\partial G}{\partial x} + B_0 \frac{\partial Y_s}{\partial t} = 0 \qquad (2.30)$$

Where: Bo = width of movable bed; t = time; G = average sediment discharge rate during time step Δt; x = distance along the channel; Ys = depth of sediment in control volume

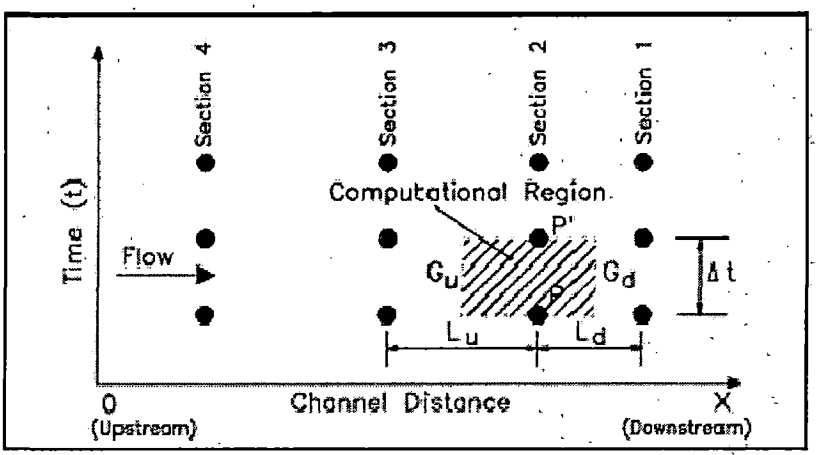

Fig: 2.8 Computation Grid

Equations (2.31) and (2.32) represent the Exner Equation expressed in finite difference form for point P using the terms shown in Fig: 2.8.

$$\frac{G_d - G_u}{0.5(L_d - L_u)} + \frac{B_{sp}(Y'_{sp} - Y_{sp})}{\Delta t} = 0 \qquad (2.31)$$

$$Y'_{sp} = Y_{sp} - \frac{\Delta t}{(0.5)B_{sp}} \cdot \frac{G_d - G_u}{L_d + L_u} \qquad (2.32)$$

Where: Bsp = width of movable bed at point P; Gu, Gd = sediment loads at the upstream and downstream cross sections, respectively; Lu, Ld = upstream and downstream reach lengths, respectively, between; cross sections Ysp, Y'sp = depth of sediment before and after time step, respectively, at point P; 0.5 = the "volume shape factor" which weights the upstream and downstream reach lengths; Δt = computational time step.

The initial depth of bed material at point P defines the initial value of Ysp. The sediment load, Gu, is the amount of sediment, by grain size, entering the control volume from the upstream control volume. For the upstream-most reach, this is the inflowing load boundary condition provided by the user. The sediment leaving the control volume, Gd, becomes the Gu for the next downstream control volume. The sediment load, Gd, is calculated by considering the transport capacity at point P, the sediment inflow, availability of material in the bed, and armoring. The difference between Gd and Gu is the amount of material deposited or scoured in the reach labeled as "computational region" on Fig: 2.8, and is converted to a change in bed elevation using Eq: 2.32.

The transport potential of each grain size is calculated for the hydraulic conditions at the beginning of the time interval and is not recalculated during that interval. Therefore, it is important that each time interval be short enough so that changes in bed elevation due to scour or deposition during that time interval do not significantly influence the transport potential by the end of the time interval. Fractions of a day are typical time steps for large water discharges and several days or even months may be satisfactory for low flows. The amount of change in bed elevation that is acceptable in one time step is a matter of judgment. Good results have been

achieved by using 10% of the water depth, whichever is less, as the allowable bed change in a computational time interval. The gradation of the bed material, however, is recalculated during the time interval because the amount of material transported is very sensitive to the gradation of bed material. If transport capacity is greater than the load entering the control volume, available sediment is removed from the bed to satisfy continuity. (HEC, 1981).

2.10 RIVER CHANNEL RECTIFICATION MEASURES

2.9.1 Submerged Vanes

A technique for which potentials as a control measure have not been fully explored is the submerged-vane technique. Both laboratory and field tests suggest that this technique has a broad range of applications. The vanes are small flow-training structures (foils), designed to modify the near-bed flow pattern and redistribute flow and sediment transport within the channel cross section. The structures are installed at an angle of attack of 15-25° with the flow, and their initial height is 0.2-0.4 times local water depth at design stage. The vanes function by generating secondary circulation in the flow.

The circulation alters magnitude and direction of the bed shear stresses and causes a change in the distributions of velocity, depth, and sediment transport in the area affected by the vanes. As a result, the river bed aggrades in one portion of the channel cross section and degrades in another.

Although the literature indicates that vanes, or panels, similar to those discussed here, have been used in the past for river-channel stabilization, little is documented on vane design and performance. The first known attempts to develop a theoretical design basis were aimed at designing a system of vanes to stop or reduce bank erosion in river curves. In such an application, the vanes are laid out so that the vane-generated secondary current eliminates the centrifugally induced secondary current, which is the root cause of bank undermining. The centrifugally induced secondary current in river bends, also known as the transverse circulation or helical motion, results from the difference in centrifugal acceleration along a vertical line in the flow because of the nonuniform vertical profile of the velocity. The secondary current forces high-velocity surface current outward and low-velocity near-bed current inward. The increase

in velocity at the outer bank increases the erosive attack on the bank, causing it to fail. By directing the near-bed current toward the outer bank, the submerged vanes counter the centrifugally induced secondary current and, thereby, inhibit bank erosion. The vanes can be laid out to make the water and sediment move through a river curve as if it were straight. The technique was subsequently developed to ameliorate shoaling problems in rivers. Significant changes in depth were achieved without causing significant changes in cross-sectional area, energy slope, and downstream sediment transport. The changes in cross-sectional average parameters are small because the vane-induced secondary current changes the direction of the bed shear stress by only a small amount.

Theory

The theory develops the relationship between vane characteristics and induced bed shear stresses. This relationship is then incorporated into the governing flow equations, which are solved to obtain flow and depth distributions in the channel.

Vane-Induced Bed Shear Stresses

A submerged vane at a small angle of attack with the flow, a, induces a horizontal circulation in the flow downstream. The circulation arises because the vertical pressure gradients on the two surfaces of the vane (the pressure increasing from bottom to top on the low-pressure side, decreasing from bottom to top on the high-pressure side) cause the fluid flowing along the high-pressure side to acquire an upward velocity component, while on the low-pressure side there is a downward velocity component. The resulting vortices (vortex sheet) at the trailing edge of the vane roll up to form a large vortex springing from a position near the top of the vane. This vortex (tip vortex) is carried with the flow downstream, where it gives rise to a secondary or helical motion of the flow and associated changes in bed shear stress and bed topography (Fig. 2). These changes can be calculated. The tip vortex is described as a steady potential vortex. Its strength decays because of viscous diffusion as the vortex is transported downstream. In an unbounded flow field, the tangential velocity perpendicular to the core axis of such a vortex is

$$v_\theta = \frac{\Gamma}{2\pi r} \times [1 - e^{(-\frac{u}{4\varepsilon s} r^2)}]$$

in which r = distance from core of vortex; ε = eddy viscosity; s = downstream distance; u = velocity of fluid transporting the vortex or velocity approaching vane; and Γ = horizontal circulation at $s = 0$. In a bounded flow field, v_θ is obtained by the method of images. With the boundaries in a river channel being the stream bed and free surface, the transverse component of v_θ (the component perpendicular to the z-axis) at distance z from the stream bed is

$$v_n = \sum_{i=1}^{\infty} (-1)^{i+1} \frac{\Gamma}{2\pi r_i} \times [1 - e^{(-\frac{u}{4\varepsilon s} r_i^2)}](\frac{z_i - z}{r_i}) + \sum_{j=1}^{\infty} (-1)^{j+1} \frac{\Gamma}{2\pi r_j} \times [1 - e^{(-\frac{u}{4\varepsilon s} r_j^2)}](\frac{z_j - z}{r_j})$$

in which the first summation includes contributions from the real vortex and images above the free surface; the second summation is the contributions from the images below the stream bed; r, and r, = distances from the core of vortex i and j, respectively; and z, and z, = vertical distances from stream bed to core of vortex i and j, respectively. Because of the pressure difference between the vane's pressure and suction sides, the vortex core is somewhat below the top elevation of the vane. Calculations [see Milne-Thomson (1966), page 209] and data (Odgaard and Spoljaric 1989; Wang 1990) show that the core is about 0.2 times the vane height below the top elevation of the vane. The horizontal circulation T can be evaluated by relating it to the horizontal lift force, *FL,* which the vane exerts on the flow (Fig. 1). This lift force has the same magnitude as the force that the flow exerts on the vane, which, according to the Kutta-Joukowskii theorem (Sabersky and Acosta 1964), is proportional to the vertical circulation around the vane associated with the shift of the rear stagnation point to the trailing edge of the vane. This vertical circulation, in turn, is equal to the horizontal circulation T (Helmholz's second theorem). Consequently, $FL = \rho \Gamma u H$, where ρ= fluid density and H = vane height.

From the velocity field thus calculated, the near-bed transverse velocity component is obtained with z = 0

$$v_{vn} = \frac{F_L}{\pi \rho u H} \sum_{j=1}^{\infty} \frac{(-1)^{j+1}}{r_j} \times [1 - e^{(-\frac{u}{4\varepsilon s} r_j^2)}] \frac{z_j}{r_j}$$

in which subscript *n* denotes the transverse direction. In this equation, it is assumed that there are as many vortices above the stream bed (including the real vortex) as there are below.

The induced transverse bed shear stress, τ_{vn} can now also be calculated. The assumption is made that τ_{vn} has the same ratio to the stream-wise bed shear stress τ_{bs} as v_{vn} „ to a certain streamwise near-bed velocity u_b.

$$\frac{\tau_{vn}}{\tau_{bs}} = \frac{v_{vn}}{u_b}$$

To proceed, a power-law velocity profile is adopted

$$u = \frac{m+1}{m} \left(\frac{z}{d}\right)^{1/m} . \bar{u}$$

in which u = point velocity at height z above the bed; d = flow depth; ū = depth-averaged velocity; and m = resistance coefficient, which is related to the Darcy-Weisbach friction factor / as $m = k\sqrt{(8/f)}$; k = von Karman constant (— 0.4). Hence, $m = k\bar{u}/\sqrt{(gSd)}$, where S = longitudinal slope of the water surface, and g = acceleration due to gravity. With this velocity profile, τ_{bs}, vane-approach velocity u_a and u_b are related to u as $\tau_{bs} = pk^2 \bar{u}^2/m^2$, $u_a = \bar{u}(H/d)^{1/m}$ (average over
height of vane) and $u_b = \bar{u}/K$, where K = function of m. The downstream decay of τ_{vn} , and v_{vn}, is controlled by ε. Since bed resistance is the major factor causing decay ε is obtained from the power law and an assumed linearly distributed primary-flow shear stress, so that,
$\varepsilon = k^2\bar{u}d/[6m(1 + 1/m)(1 - 1/2m)(1 - 1/3/m)]$. By substituting Eq. 3 into Eq. 4, the transverse bed shear stress is

$$\tau_{vn} = F_L.f_v$$

where

$$f_v = \frac{Kk^2}{\pi m^2 H} \frac{\bar{u}}{u_a} \sum_{j=1}^{\infty} \frac{(-1)^{j+1}}{r_j} \times [1 - e^{(-\frac{u}{4\varepsilon s} r_j^2)}] \frac{Z_j}{r_j}$$

It follows that the streamwise *(s)* component of the induced bed shear stress is

$$\tau_{vs} = F_D . f_v$$

where F_D = drag force associated with F_L. Both FL and FD are most easily calculated by relating them to dynamic pressure as

$$F_L = \frac{1}{2} c_L \rho L \int_0^H u^2 \, dz$$

and

$$F_D = \frac{1}{2} c_D \rho L \int_0^H u^2 \, dz$$

in which L = vane length; and c_L, c_D = lift and drag coefficients. By substituting Eq. 5 into Eqs. 9 and 10, the lift and drag forces are

$$F_L = \frac{1}{2} c_L \rho H L \bar{u}^2 \left(\frac{(m+2)^2}{m(m+1)}\right) \left(\frac{H}{d}\right)^{2/m}$$

and

$$F_D = \frac{c_D}{c_L} F_L$$

By assuming that the distribution of the vertical circulation around the vane is elliptical, maximum at the bed and zero at the top of the vane, the lift coefficient is

$$c_L = \frac{2\pi\alpha}{1 + \frac{L}{H}}$$

The corresponding drag coefficient is determined by

$$c_D = \frac{1}{2\pi}\frac{L}{H} c_L^2$$

The area of stream bed affected by a single vane is limited. In the transverse direction, the vane has little impact beyond about three times vane height. A wider area is affected if two or more vanes are employed. If the vanes are arranged in an array, as shown in Figs. 3 and 4, the width of the affected area is increased. However, because of interaction between tip vortices, the strength of the induced circulation is then less than that obtained by simple superposition of individual vorticity fields. The interaction between two or more tip vortices, and its effect on total induced circulation, is described by an interaction model similar to that used for biplanes. According to this model, the total circulation induced by an array of equally sized, equally angled vanes is obtained by adding the circulations of individual vanes, provided these are adjusted by an interaction coefficient λ, which is a function of vane spacing δ_n and vane dimensions H and L. It follows from this model that for a vane array to generate a coherent circulation downstream, vane spacing must be less than about two to three times vane height. When the spacing is two to three times the vane height, λ is of the order 0.9. If the spacing is larger, the vane array will generate a system of individual vortices and be less efficient. By incorporating the coefficient λ in the function f_v, the resulting stress distribution downstream from a vane array is obtained by summation of the stress distributions associated with the individual vanes in the array.

To sustain a certain induced circulation and induced bed shear stress downstream, the vane array must be repeated at intervals in the downstream direction. The distance between the arrays, δ_s, depends on the design objective, which must stipulate lower limits on induced stresses. Within a vane field consisting of equal-sized, equal-spaced vanes, the area averaged induced bed shear stresses are

$$\tau_{vn} = \frac{F_L \lambda \beta}{A_v}$$

and

$$\tau_{vs} = \frac{F_D \lambda \beta}{A_v}$$

in which $A_v = \delta_s \delta_n$; overbars indicate area averaging; and β = factor arising from averaging process (Wang 1990).

It follows that, if the vane field covers an area A and the total number of vanes is N, $A_v = A/N$.

Chapter -3

NUMERICAL MODELING AND FLOW SIMULATION STUDY

3.1 INTRODUCTION

Gandak, being one of the youngest river system with varied nature of drainage areas from snow peak mountains in Nepal to lower flood valley of the Northern Bihar and the complexity exuberated by high sediment yielding geological surfaces it has been a very formidable task to quantify all the embodied "fluvial-river-morphological characteristics" to explain the ever changing characteristics of the river. The high degree of braiding of the main channel, especially when it enters the Northern Bihar valley because of a steep valley gradient, and deforestation in upstream region in Nepal, the fall in the hydraulic competency due to braiding is reflected to sediment transportation and downstream aggradation. Due to very unstable hydraulic geometry, the changing river channel morphology in the spatial and temporal space hinders the formulation of idealised hydraulic models. Moreover, the researches and the literatures on braided channels are less compared to single channel in alluvium region. Due to high non linearity involved in the interdependencies of the hydrological – morphological and hydraulic parameters, majority of relationships developed relating hydrological and hydraulic parameters are empirical.

The river Gandak is one of the rivers which are well under the observation of different government offices in Bihar. The sediment discharges and flood discharges at certain locations have been continuingly recorded and the river cross sections surveyed. Still, the limitation in the human capacity, instrumentation, the ambience of the measurement and the risk involved since major region is densely forested, the actual data acquisition often remain off-set by errors. The importance of the information that could be derived from the analysis of the data is very high in the design, management and future risk and hazard strategies.

Taking in to account the situation as described above, the present study is a formative attempt to implement a flow simulation model HEC-RAS for the study reach. The algorithms established by the researchers /modellers in the various literatures advocate success of flow simulation model application depends on the size of the data covering wide patterns of phenomena .More the data

sets better is the results' reliability. In the assessment of the available data, data sorting, data generation supporting further analysis, modelling and deriving inferences HEC-RAS has been known to be robust. As the technique is a data driven model requiring gamut of data patterns representing the actual phenomena to accommodate all the possibilities within the patterns of independent and dependent variables.

In the near future, more work with more expertise on this line would be enhancing the dependability on the strength of the technique in the more complex analysis.

3.2 DATA SOURCES AND DATA TYPES

3.2.1 HYDROGRAPHIC DATA

Morpho-metric data: the reduced levels of the river cross-sections of post-monsoon period for the year 2010 have been collected in respect of all the pre-defined river cross-sections from the Bihar Rajya Pul Nigam Ltd., Government of Bihar, India.

Also survey data of reduced levels at different positions at around the river channel and adjacent area have been obtained from Bihar Rajya Pul Nigam Ltd., Government of Bihar, India.

3.2.2 DISCHARGE AND STAGE DATA

Discharge and stage data of the river Gandak, collected for various cross-sections from Central Water Commission (CWC), Bihar Rajya Pul Nigam Ltd. have constituted main data resource to the model implementation.

3.2.3. REMOTE SENSING DATA

IRS LISS III images of from a period of 1988 to 2010 are collected from United States Geological Survey (USGS). These satellite images are used to analysis the changing pattern of the channel at the vicinity of the bridge site.

Table: 3.1 Digital satellite image used

S.No	Satellite	Sensor	Image acquisition Year
1	IRS	LISS III	1988
2	IRS	LISS III	2001
3	IRS	LISS III	2006
4	IRS	LISS III	2010

3.2.4 SEDIMENT DATA

Sediment data obtained from the monthly suspended sediment data in respect of the upstream cs-29 and average monthly discharge (cumecs) has been used in the study. Characteristic sediment particle size distribution at the cross-sections was collected from Bihar Rajya Pul Nigam Ltd., after they have obtained the sample and conducted particle size analysis.

3.3 PRE- PROCESSING OF HYDRO GRAPHIC DATA

As a certain degree of uncertainty is associated with hydrologic frequency distributions on relative time scales, the sensitive response function of the river / stream as Stage - Discharge (G-Q) relationships , Sediment discharge Rating (Q_t –Q) curves, Stream flow Hydrographs, etc needs to adequately represented from the observed field data. The Gandak River Basin in terms of its complexity calls for well-defined response models. In the study, some of the significant steps followed are outlined as:

(i) The first step is the abstraction of outliers and errors in the data sets. Conceptual or statistical tools as regression and curve fitting were implemented on the variables pertaining to specific river / stream to identify the irrational points; they were either discarded or rectified based on the earlier trends or pattern of the data.

(ii) The datasets are then sorted strictly on a base time scale. Monthly average record data sets pertaining to the main river are chosen for the study, the period between December 2009 and December 2010 has been adopted as the base time scale for the framing of the channel response parameters and the model formulation.

3.4 DEVELOPMENT OF FLOW SIMULATION MODEL IN 'HEC-RAS'

The system contains three one-dimensional hydraulic analysis components for: (1) steady flow water surface profile computations; (2) unsteady flow simulation; and (3) movable boundary sediment transport computations. A key element is that all three components will use a common geometric data representation and common geometric and hydraulic computation routines. In addition to the three hydraulic analysis components, the system contains several hydraulic design features that can be invoked once the basic water surface profiles are computed.

HEC-RAS is designed to perform one-dimensional hydraulic calculations for a full network of natural and constructed channels. Theoretical basis for one-dimensional calculation in HECRAS is briefed in chapter-2.

3.4.1 DATA REQUIREMENTS AND INPUT

The basic input data required for sedimentation analysis by HEC-RAS model can be grouped into four categories as below.

3.4.1.1 GEOMETRIC DATA

Geometry of the physical system is represented by cross sections, specified by coordinate points (stations and elevations), and the distance between cross sections. Hydraulic roughness is measured by Manning's n-values and can vary from cross section to cross section. At each cross section n-values may vary vertically and horizontally. The program raises or lowers cross-section elevations to reflect deposition or scour and thus generates data during the course of its execution.

THE RIVER SYSTEM SCHEMATIC

The river system schematic is required for any geometric data set within the HEC-RAS system. The schematic defines how the various river reaches are connected, as well as establishing a naming convention for referencing all the other data. The river system schematic is developed by drawing and connecting the various reaches of the system within the geometric data editor (Fig: 3.1). Another way, it can also be imported from geographically referenced images with the help of HECGEO-RAS extension for ARCGIS. Each river reach on the schematic is given a unique identifier. As other data are entered, the data are referenced to a specific reach of the schematic. Here the data is extracted from IRS- 1C LISS III satellite image of the area.

Each river reach on the schematic is given a unique identifier. As other data are entered, the data are referenced to a specific reach of the schematic. For example, each cross section must have a "River", "Reach" and "River Station" identifier. The river and reach identifiers defines which reach the cross section lives in, while the river station identifier defines where that cross section is located within the reach, with respect to the other cross sections for that reach.

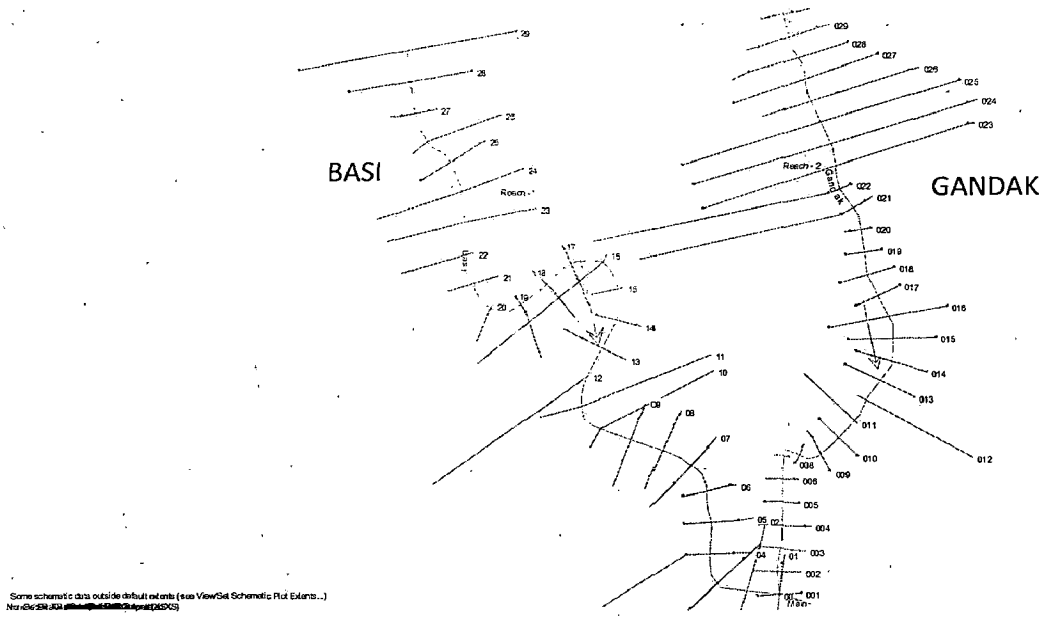

Fig: 3.1 Schematic Plot of the Study Reach of Basi (Left Stream of Gandak) River in the Program Module

The connectivity of reaches is very important in order for the model to understand how the computations should proceed from one reach to the next. It is required to draw each reach from upstream to downstream, in what is considered to be the positive flow direction.

CROSS SECTION GEOMETRY

Boundary geometry for the analysis of flow in natural streams is specified in terms of ground surface profiles (cross sections) and the measured distances between them (reach lengths). Cross sections are located at intervals along a stream to characterize the flow carrying capability of the stream and its adjacent floodplain. They should extend across the entire floodplain and should be perpendicular to the anticipated flow lines. Occasionally it is necessary to layout cross-sections in a curved or dog-leg alignment to meet this requirement. Every effort should be made to obtain cross sections that accurately represent the stream and floodplain geometry.

Cross sections are required at representative locations throughout a stream reach and at locations where changes occur in discharge, slope, shape, or roughness, at locations where levees begin or

end and at bridges or control structures such as weirs. Where abrupt changes occur, several cross sections should be used to describe the change regardless of the distance. Cross section spacing is also a function of stream size, slope, and the uniformity of cross section shape. In general, large uniform rivers of flat slope normally require the fewest number of cross sections per km. The purpose of the study also affects spacing of cross sections. For instance, navigation studies on large relatively flat streams may require closely spaced (e.g., 200 feet) cross sections to analyze the effect of local conditions on low flow depths, whereas cross sections for sedimentation studies, to determine deposition in reservoirs, may be spaced at intervals on the order of km.

Each cross section in an HEC-RAS data set is identified by a River, Reach, and River Station label. The cross section is described by entering the station and elevation (X-Y data) from left to right, with respect to looking in the downstream direction. The River Station identifier may correspond to stationing along the channel, mile points, or any fictitious numbering system. The numbering system must be consistent, in that the program assumes that higher numbers are upstream and lower numbers are downstream.

Each data point in the cross section is given a station number corresponding to the horizontal distance from a starting point on the left. Up to 500 data points may be used to describe each cross section. Cross section data are traditionally defined looking in the downstream direction. The program considers the left side of the stream to have the lowest station numbers and the right side to have the highest. Cross section data are allowed to have negative stationing values. Stationing must be entered from left to right in increasing order. However, more than one point can have the same stationing value. The left and right stations separating the main channel from the over bank areas must be specified on the cross section data editor. End points of a cross section that are too low (below the computed water surface elevation) will automatically be extended vertically and a note indicating that the cross section had to be extended will show up in the output for that section. The program adds additional wetted perimeter for any water that comes into contact with the extended walls.

Other data that are required for each cross section consist of downstream reach lengths; roughness coefficients; and contraction and expansion coefficients. These data are discussed in detail here in this chapter. Numerous program options are available to allow easily adding or modifying cross section data.

REACH LENGTHS

The measured distances between cross sections are referred to as reach lengths. The reach lengths for the left over bank, right over bank and channel are specified on the cross section data editor. Channel reach lengths are typically measured along the thalweg. Over bank reach lengths should be measured along the anticipated path of the center of mass of the over bank flow. Often, these three lengths will be of similar value. There are, however, conditions where they will differ significantly, such as at river bends, or where the channel meanders and the over banks are straight. Where the distances between cross sections for channel and over banks are different, a discharge-weighted reach length is determined based on the discharges in the main channel and left and right over bank segments of the reach. In the selected reach of Gandak, all three lengths are mostly dissimilar as the river is meandering at multiple points.

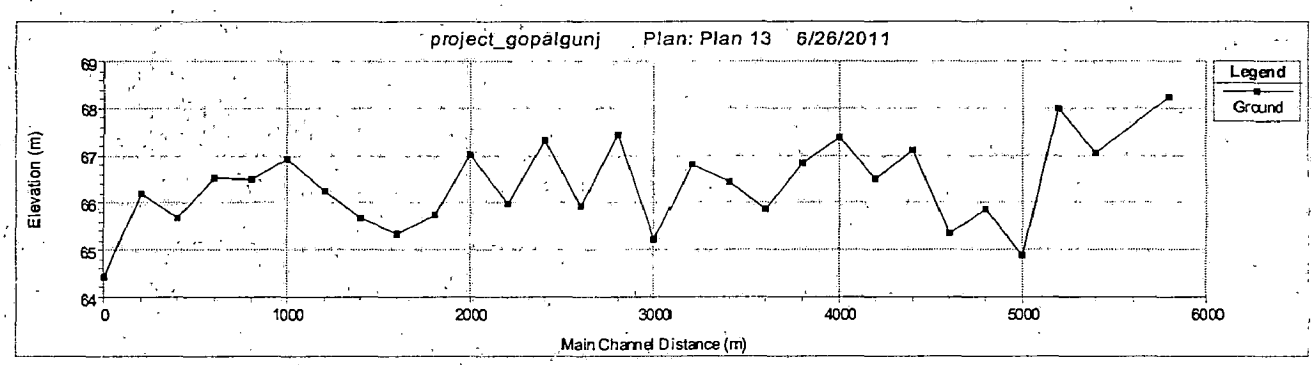

Fig: 3.2 Deepest Bed Level of Study Reach (BASI)

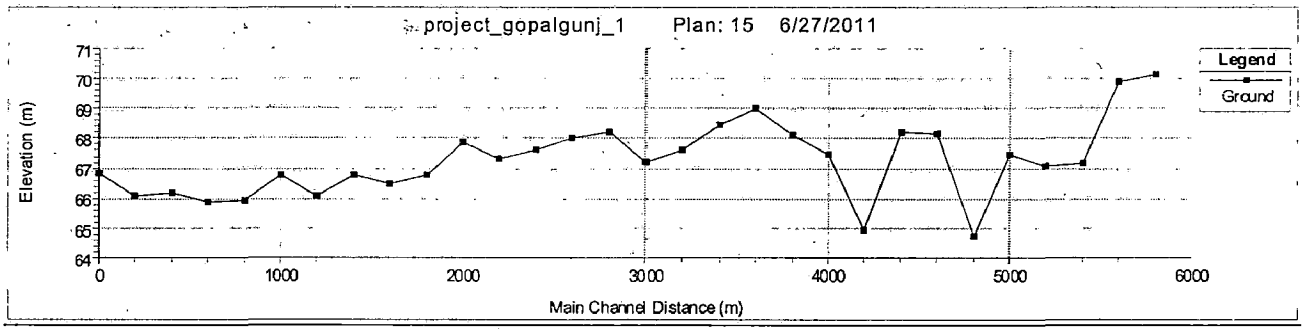

Fig: 3.3 Deepest Bed Level of Study Reach (GANDAK)

ENERGY LOSS COEFFICIENTS

Several types of loss coefficients are utilized by the program to evaluate energy losses: (1) Manning's n values or equivalent roughness "k" values for friction loss, (2) contraction and expansion coefficients to evaluate transition (shock) losses.

Manning's n: Selection of an appropriate value for Manning's n is very significant to the accuracy of the computed water surface profiles. The value of Manning's n is highly variable and depends on a number of factors including: surface roughness; vegetation; channel irregularities; channel alignment; scour and deposition; obstructions; size and shape of the channel; stage and discharge; seasonal changes; temperature; and suspended material and bed load.

In general, Manning's n values should be calibrated whenever observed water surface profile information (gage data, as well as high water marks) is available. As water surface profile information is adequately available for the study reach, so Manning's n values were calibrated in fixed bed module with spatial as well as based on discharge variation and values fed into sediment module of flow simulation for further analysis.

There is a difference in Manning's n between fixed and movable bed situations. Fixed bed n's are values which do not depend on the characteristics of the movable boundary, movable bed n's are values which may depend on the rate of sediment transport and, hence, the discharge. Appropriate values for Manning's n were initially determined by executing HEC-RAS in fixed bed mode, i.e., as a step-backwater program. This is necessary to properly compare calculated water surface elevations with observed water surface profiles, with established rating curves, during the analysis of geometric data and calibration of n values, many program executions were required. Study

reach has been subdivided into separate segments, cross-section were interpolated to appropriate numbers and program is executed for different value of n until computed water surface profiles at approximately matched with observed ones. Finally, calibrated n with discharge variation and spatial variation obtained.

Changing n values with distance should be justified based on changes in vegetation, channel form, structures, or sediment size. The technique assumes that the entire bed of the river is stationary and does not move or change roughness during a flood event. Before focusing on sediment transport, however, Manning's n value for the channel is appropriate for a movable boundary analyzed and whatever required minor adjustments, were made to ensure that the n value for the movable portion of the cross section is in reasonable agreement with that obtained from bed roughness predictors.

SELECTION OF CONTRACTION AND EXPANSION COEFFICIENTS

Information for contraction and expansion losses is sparser than that for n values. King and Brater (1963) give values of 0.5 and 1.0 respectively for a sudden change in area accompanied by sharp corners, and values of 0.05 and 0.10 for the most efficient transitions. Design values of 0.1 and 0.2 are suggested. They cite Hinds (1928) as their reference. Values often cited by the Corps of Engineers (HEC, 1990a) are 0.1 and 0.3, contraction and expansion respectively, for gradual transitions .So in the present study, contraction and expansion coefficient are by default taken as 0.1 and 0.30.

3.4.1.2 HYDROLOGIC DATA

The hydrologic data consist of water discharges, temperatures and flow durations. The discharge hydrograph is approximated by a sequence of steady inflow discharges each of which occurs for a specified numbers of days. Water surface profiles are calculated by using the standard step method to solve the energy equation. Friction loss is calculated by Manning's equation, and

expansion and contraction losses will be included if the representative loss coefficients are specified.

STEADY FLOW DATA

Steady flow data were required in order to perform a steady water surface profile calculation and consequently calibration of 'n' worked out. Steady flow data consist of flow regime, boundary conditions and discharge information.

Boundary conditions are necessary to establish the water surface at the ends of the river system (upstream and downstream). A starting water surface is necessary in order for the program to begin the calculations. In a sub critical flow regime, boundary conditions are only necessary at the downstream ends of the river system. If a supercritical flow regime is going to be calculated, boundary conditions are only necessary at the upstream ends of the river system. If a mixed flow regime calculation is going to be made, then boundary conditions must be entered at all ends of the river system. Observed monthly flow profile were fed as input in different cross-section segmental reach and program were run separately to compute water surface elevation at d/s and compared with observed one to estimate n .

QUASI-UNSTEADY FLOW DATA

Current sediment capabilities in HEC-RAS are based on quasi-unsteady hydraulics. The quasi-unsteady approach approximates a flow hydrograph by a series of steady flow profiles associated with corresponding flow durations. Boundary conditions were flow series (flow hydrograph) at upstream boundary (c/s-29) for Basi river reach and (c/s-30) for Gandak river reach. At downstream boundary at (c/s-1) for Basi reach and (c/s-1) for Gandak reach, stage time series /rating curve applied. The stage -time series boundary condition allows inputting a time series of stages at the downstream boundary.

As sensitive inputs to the Model boundary values, the Stage-Discharge relations, the G-Q relations of the major rivers/ streams under consideration needs to sufficiently dictate the hydraulic behaviour.

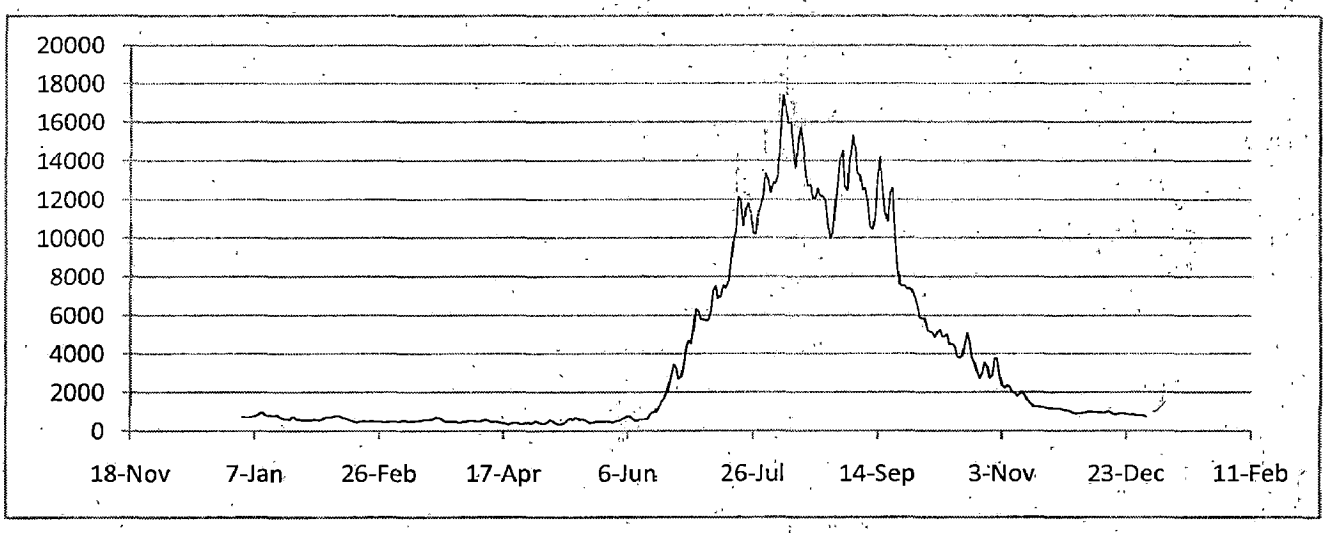

Fig 3.4 Simulation Hydrograph at c/s-29 (Basi Reach)

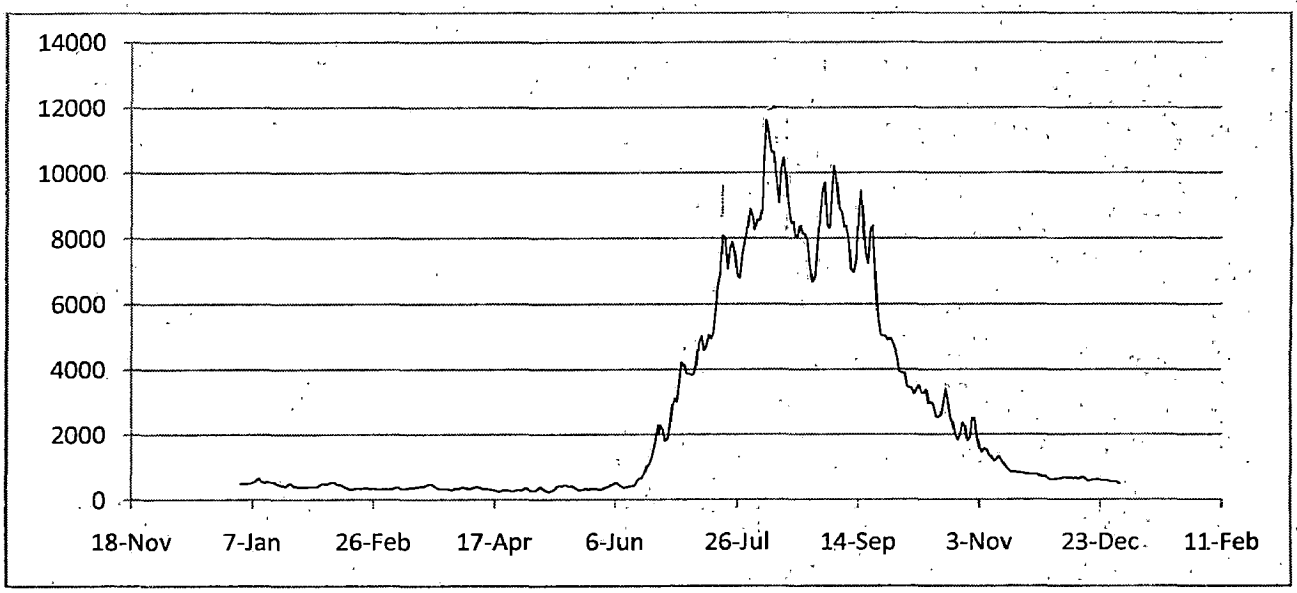

Fig 3.5 Simulation Hydrograph at c/s-30 (Gandak Reach)

Stage-Discharge Relation at extreme d/s boundary of reach which contains combined flow is plotted in Fig: 3.6, similarly Discharge hydrograph at extreme u/s boundary is also plotted in Fig 3.4 and Fig 3.5 for the reaches Basi and Gandak respectively, which has also been taken as inputs for simulating flow for specific period.

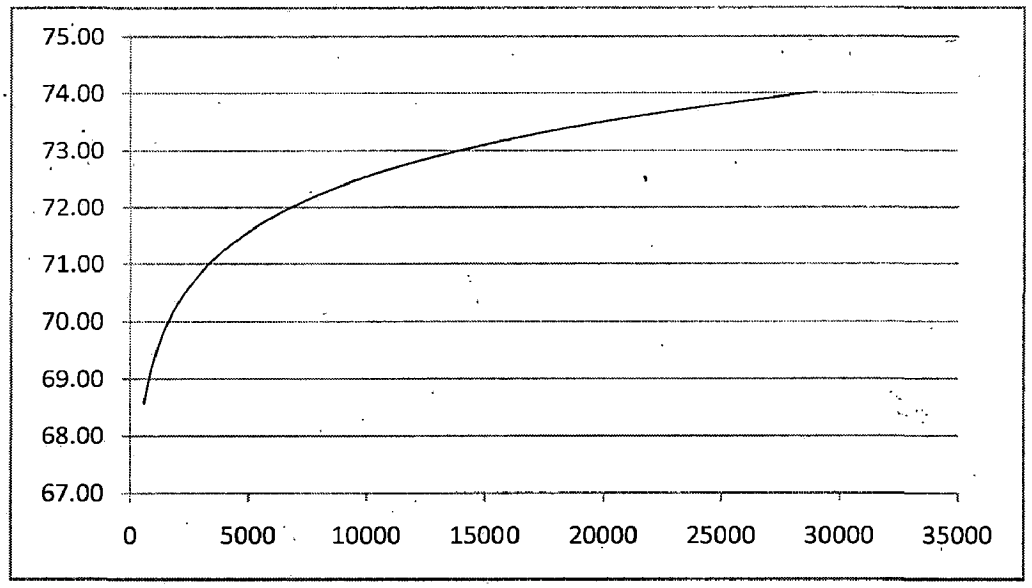

Fig: 3.6 Stage – Discharge Relation at extreme downstream c/s

3.4.1.3 SEDIMENT DATA

The sediment data consist of inflowing sediment load data, gradation of material in the stream bed and information about sediment properties. The inflowing sediment load is related to water discharge by a rating table at the upstream end of the model.

Sediment mixtures are classified by grain size using the American Geophysical union scale. The program accommodates clay (up to 0.004 mm), four classes of silt (0.004 – 0.0625 mm), five classes of sand (very fine sand 0.0625 mm to very course sand 0.2 mm) and five classes of gravel (very fine gravel 0.2mm to very coarse gravel 0.64mm).Sediment transport capacity is calculated at each cross section by using hydraulic data obtained during the calculation of water surface profiles and the gradation of bed material for that cross section.

The variations in the sediment load discharge with the flow is calibrated from the Sediment Discharge Rating Curves and entered to the model input.

Each cross-section must have an associated bed gradation. Possession of data in regard to bed material for all cross section couldn't be done. But character of bed material within the study reach can presumed to be similar in nature so far sediment transport is concerned. Bed material gradation between cross sections -29 and 28 of Basi reach is taken as representative bed gradation (Fig: 3.7) throughout the alluvial study reach.

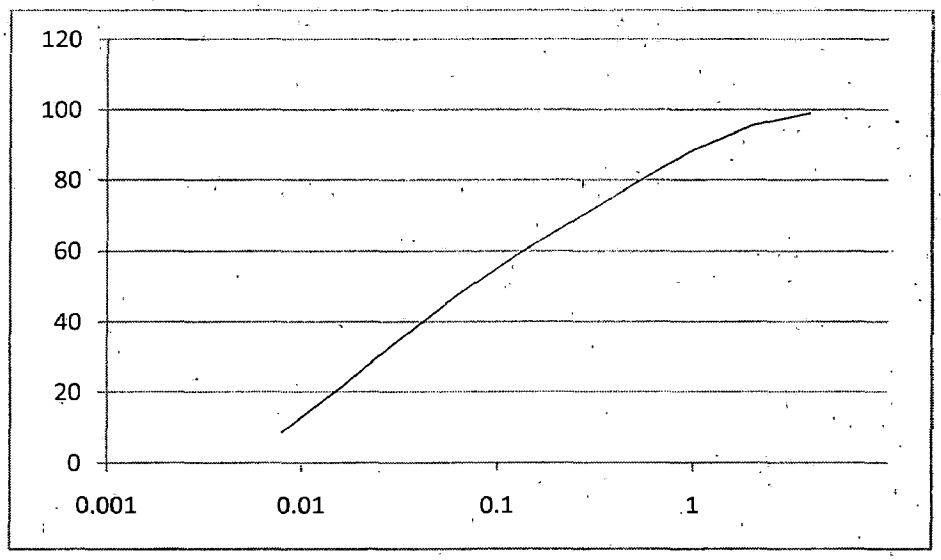

Fig: 3.7 Representative Bed Gradation (semi-log) Plot of the Study Reach

SEDIMENT BOUNDARY CONDITIONS

For sediment transport analysis sediment boundary conditions must be applied. Usually boundary conditions are applied at extreme u/s and d/s cross sections .Internal boundary conditions were applied where flow change is occurring i.e. where tributaries are meeting the main stream. In model formulated sediment rating curves were applied for simulating sediment transport. Sediment rating curve at c/s-29 of Basi reach is plotted and depicted in Figs. 3.8. (Sediment inflow in y axis and discharge in x axis). A rating curve determines a sediment inflow based on water flow.

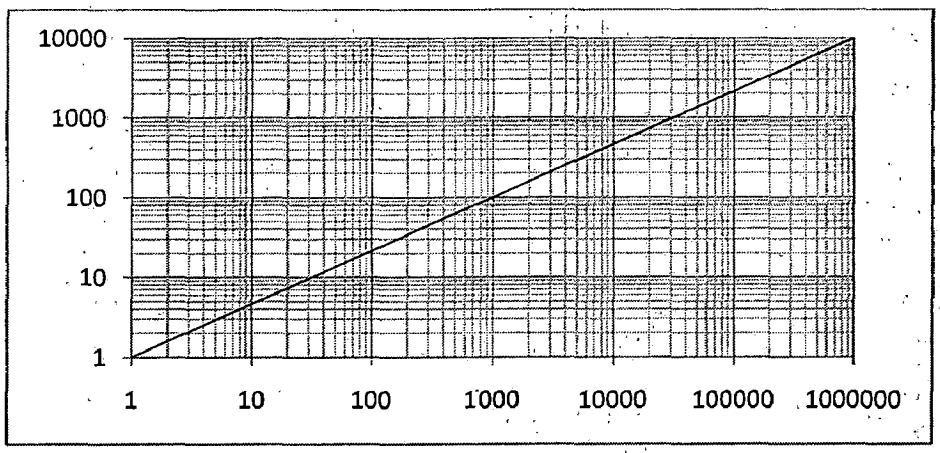

Fig: 3.8 Sediment Rating Curve

Besides the hydrologic data, sediment data and roughness coefficients, other bound values accorded are the depth of sediment bed control volume (adopted as 5.0 meter wherever necessary) and the water temperature. The sensitivity of the variation in water temperature (^{0}C) over the sediment transport rates and water surface is also simulated as presented in the result summary tables. Average monthly variation of temperature as per field data (Based on average. Temperature record in Gopalgunj) is adopted (Table 4.2) for the study.

Table 3.2 Average Monthly Temperature Variations

Month	Avg. Temp	Month	Avg. Temp
January	19.03	July	39.22
February	22.52	August	36.12
March	28.20	September	33.07
April	36.00	October	29.72
May	39.47	November	25.09
June	41.92	December	20.52

3.4.2 PROGRAM ORGANISATION

The HEC-RAS program in its present form has been organized into two major modules. Modules run with various sub-programs where data have been transferred for specific output generation. The functional flowchart of the program is shown in Fig. 4.15.

3.4.2.1 HYDRODYNAMIC MODELING AND CALIBRATION OF 'N'

Roughness Coefficients

Roughness coefficients are one of the main variables used in calibrating a hydraulic model. Generally, for a free flowing river, roughness decreases with increased stage and flow However, if the banks of a river are rougher than the channel bottom (due to trees and brushes), then the composite n value will increase with increased stage. Sediment and debris can also play an

important role in changing the roughness. More sediment and debris in a river will require the modeler to use higher n values in order to match observed water surfaces.

3.4.2.2 SEDIMENT TRANSPORT ANALYSIS (QUASI-UNSTEADY FLOW ANALYSIS)

The outputs obtained from first module were to be applied in this module for calibration and testing of the model. Calibrated value of roughness parameter n from first module gave the idea of n and its relation with discharge and also its variation with distance. With slight processing the calibrated set of Manning's n were fed into sediment module. In this module the whole study reach were taken as geometric data. The study has been conducted in two parts, for Basi and Gandak reach Some intermediate cross-sections were linearly interpolated to assure stability to running of the module.

Other sediment data like representative bed gradation at each cross-section /sediment inflow at u/s locations as well as flow change locations were fed into the module. Flow series at u/s boundary and lateral flow series at internal boundaries as well as stage series at d/s is fed into the module. Simulation plans for varying sediment predictors as well as different time series were designated and executed and outputs were obtained. A detailed discussion on outputs will be done later.

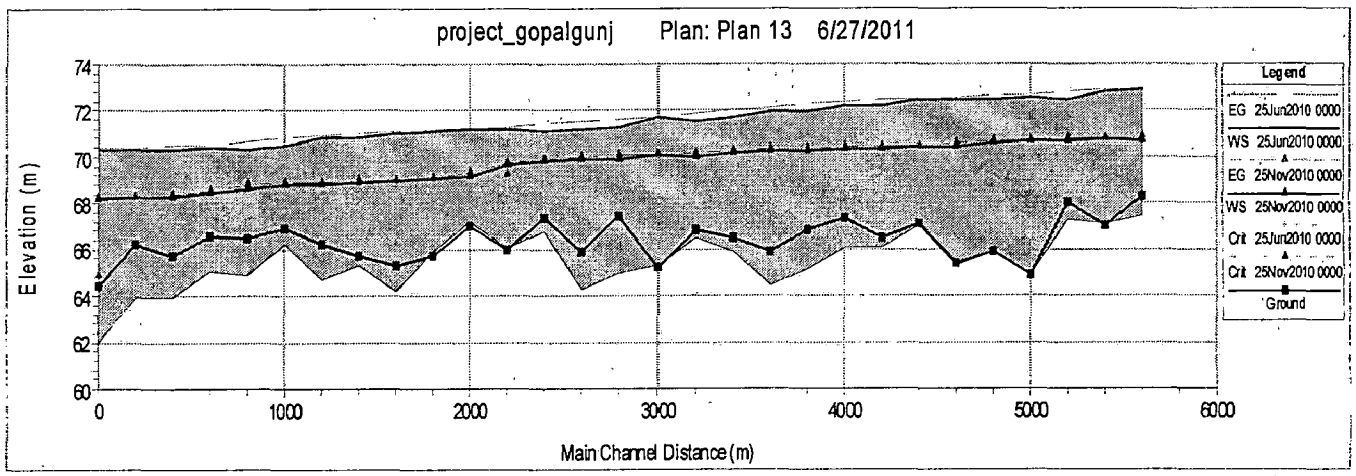

Fig 3.9 Sediment Transport Analysis and Prediction of Bed Profile for 25 June 2010 and 25 November 2010 for Basi Reach

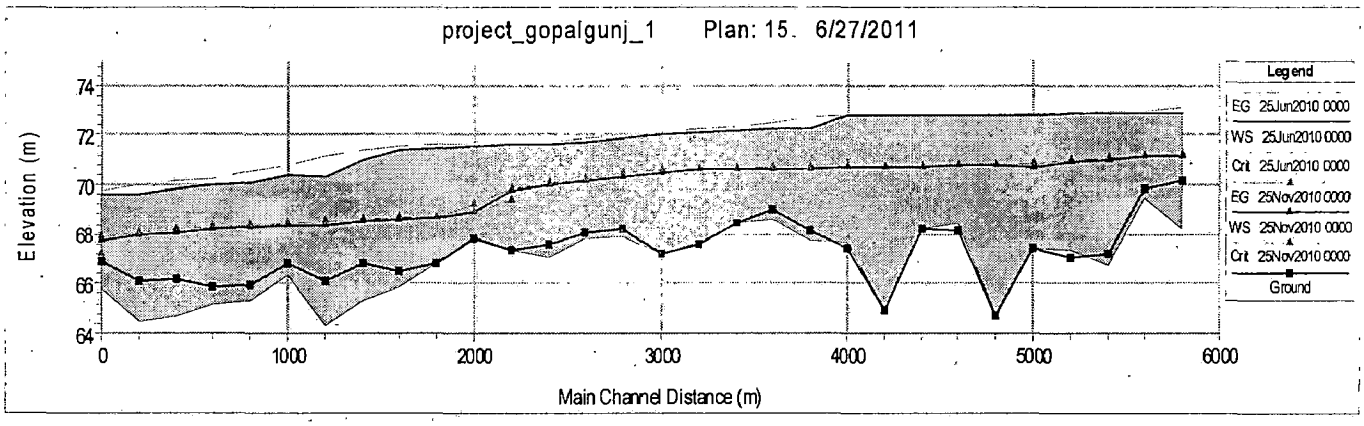

Fig 3.10 Sediment Transport Analysis and Prediction of Bed Profile for 25 June 2010 and 25 November 2010 for Gandak Reach

Chapter -4

PHYSICAL MODELING AND FLOW SIMULATION STUDY

4.1 INTRODUCTION

Three categories of methods for predicting river hydraulic conditions were identified by Rouse (1959). The first and oldest uses engineering experience acquired from previous practice by an individual. The second utilizes laboratory scale models (physical models) to replicate river hydraulic situations at a specific site or for general types of structures. Laboratory modeling has been in extensive and successful use for at least the past 60 years. The third category is application of analytical (mathematical) procedures and numerical modeling. Recent use of physical and numerical modeling in combination, guided by engineering experience, is termed "hybrid modeling" and has been very successful.

The most thorough contemporary strategy for analyzing and predicting river behavior and response to imposed changes combines all three of the methods mentioned above; this is known as hybrid modelling.

Hybrid modeling is attempted in the Gandak River study. One dimensional HECRAS 4.1 model and PHYSICAL MODEL is used. The study is supplemented by the application of satellite based spatio-temporal variation of channel migration in the vicinity of study area.

4.2 DATA SOURCES AND DATA TYPES

4.2.1 HYDROGRAPHIC DATA

Morpho-metric data: the reduced levels of the river cross-sections of post-monsoon period for the year 2010 have been collected in respect of all the pre-defined river cross-sections from the Bihar Rajya Pul Nigam Ltd., Government of Bihar, India.

Also survey data of reduced levels at different positions at around the river channel and adjacent area have been obtained from Bihar Rajya Pul Nigam Ltd., Government of Bihar, India.

4.2.2 DISCHARGE AND STAGE DATA

Discharge and stage data of the river Gandak, collected for various cross-sections from Central Water Commission (CWC), Bihar Rajya Pul Nigam Ltd. have constituted main data resource to the model implementation.

4.2.3. REMOTE SENSING DATA

IRS LISS III images of from a period of 1988 to 2010 are collected from United States Geological Survey (USGS). These satellite images are used to analysis the changing pattern of the channel at the vicinity of the bridge site.

Table: 4.1 Digital satellite image used

S.No	Satellite	Sensor	Image acquisition Year
1	IRS	LISS III	1988
2	IRS	LISS III	2001
3	IRS	LISS III	2006
4	IRS	LISS III	2010

4.2.4 SEDIMENT DATA

Sediment data obtained from the monthly suspended sediment data in respect of the upstream cs-29 and average monthly discharge (cumecs) has been used in the study. Characteristic sediment particle size distribution at the cross-sections was collected from Bihar Rajya Pul Nigam Ltd., after they have obtained the sample and conducted particle size analysis.

4.3. PHYSICAL MODEL DEVELOPMENT

Main purpose of this physical model design is to understand the scour and deposition effects, due to sediment transport, for design and nominal discharge at the bridge construction site on Gandak River. For this particular kind of study movable-bed type models are recommended (Peterson 1986, Julian 2002).

The model is constructed at outfield lab of WRDM. To fix the model bed level for initial condition, survey conducted in 2010 is used. Other model parameters are determined based on design discharge, availability of space and personal field experience. The model is constructed to represent about 8.5km in total upstream and downstream of the bridge site in the river direction. The model is also supplemented by steady and quasi steady analysis of one dimensional numerical model (conducted on previous chapter) and river channel change pattern based on historical satellite images.

Procedure for determination of scale for the model is followed from Julian (2002). To model 8.5km of the river reach with available space a longitudinal scale of 1 to 400 is used. According Julian (2002), if Shields parameter of the prototype is greater than 0.06, there is sediment transport.

Table: 4.2 Physical Model Parameters

Parameter	Value	Comment
ds	0.08 mm	Approximate value
Average slope	0.0003	
Maximum depth of flow (h)	8.33 m	At bridge site
Longitudinal scale	1/400	Governed by space
Sediment specific gravity	2.65	

$\tau_{*p} = \frac{h_p S_p}{(G-1)_p d_{sp}} = 18.93 > 0.06$, hence the use of mobile-bed model is justified. As discussed in Chapter two, there are two options of mobile-bed model. Complete and incomplete mobile bed similitude. Other parameters of the model are calculated in the assumption of complete mobile bed calculation procedures based on Julian (2002). The value of m is given as

$m = [1/(\ln 12.2\frac{h}{d_s})] = 0.071$

Table: 4.3 Model scale ratio parameters

Parameter	Equation Complete/ Incomplete	Calculated	Adopted
Depth	z_r		50
Width	y_r		400
Length	$z_r^{(1+4m)/(1+m)}$	108.85	
	$z_r^2 d_{sr}^2$	2500	
Particle diameter	$z_r^{(2m-1)/(2+2m)}$	0.209	3.252
	d_{sr}	1	
Velocity	$z_r^{1/2}$	7.07	
	$z_r^m d_{sr}^{-1-m}$	1.32	
Shear velocity	$z_r^{(1-2m)/(2+2m)}$	4.79	
	d_{sr}^{-1}	1	
Settling velocity	$z_r^{(1-2m)/(2+2m)}$	4.79	
	d_{sr}^{-1}	1	
Discharge	$y_r z_r^{1.5}$	141421.4	
	$y_r z_r^{1+m} d_{sr}^{-1-m}$	26403.22	
Time (flow)	$z_r^{(1+7m)/(2+2m)}$	15.4	
	$z_r^{2-m} d_{sr}^{3+m}$	1893.71	
Time (bed)	$z_r^{(2+5m)/(1+m)}$	5442.9	
	$z_r^3 d_{sr}^2$	125000	
Froude	1	0.186	0.186
	$z_r^{m-0.5} d_{sr}^{-1-m}$		
Slope	$z_r^{(-3m)/(1+m)}$	0.46	1
	$z_r^{-1} d_{sr}^{-2}$	0.02	
Reynolds	$z_r^{3/2}$	353.55	353.55
	1		
Sediment density $(G-1)_r$	$z_r^{(3-6m)/(2+2m)}$	110.06	1
	d_{sr}^{-3}	1	

Based on the calculated model scale ratios it is impossible to attain complete mobile bed similitude. For example sediment density ratio of 96 will imply that for model sediment specific gravity of 1.02. Even less than polystyrene which has specific gravity of 1.036 and this necessitates to resorting to incomplete mobile bed similitude. Because the conditions for complete similitude are not practically possible, some constraints are sacrificed in order to benefit from an additional degree of freedom in adopting scale factors. And also at the site there is no available material that can be used for complete mobile bed similitude.

One option of incomplete mobile bed similitude is the use of non-Froudian models, Julian (2002), i.e. it is possible to use different values of the Froude number for the model and the prototype as long as the flow remains subcritical in both systems. When the same density of sediment is used, the similitude in dimensionless particle diameter d^* implies that $(G-1)_r = 1/ d_{sr}^3$; thus the sediment must have the same density and particle diameter. In this case Froude number is $F_r = z_r^{m-0.5} d_{sr}^{-1-m}$. This type of model allows the use of the same sediment in the model and the prototype.

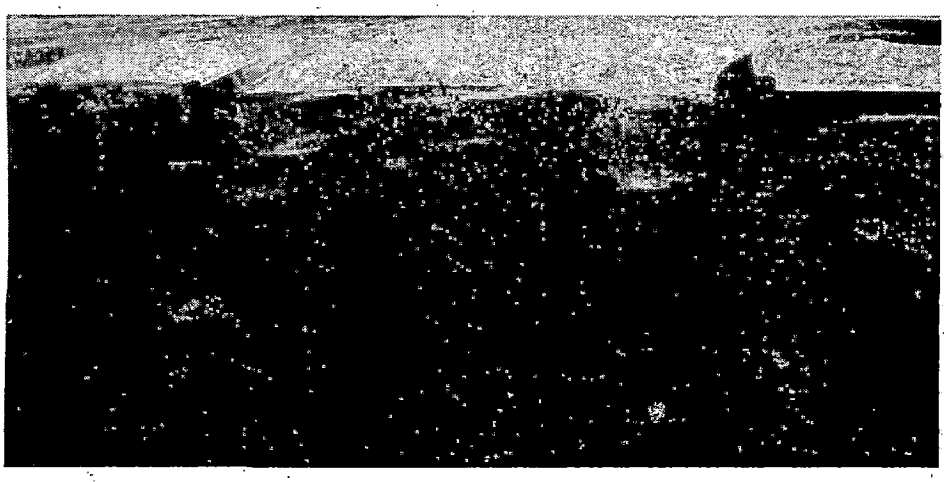

Fig: 4.1
Constructed Model

Fig: 4.2
Test Run

Fig: 4.3
Water Level Gauge

4.4. RESULTS AND DISCUSSIONS

4.4.1. GENERAL

The satellite images shows that the river is constantly changing and in lights of that the physical model was run to assess the impact of having one river channel on the bridge guide bank. The model is run for two scenarios, one with clear water scenarios and the other for sediment concentration of 2000 ppm. Model dimension of 25m by 12m .With clear water simulation the model is verified against observed stage and discharge. In the verification stage, there were noticeable erosion and disposition phenomenon. The clear water erodes the bed from the upstream section and deposits them at back side of left guide bank.

12kg of sediment is fed each minute for 20 minute to represent 8 hrs of flow in the prototype. After the simulation is over the bed change is surveyed for both clear water simulation experiment and sediment fed experiment. Three bed levels are compared and the results are plotted below.

4.4.2. SCOUR AND DEPOSITION

Local sour of alluvial river bed around obstructions such as abutments and guide banks is ever existing problem and continuing interest to many researchers. The complex three-dimensional flow and sediment transport around such structures have defied an analytical solution to the problem and its is not the scope of this study to investigate them, rather it is to determine the locations where local scour as well as deposition has occurred and to identify appropriate measure to safe guard the structure.

Observations show that deposition is occurring in the middle of the channel between the abutments and erosion and scouring is taking place at the toe of the guide bank. And it is also observed that the left guide bank is under more attack due to the secondary flow generated at the upstream section of the guide bank.

A closer look at the model indicates occurrence of deposition along the inner section of the guide bank and subsequent erosion and deposition at the central portion of the channel. In successive chapters an appropriate design will be suggested for addressing the problem.

RESULTS AND DISCUSSIONS OF FLOW SIMULATION STUDIES

5.1 INTRODUCTION

This chapter is focused on the results of the flow simulation studies conducted by HECRAS 4.0 regarding steady and quasi-steady flow analysis generating a quantitative measurement of the sediment transport in the river system around the study area. The inputs and the procedural steps are mentioned in chapter 3.

5.2 HYDRODYNAMIC MODELING AND CALIBRATION OF 'N'

Study Reach Length (5.6 km) of Basi Reach was sub divided into 28 segments each of the segment comprised of two cross-section like c/s 1 to c/s 2, then c/s 2 to c/s 3 and so on, considering bed profile of the reach as in 2010, constant discharge at upstream and observed water surface level at d/s of the reach, the hydrodynamic model is run for steady flow. Initial value of Manning's is taken 0.033. The computed water surface profile is compared with the observed ones for the best matching of the profile; the value of n is chosen.

Such computation is done for all the monthly discharges of year 2010 and correspondingly the value of n is assessed.

Segment-wise assessed Manning's values for the year 2010 are plotted in Fig: 5.1. The reach selected for study is situated in lower reach of Gandak.

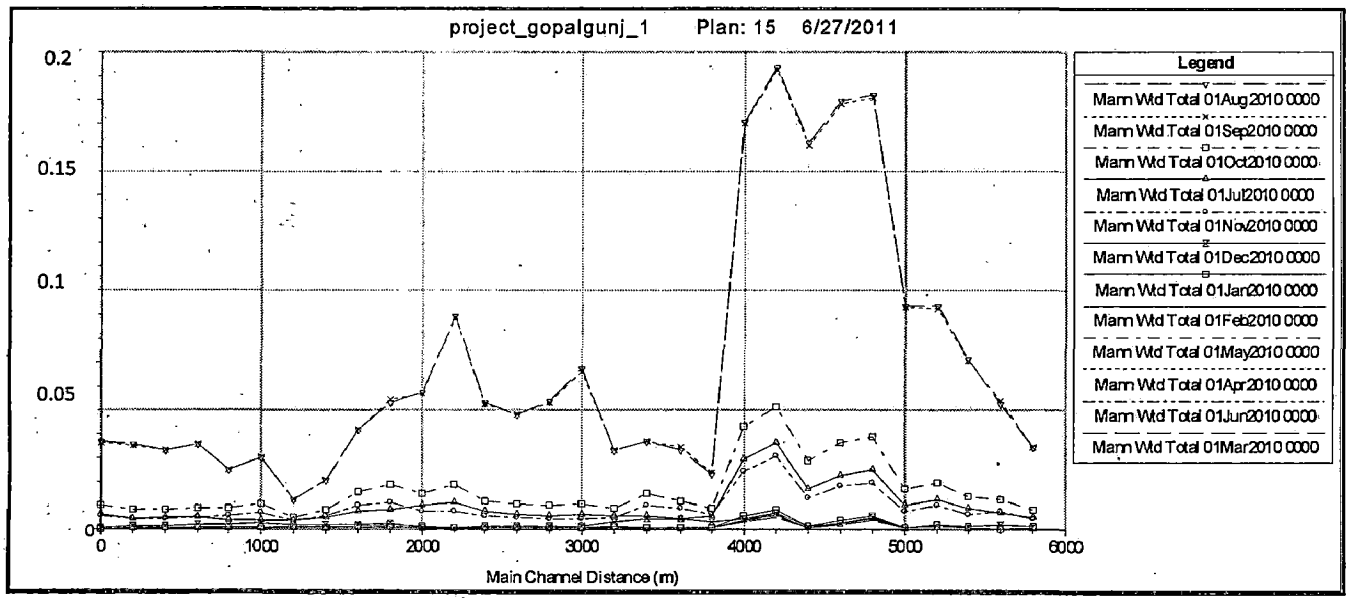

Fig: 5.1 Spatial Variation of Manning's n (Year 2010) in the Study Reach

If one analyze Fig: 5.1 which give the n variation with discharge for year 2010, one can easily figure out that with increasing discharge, there is an increase in Manning's n, which advocates the theory of bed form changes from ripples to dunes, which is supported by the fact that dunes are formed in alluvial channels at Froude Numbers much less than unity. Moreover increase in roughness with discharges in different segment also varies. Also in some segmental reaches n variation with discharges are minimal which implies that these sections are less prone to bed form changes and roughness mainly depends on grain roughness. It also gives the idea that bed in these segmental reaches is somehow coarse in nature. So in some areas shoal formations may be possible due to high discharge while some areas remain unaffected.

5.3 SEDIMENT TRANSPORT ANALYSIS/BED VARIATION ANALYSIS

In this module, designed roughness parameter along with various sediment parameters were selected and fed into the formulated quasi-unsteady flow model of HEC-RAS. Various input parameters like bed gradation for the study reach, sediment rating curve as boundary conditions at u/s and d/s boundary as well as flow change locations, gradation of suspended sediment were appropriately fed into the module as sediment data. Sediment transport parameters like transport functions, maximum erodable depth, fall velocity method, sorting method were appropriately selected. For this module maximum erodable depth is taken 5.0 meter wherever necessary. Fall velocity method selected is Ruby and Exner is selected as sorting method. Transport functions selected were Yang, Acker-White and Engelund-Hansen for running different modules for prediction of thalweg changes. Modules were run and corresponding outputs for bed variation for the period 2010 were analyzed for in-depth examination of thalweg changes. For the Study Reaches, three sediment predictors were used to predict the changes in bed during the simulation time.

5.3.1 ACKER- WHITE SEDIMENT MODULE FOR BED PROFILE FORCASTING

In this Module, Acker-White sediment transport function is applied for the prediction of bed profile for the period 2010 in the stretch keeping the base month as January. Model is run for the u/s inflow hydrograph and sediment inflow for twelve months with d/s boundary conditions observed water surface profile and initial condition as in January 2010 for the two reaches. Monthly bed profile prediction were computed and presented in tabular form in Table 5.1. and 5.2 for Basi and Gandak reaches respectively.

Figures 5.2 and 5.3 shows the monthly predicted profile using Acker-White Predictor, for the reaches Basi and Gandak respectfully. Fig: 5.2 and 5.3 depicts that there is significant aggrading tendency throughout the reach.

Table: 5.1 Monthly Predicted Profile Using Acker-White Predictor for the Reach Basi

S No.	Reach Station	Channel Distance	Bed Profile (m)											
			JAN	FEB	MAR	APR	MAY	JUN	JUL	AUG	SEP	OCT	NOV	DEC
1	29.0	200.0	68.2	67.6	67.6	67.5	67.5	67.5	67.5	67.5	67.5	67.5	67.5	67.4
2	28.0	200.0	67.0	67.1	67.1	67.1	67.1	67.1	67.0	66.8	66.6	66.3	66.1	66.1
3	27.0	200.0	68.0	67.3	67.3	67.3	67.3	67.3	67.2	65.7	65.5	65.5	65.5	65.5
4	26.0	200.0	64.9	64.9	64.9	64.9	64.9	64.9	64.9	64.9	64.9	63.6	63.6	63.6
5	25.0	200.0	65.9	65.9	65.9	65.9	65.9	65.9	65.9	66.0	66.0	66.0	66.0	65.9
6	24.0	200.0	65.3	65.3	65.3	65.3	65.3	65.3	65.3	65.3	65.4	65.4	65.4	65.3
7	23.0	200.0	67.1	67.1	67.1	67.1	67.1	67.1	67.0	67.0	67.0	67.1	67.1	67.1
8	22.0	200.0	66.5	66.2	66.2	66.2	66.1	66.1	66.1	66.0	64.7	64.6	64.6	64.7
9	21.0	200.0	67.4	67.3	67.3	67.3	67.3	67.3	66.0	65.5	65.4	65.1	65.0	65.0
10	20.0	200.0	66.8	66.2	66.2	66.2	65.7	65.6	65.0	64.8	64.6	64.4	64.3	64.4
11	19.0	200.0	65.9	65.1	65.1	65.1	65.1	65.1	64.4	64.4	64.4	64.4	64.1	64.0
12	18.0	200.0	66.5	66.0	66.0	65.9	65.9	65.9	65.9	66.0	65.9	65.9	65.9	65.0
13	17.0	200.0	66.8	66.5	66.5	66.5	66.5	66.5	66.4	66.6	66.6	66.7	66.6	66.5
14	16.0	200.0	65.2	65.3	65.3	65.3	65.3	65.3	65.3	65.3	65.3	65.3	65.3	65.4
15	15.0	200.0	67.5	66.3	66.3	66.3	66.3	66.3	65.0	65.0	65.0	65.0	65.0	65.0
16	14.0	200.0	65.9	65.4	65.3	64.9	64.9	64.8	64.2	63.4	63.4	63.4	63.4	63.4
17	13.0	200.0	67.3	66.8	66.7	66.7	66.7	66.7	66.7	67.0	66.9	66.9	66.7	66.6
18	12.0	200.0	66.0	66.0	66.0	66.0	66.0	66.0	66.0	66.2	66.3	66.4	66.4	66.2
19	11.0	200.0	67.0	67.0	67.1	67.1	67.0	67.0	67.1	67.2	67.3	67.4	67.4	67.2
20	10.0	200.0	65.7	65.8	65.8	65.8	65.8	65.8	65.9	65.8	65.8	65.8	65.9	66.1
21	9.0	200.0	65.3	64.8	64.7	64.7	64.7	64.7	64.2	63.7	63.7	63.6	63.6	64.2
22	8.0	200.0	65.7	65.4	65.3	65.3	65.3	65.3	65.3	65.2	65.2	64.2	64.2	64.2
23	7.0	200.0	66.3	66.1	66.0	66.0	66.0	65.8	64.7	64.7	64.7	64.6	64.6	64.6
24	6.0	200.0	66.9	66.5	66.4	66.4	66.4	66.3	65.0	64.7	64.5	64.4	64.5	64.5
25	5.0	200.0	66.5	65.6	65.6	65.6	64.8	64.9	64.9	64.9	65.0	64.9	64.8	64.8
26	4.0	200.0	66.5	66.2	66.1	66.1	66.0	65.0	65.1	65.1	65.2	65.3	65.3	65.2
27	3.0	200.0	65.7	65.3	65.3	65.2	63.9	63.8	64.0	64.0	64.0	64.1	64.1	64.1
28	2.0	200.0	66.2	65.2	65.2	64.3	64.1	63.9	64.0	63.9	63.9	63.9	64.0	64.2
29	1.0	0.0	64.4	64.1	62.5	62.6	62.6	61.9	62.0	62.0	62.0	62.0	62.0	62.0

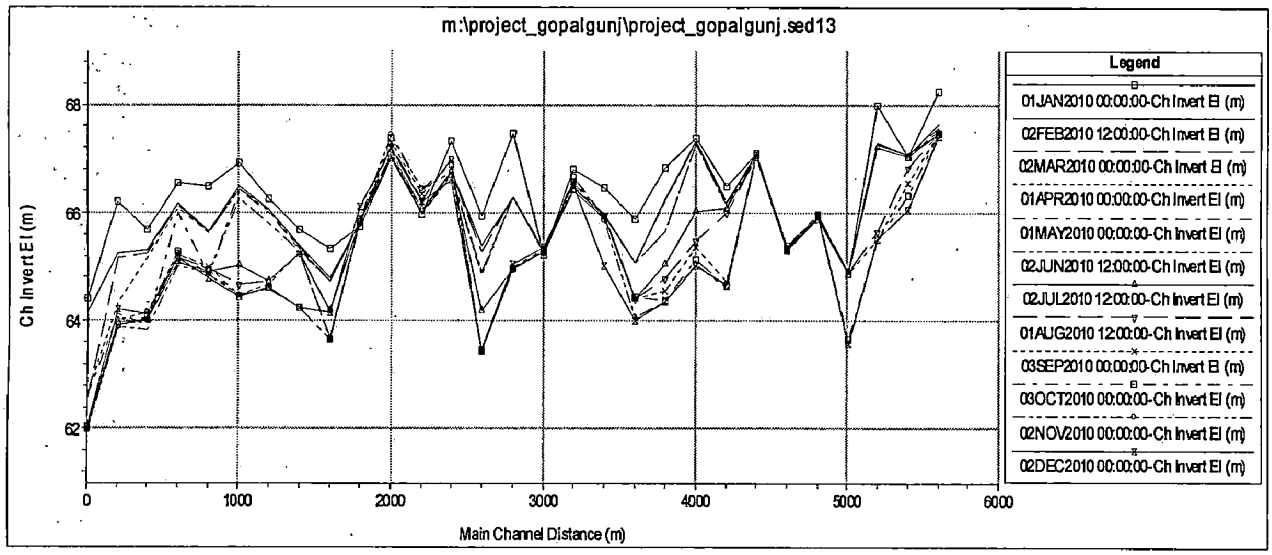

Fig: 5.2 Monthly Predicted Profile Using Acker-White Predictor for the Reach Basi

Table: 5.2 Monthly Predicted Profile Using Acker-White Predictor for the Reach Gandak

S No	Reach Statio	Channel Distanc	Bed Profile (m)											
			JA	FEB	MAR	AP	MA	JU	JU	AU	SEP	OC	NO	DE
1	30.0	200.0	70.2	69.5	69.3	69.0	68.7	68.4	67.7	67.7	67.7	67.7	67.7	67.7
2	29.0	200.0	70.5	70.1	70.1	70.0	70.0	69.7	69.5	69.3	69.0	68.8	68.7	68.6
3	28.0	200.0	67.2	66.8	66.8	66.8	66.8	66.8	66.8	66.8	66.8	66.8	66.8	66.8
4	27.0	200.0	67.1	67.2	67.3	67.3	67.3	67.3	67.3	67.3	67.3	67.3	67.3	67.3
5	26.0	200.0	67.5	67.4	67.4	67.4	67.5	67.5	67.5	67.5	67.5	67.5	67.5	67.5
6	25.0	200.0	64.7	64.7	64.7	64.7	64.7	64.7	64.8	64.8	64.8	64.8	64.8	64.8
7	24.0	200.0	68.2	68.3	68.3	68.3	68.3	68.4	68.4	68.4	68.4	68.4	68.4	68.3
8	23.0	200.0	68.2	68.2	68.2	68.2	68.2	68.2	68.2	68.2	68.2	68.2	68.2	68.0
9	22.0	200.0	66.8	66.9	66.9	66.9	66.9	66.9	66.9	66.9	66.9	66.9	66.9	66.9
10	21.0	200.0	67.5	67.6	67.6	67.6	67.6	67.6	67.6	67.6	67.6	67.7	67.8	68.2
11	20.0	200.0	68.1	67.9	67.8	67.8	67.8	67.8	66.0	65.6	65.6	65.6	65.6	65.7
12	19.0	200.0	69.0	68.7	68.7	68.7	68.6	68.6	66.9	66.6	66.5	66.5	66.5	66.5
13	18.0	200.0	68.5	68.4	68.4	68.4	68.4	68.4	68.5	68.5	66.9	66.8	66.8	66.8
14	17.0	200.0	67.6	67.6	67.6	67.6	67.6	67.6	67.7	67.7	67.7	67.6	66.7	66.7
15	16.0	200.0	67.2	67.2	67.2	67.2	67.2	67.2	67.3	67.3	67.3	67.3	67.2	67.2
16	15.0	200.0	68.2	68.0	67.9	67.9	67.9	67.9	67.9	68.0	68.0	67.9	67.9	67.9
17	14.0	200.0	68.0	67.9	67.9	67.9	67.8	67.8	67.8	67.8	67.8	67.8	67.8	67.8
18	13.0	200.0	67.6	67.1	67.1	67.1	67.1	67.0	67.1	67.1	67.1	67.1	67.1	67.0
19	12.0	200.0	67.3	67.3	67.3	67.3	67.3	67.3	67.4	67.4	67.5	67.5	67.5	67.4
20	11.0	200.0	67.9	67.9	67.9	67.9	67.9	67.9	67.9	67.9	67.9	68.0	68.0	67.9
21	10.0	200.0	66.8	66.8	66.8	66.8	66.8	66.8	65.8	65.7	65.5	65.5	65.7	65.6
22	9.0	200.0	66.5	66.4	66.4	66.4	65.9	65.9	65.6	65.5	64.4	64.4	64.5	64.8
23	8.0	200.0	66.8	65.5	65.5	65.4	65.4	65.4	64.3	64.3	64.3	64.3	64.3	64.3
24	7.0	200.0	66.1	65.2	65.2	65.3	65.4	65.2	63.6	63.6	63.6	63.6	63.6	63.6
25	6.0	200.0	66.8	66.5	66.5	66.5	66.4	66.4	64.5	64.3	64.3	64.3	64.3	64.3
26	5.0	200.0	65.9	65.5	65.5	65.4	65.4	65.3	65.5	65.3	64.0	63.7	63.6	63.6
27	4.0	200.0	65.9	65.7	65.1	65.1	65.1	65.1	65.3	65.3	65.2	65.2	65.1	64.4
28	3.0	200.0	66.2	65.7	65.6	65.6	65.6	65.6	64.9	64.9	64.9	64.9	64.8	64.8
29	2.0	200.0	66.1	64.8	64.8	64.8	64.5	64.5	64.5	64.5	64.5	64.5	64.5	64.5
30	1.0	0.0	66.8	65.9	65.8	65.8	65.8	65.8	65.9	65.9	65.9	65.9	65.9	65.8

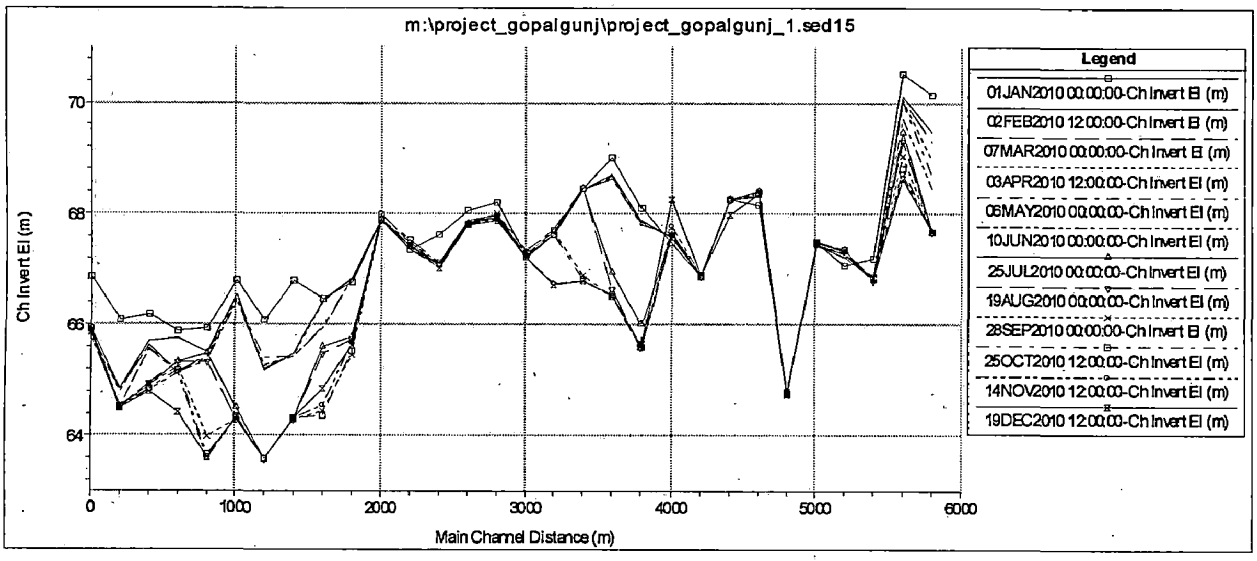

Fig: 5.3 Monthly Predicted Profile Using Acker-White Predictor for the Reach Gandak

5.3.2 YANG SEDIMENT MODULE FOR BED PROFILE FORECASTING

In this Module, Yang sediment transport function is applied for the prediction of bed profile for the period 2010 in the stretch keeping the base month as January. Model is run for the same input data as discussed in section 5.3.1. Monthly bed profile prediction were computed and presented in tabular form in Table 5.3 and 5.4 for Basi and Gandak reaches respectively.

Figures 5.4 and 5.5 shows the monthly predicted profile is nearly same as Acker-White Predictor, for the reaches Basi and Gandak respectfully. Fig: 5.4 and 5.5 depicts that there is significant aggrading tendency throughout the reach.

Table: 5.3 Monthly Predicted Profile Using Yang Predictor for the Reach Basi

S No.	Reach Station	Channel Distance	Bed Profile (m)											
			JAN	FEB	MAR	APR	MAY	JUN	JUL	AUG	SEP	OCT	NOV	DEC
1	29.0	200.0	68.2	67.7	67.7	67.6	67.6	67.6	67.6	67.6	67.6	67.6	67.6	67.6
2	28.0	200.0	67.0	67.1	67.1	67.1	67.1	67.1	67.0	66.7	66.5	66.3	66.1	66.1
3	27.0	200.0	68.0	67.9	67.9	67.9	67.8	67.8	66.4	65.7	65.5	65.5	65.5	65.5
4	26.0	200.0	64.9	64.9	64.9	64.9	65.0	65.0	64.9	64.9	64.9	64.5	64.1	64.1
5	25.0	200.0	65.9	65.9	65.9	65.9	65.9	65.9	66.0	66.2	66.2	66.2	66.0	66.0
6	24.0	200.0	65.3	65.3	65.3	65.3	65.2	65.2	65.2	65.3	65.3	65.3	65.3	65.3
7	23.0	200.0	67.1	67.1	67.1	67.1	67.1	67.0	67.0	67.1	67.1	67.1	67.1	67.1
8	22.0	200.0	66.5	66.4	66.4	66.4	66.3	66.3	66.2	66.2	66.2	66.2	66.2	66.2
9	21.0	200.0	67.4	67.3	67.3	67.3	67.3	67.3	66.9	66.9	66.9	66.9	66.9	66.9
10	20.0	200.0	66.8	66.6	66.6	66.4	66.4	66.4	65.4	65.1	65.1	65.1	65.2	65.2
11	19.0	200.0	65.9	65.1	65.0	65.0	65.0	65.0	64.6	64.3	64.1	63.9	63.8	63.8
12	18.0	200.0	66.5	66.3	66.0	66.0	66.0	66.0	66.0	65.2	65.1	64.9	64.7	64.7
13	17.0	200.0	66.8	66.8	66.8	66.8	66.8	66.7	66.7	66.8	66.8	66.8	66.6	66.5
14	16.0	200.0	65.2	65.3	65.3	65.3	65.3	65.3	65.3	65.3	65.3	65.2	65.3	65.3
15	15.0	200.0	67.5	67.1	67.1	67.1	67.1	67.1	65.1	65.0	65.0	65.0	65.0	65.1
16	14.0	200.0	65.9	64.8	64.8	64.8	64.7	64.7	64.1	63.4	63.4	63.4	63.4	63.4
17	13.0	200.0	67.3	67.2	67.1	67.1	67.0	67.0	67.2	67.6	67.5	67.4	66.6	66.0
18	12.0	200.0	66.0	66.0	66.0	66.0	66.0	66.0	66.1	66.3	66.4	66.6	66.6	66.3
19	11.0	200.0	67.0	67.1	67.1	67.1	67.1	67.1	67.3	67.3	67.4	67.4	67.5	67.5
20	10.0	200.0	65.7	65.8	65.8	65.8	65.9	65.9	65.9	65.9	65.9	65.9	65.9	66.1
21	9.0	200.0	65.3	65.2	65.2	65.2	65.2	65.2	64.8	64.8	64.8	64.8	64.6	64.6
22	8.0	200.0	65.7	65.5	65.5	65.4	65.4	65.4	65.4	65.4	65.4	65.4	65.4	65.4
23	7.0	200.0	66.3	66.1	66.1	66.1	66.1	66.1	66.1	66.1	66.1	66.0	65.9	65.9
24	6.0	200.0	66.9	66.7	66.6	66.6	66.5	66.5	66.5	66.5	66.5	66.5	66.5	66.5
25	5.0	200.0	66.5	65.1	65.1	64.9	64.6	64.5	64.6	64.6	64.6	64.6	64.6	64.6
26	4.0	200.0	66.5	66.2	66.2	66.2	66.2	66.2	66.2	66.2	66.2	66.2	66.2	66.0
27	3.0	200.0	65.7	65.2	65.2	64.2	64.2	64.2	64.3	64.3	64.3	64.3	64.4	64.2
28	2.0	200.0	66.2	64.6	64.7	64.7	64.5	64.4	64.4	64.4	64.4	64.4	64.5	64.6
29	1.0	0.0	64.4	63.5	61.9	62.0	62.0	61.9	62.0	62.0	62.0	62.0	62.1	62.1

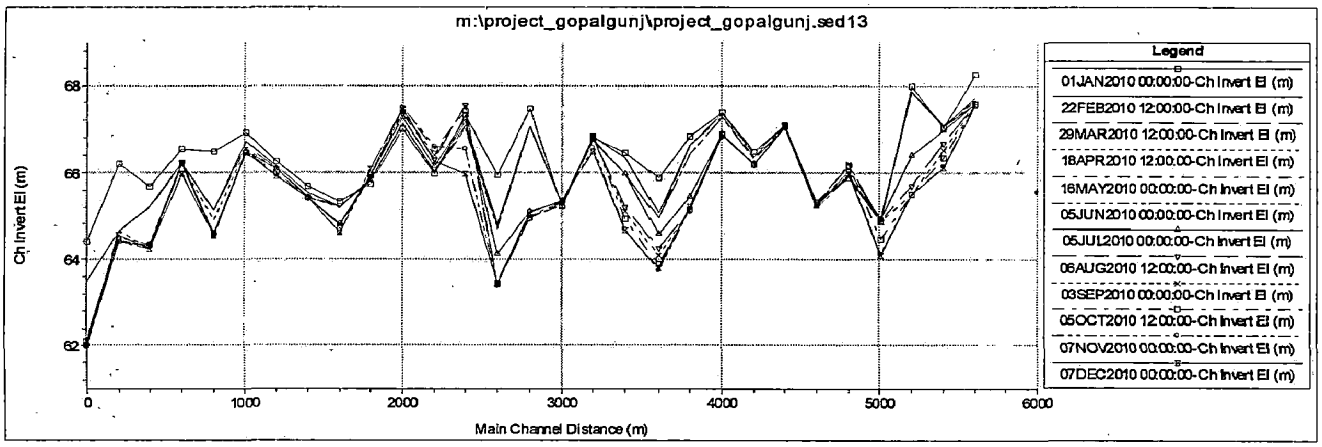

Fig: 5.4 Monthly Predicted Profile Using Yang Predictor for the Reach Basi

Table: 5.4 Monthly Predicted Profile Using Yang Predictor for the Reach Gandak

S No	Reach Statio	Channel Distanc	Bed Profile (m)											
			JA	FEB	MAR	AP	MA	JU	JU	AU	SEP	OC	NO	DE
1	30.0	200.0	67.7	70.2	69.6	69.6	69.5	69.5	69.5	68.8	68.2	67.7	67.7	67.7
2	29.0	200.0	68.0	70.5	70.1	70.1	70.1	70.1	69.8	69.7	69.7	69.7	69.6	69.3
3	28.0	200.0	66.9	67.2	67.0	66.9	66.7	66.7	66.7	66.7	66.7	66.7	66.7	66.7
4	27.0	200.0	67.6	67.1	67.3	67.4	67.6	67.6	67.6	67.6	67.6	67.6	67.6	67.6
5	26.0	200.0	67.5	67.5	67.5	67.5	67.5	67.5	67.5	67.5	67.5	67.5	67.5	67.5
6	25.0	200.0	64.8	64.7	64.7	64.7	64.8	64.8	64.8	64.8	64.8	64.8	64.8	64.8
7	24.0	200.0	68.4	68.2	68.2	68.2	68.2	68.2	68.2	68.2	68.2	68.2	68.2	68.3
8	23.0	200.0	68.3	68.2	68.2	68.2	68.3	68.3	68.3	68.3	68.3	68.3	68.3	68.3
9	22.0	200.0	67.1	66.8	66.9	66.9	66.9	66.9	66.9	66.9	66.9	66.9	66.9	67.0
10	21.0	200.0	67.6	67.5	67.5	67.5	67.5	67.5	67.5	67.5	67.5	67.5	67.5	67.5
11	20.0	200.0	65.6	68.1	68.0	68.0	68.0	68.0	67.9	67.9	67.9	67.0	66.2	66.1
12	19.0	200.0	66.5	69.0	68.9	68.8	68.8	68.8	68.7	68.7	68.7	68.7	68.3	68.3
13	18.0	200.0	66.8	68.5	68.5	68.5	68.5	68.5	68.4	68.4	68.4	68.4	68.4	68.4
14	17.0	200.0	67.0	67.6	67.6	67.7	67.7	67.7	67.7	67.6	67.3	66.8	66.8	66.8
15	16.0	200.0	67.2	67.2	67.2	67.2	67.2	67.2	67.2	67.2	67.2	67.2	67.0	66.7
16	15.0	200.0	67.5	68.2	68.1	68.1	68.0	68.0	68.0	68.0	68.0	68.1	68.0	68.0
17	14.0	200.0	67.7	68.0	68.0	67.9	67.9	67.9	67.9	67.9	67.9	67.9	67.9	67.9
18	13.0	200.0	67.0	67.6	67.4	67.4	67.3	67.3	67.3	67.3	67.3	67.2	67.2	67.0
19	12.0	200.0	67.4	67.3	67.4	67.4	67.4	67.3	67.3	67.4	67.4	67.4	67.6	67.5
20	11.0	200.0	67.9	67.9	68.0	68.0	68.0	68.0	68.0	68.0	68.0	68.0	68.1	68.0
21	10.0	200.0	66.3	66.8	66.8	66.9	66.9	66.9	66.9	66.9	66.8	66.8	66.7	66.8
22	9.0	200.0	64.6	66.5	66.5	66.4	66.4	66.4	66.4	66.3	66.0	65.2	64.8	65.1
23	8.0	200.0	64.3	66.8	66.4	66.3	66.2	65.9	65.8	65.7	65.7	64.4	64.3	64.6
24	7.0	200.0	63.6	66.1	65.1	65.1	65.1	65.3	65.4	65.1	65.1	65.1	63.6	63.6
25	6.0	200.0	64.3	66.8	66.7	66.7	66.6	66.5	66.5	65.3	65.3	65.3	65.3	65.3
26	5.0	200.0	63.4	65.9	65.7	65.6	65.5	65.5	64.0	64.0	64.0	64.0	64.0	64.0
27	4.0	200.0	63.4	65.9	65.8	65.7	64.3	64.3	64.5	64.3	64.3	64.3	64.3	64.3
28	3.0	200.0	64.3	66.2	65.8	65.1	65.1	65.1	65.1	65.1	64.1	64.0	63.9	63.7
29	2.0	200.0	63.6	66.1	64.7	64.7	64.7	64.7	64.7	64.7	64.7	64.7	64.7	64.7
30	1.0	0.0	65.2	66.8	64.4	64.4	64.4	64.4	64.4	64.5	64.5	64.5	64.4	64.4

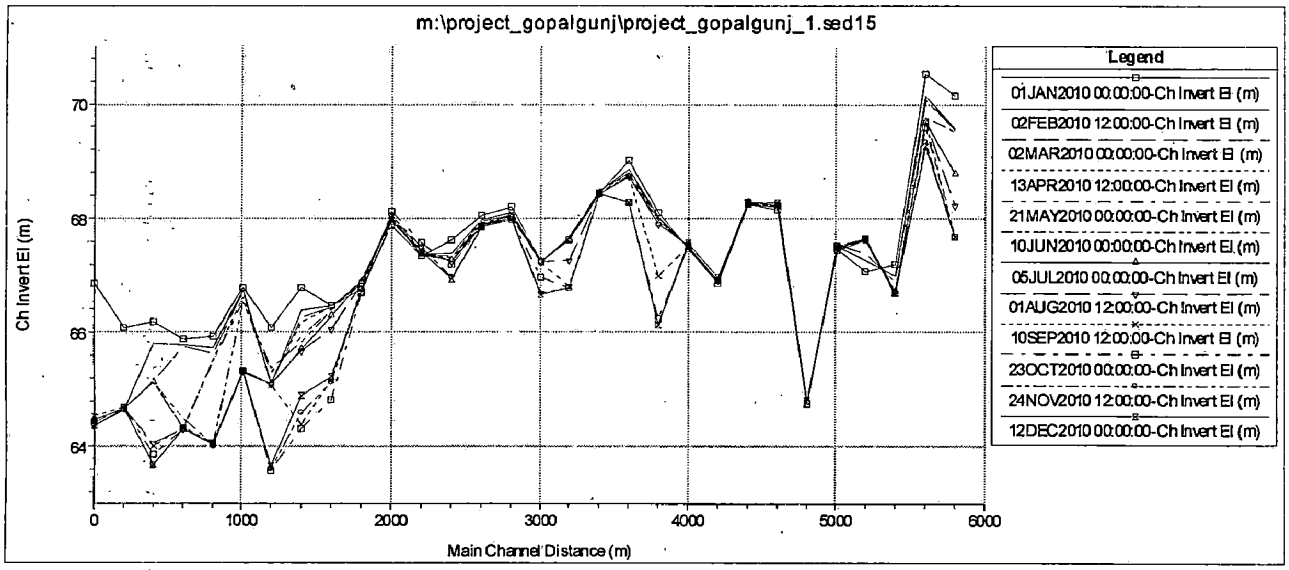

Fig: 5.5 Monthly Predicted Profile Using Yang Predictor for the Reach Gandak

5.3.3 ENGELUND-HANSEN SEDIMENT MODULE FOR BED PROFILE FORECASTING

Using the input data of section 5.3.1 and Engelund- Hansen sediment module, bed profiles have been forecasted for the same time period. Monthly bed profile prediction were computed and presented in tabular form in Table 5.5 and 5.6 for Basi and Gandak reaches respectively.

Figures 5.6 and 5.7 shows the monthly predicted profile is nearly same as Yang Predictor, for the reaches Basi and Gandak respectfully. Fig: 5.6 and 5.7 depicts that there is significant aggrading tendency throughout the reach.

Table: 5.5 Monthly Predicted Profile Using Engelund-Hansen Predictor for the Reach Basi

S No.	Reach Station	Channel Distance	Bed Profile (m)											
			JAN	FEB	MAR	APR	MAY	JUN	JUL	AUG	SEP	OCT	NOV	DEC
1	29.0	200.0	68.2	67.7	67.5	67.4	67.4	67.2	67.2	67.2	67.2	67.1	67.0	66.9
2	28.0	200.0	67.0	67.1	67.1	67.1	67.1	67.1	66.9	66.6	66.5	66.1	66.1	66.1
3	27.0	200.0	68.0	67.8	67.7	67.6	67.5	67.4	66.5	65.7	65.5	65.5	65.5	65.5
4	26.0	200.0	64.9	64.9	64.9	64.9	64.9	65.0	65.0	65.0	64.9	64.5	64.4	64.3
5	25.0	200.0	65.9	65.9	66.0	66.0	66.0	66.0	66.1	66.3	66.3	66.3	66.1	66.0
6	24.0	200.0	65.3	65.3	65.3	65.3	65.3	65.3	65.3	65.4	65.4	65.5	65.4	65.3
7	23.0	200.0	67.1	67.1	67.1	67.1	67.1	67.1	67.1	67.1	67.1	67.1	67.2	67.2
8	22.0	200.0	66.5	66.4	66.4	66.3	66.3	66.2	65.8	65.5	65.3	65.0	65.1	65.2
9	21.0	200.0	67.4	67.3	67.2	67.2	67.2	67.2	66.3	65.4	64.9	64.9	64.9	64.9
10	20.0	200.0	66.8	66.5	66.4	66.3	66.2	66.1	64.9	64.3	64.3	64.3	64.3	64.4
11	19.0	200.0	65.9	65.4	65.3	65.2	65.1	65.0	64.9	64.7	64.3	63.4	63.4	63.4
12	18.0	200.0	66.5	66.3	66.2	66.0	66.0	65.8	65.7	65.8	65.8	65.0	64.5	64.4
13	17.0	200.0	66.8	66.9	66.9	66.8	66.8	66.7	66.8	67.0	67.1	66.8	66.2	66.1
14	16.0	200.0	65.2	65.3	65.3	65.3	65.4	65.4	65.4	65.3	65.2	65.2	65.3	65.3
15	15.0	200.0	67.5	67.0	66.9	66.9	66.9	66.7	65.0	65.0	65.0	65.0	65.0	65.1
16	14.0	200.0	65.9	65.6	65.5	65.4	65.3	65.2	64.0	63.4	63.4	63.4	63.4	63.4
17	13.0	200.0	67.3	67.2	67.1	66.9	66.8	66.7	67.0	67.2	67.3	66.9	66.0	65.9
18	12.0	200.0	66.0	66.1	66.0	65.8	65.6	65.5	65.9	66.1	66.3	66.8	66.4	66.0
19	11.0	200.0	67.0	67.1	67.1	66.9	66.7	66.7	66.9	67.0	67.0	67.3	67.3	67.1
20	10.0	200.0	65.7	65.8	65.9	65.9	65.9	66.0	66.0	66.0	66.0	66.1	66.4	66.6
21	9.0	200.0	65.3	65.2	65.2	65.1	65.0	64.7	64.5	64.4	64.4	64.2	64.4	64.7
22	8.0	200.0	65.7	65.4	65.1	64.8	64.5	64.2	64.1	64.1	64.0	63.9	63.9	64.0
23	7.0	200.0	66.3	66.0	65.5	65.0	64.9	64.8	64.8	64.8	64.7	64.6	64.7	64.8
24	6.0	200.0	66.9	66.5	66.0	65.3	65.2	65.2	65.1	64.7	64.4	64.4	64.5	64.7
25	5.0	200.0	66.5	65.3	64.7	64.0	64.0	64.0	64.1	64.2	64.1	64.0	64.0	64.0
26	4.0	200.0	66.5	65.8	65.0	64.6	64.5	64.4	64.6	64.7	64.8	65.0	64.9	64.7
27	3.0	200.0	65.7	64.8	63.6	63.2	63.2	63.2	63.4	63.4	63.5	63.6	63.7	63.8
28	2.0	200.0	66.2	64.1	63.7	63.7	63.7	63.7	63.8	63.8	63.8	63.8	64.0	64.1
29	1.0	0.0	64.4	61.9	61.9	61.9	61.9	61.9	62.0	62.0	62.0	62.0	62.1	62.2

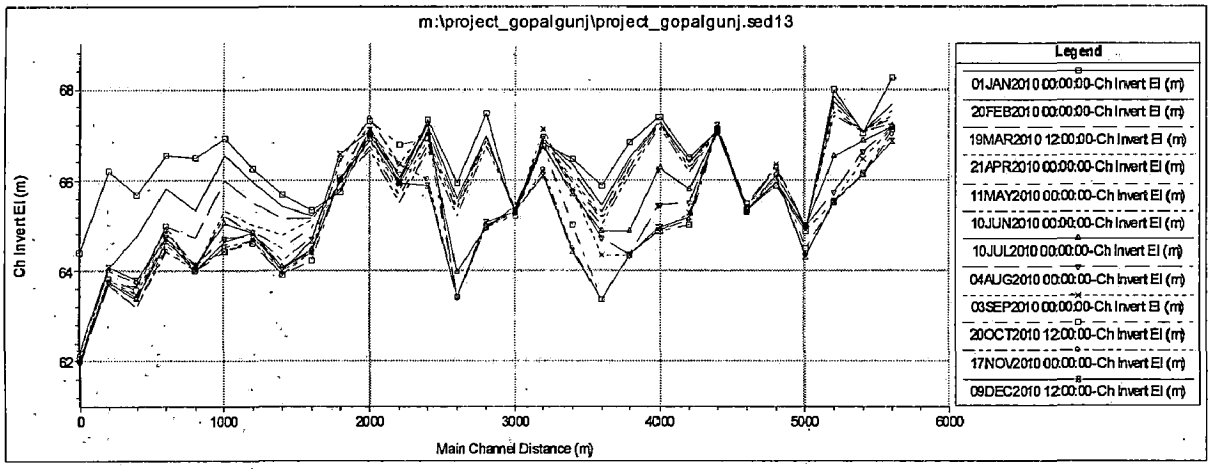

Fig: 5.6 Monthly Predicted Profile Using Engelund-Hansen Predictor for the Reach Basi

Table: 5.6 Monthly Predicted Profile Using Engelund-Hansen Predictor for the Reach Gandak

S No	Reach Statio	Channel Distanc	Bed Profile (m)											
			JAN	FEB	MA	APR	MA	JUN	JUL	AUG	SEP	OCT	NOV	DEC
1	30.0	200.0	70.2	69.4	68.9	68.5	68.4	68.2	67.7	67.7	67.7	67.7	67.7	67.7
2	29.0	200.0	70.5	70.1	69.8	69.6	69.5	69.4	69.2	68.8	68.6	68.0	68.0	68.0
3	28.0	200.0	67.2	67.0	66.9	66.8	66.8	66.7	66.8	66.8	66.9	67.0	66.9	66.8
4	27.0	200.0	67.1	67.3	67.4	67.5	67.5	67.6	67.6	67.6	67.6	67.7	67.6	67.6
5	26.0	200.0	67.5	67.5	67.6	67.6	67.6	67.5	67.5	67.5	67.5	67.6	67.5	67.3
6	25.0	200.0	64.7	64.7	64.8	64.8	64.8	64.8	64.8	64.8	64.8	64.8	64.8	64.8
7	24.0	200.0	68.2	68.2	68.3	68.3	68.3	68.4	68.4	68.4	68.4	68.4	68.4	68.5
8	23.0	200.0	68.2	68.3	68.3	68.3	68.3	68.3	68.3	68.3	68.3	68.3	68.3	68.2
9	22.0	200.0	66.8	66.9	66.9	66.9	67.0	67.0	67.0	67.0	67.0	67.0	67.1	67.1
10	21.0	200.0	67.5	67.5	67.5	67.5	67.5	67.6	67.6	67.6	67.6	67.6	67.6	67.7
11	20.0	200.0	68.1	68.0	68.0	67.9	67.9	67.8	66.3	65.6	65.6	65.6	65.6	65.6
12	19.0	200.0	69.0	68.8	68.7	68.6	68.6	68.5	67.0	66.5	66.5	66.5	66.5	66.5
13	18.0	200.0	68.5	68.5	68.5	68.5	68.4	68.4	68.6	68.4	67.7	67.0	66.8	66.8
14	17.0	200.0	67.6	67.6	67.6	67.6	67.6	67.6	67.6	67.6	67.4	67.1	67.0	66.9
15	16.0	200.0	67.2	67.2	67.2	67.2	67.2	67.2	67.2	67.3	67.4	67.3	67.2	67.0
16	15.0	200.0	68.2	68.1	68.0	67.9	67.8	67.7	67.6	67.7	67.8	67.7	67.5	67.4
17	14.0	200.0	68.0	67.9	67.9	67.8	67.8	67.8	67.7	67.7	67.7	67.7	67.7	67.7
18	13.0	200.0	67.6	67.4	67.3	67.2	67.2	67.1	66.9	66.9	66.9	67.0	67.0	66.8
19	12.0	200.0	67.3	67.3	67.3	67.2	67.2	67.1	67.2	67.3	67.3	67.5	67.4	67.2
20	11.0	200.0	67.9	68.0	68.0	67.9	67.9	67.6	67.8	67.8	67.8	67.9	67.9	67.5
21	10.0	200.0	66.8	66.8	66.8	66.8	66.8	66.5	66.5	66.4	66.3	66.2	66.3	66.3
22	9.0	200.0	66.5	66.4	66.3	66.0	65.8	65.8	65.5	65.1	64.7	64.5	64.6	65.4
23	8.0	200.0	66.8	66.3	65.8	65.5	65.5	65.3	64.3	64.3	64.3	64.3	64.3	64.3
24	7.0	200.0	66.1	65.6	65.6	65.5	65.5	65.2	63.6	63.6	63.6	63.6	63.6	63.8
25	6.0	200.0	66.8	66.7	66.1	65.7	65.6	65.5	64.3	64.3	64.3	64.3	64.3	64.4
26	5.0	200.0	65.9	65.2	64.6	64.4	64.4	64.2	64.2	63.4	63.4	63.4	63.4	63.5
27	4.0	200.0	65.9	65.1	64.6	64.4	64.3	64.2	64.4	64.3	63.8	63.4	63.4	63.4
28	3.0	200.0	66.2	64.7	64.4	64.3	64.2	64.2	64.5	64.6	64.6	64.4	64.3	64.3
29	2.0	200.0	66.1	63.9	63.8	63.6	63.6	63.6	63.6	63.6	63.6	63.6	63.6	63.6
30	1.0	0.0	66.8	64.4	64.4	64.4	64.4	64.4	64.9	65.2	65.3	65.3	65.2	65.1

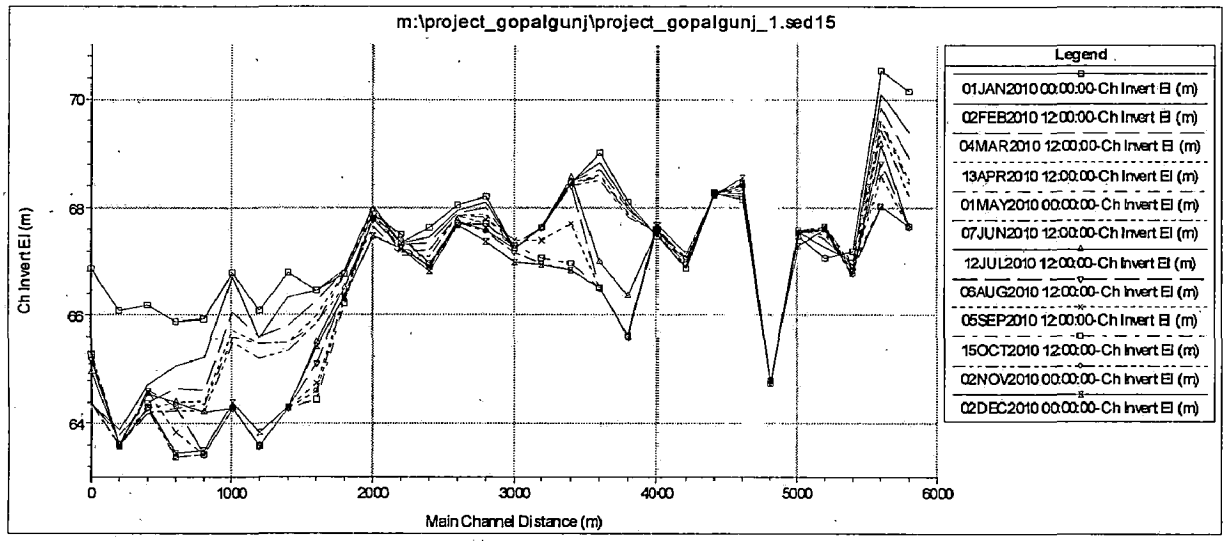

Fig: 5.7 Monthly Predicted Profile Using Engelund-Hansen Predictor for the Reach Gandak

5.4 INFERENCE

From the above study it can be conclude that considerable river morphological changes are occurring with aggradation and degradation along the thalweg supported by all three sediment flow profile predictors used here. This is supported by the physical model study as discussed in previous chapters. Hence a suitable river channel rectification is required to be designed for addressing the situation, which will be the primary focus of the next chapter.

DESIGN OF RIVER CHANNEL RECTIFICATION

6.1 INTRODUCTION

The occurrence of erosion and deposition inside the two guide banks will affect the depth of flow, which in turn may led to the breach of the guide bank in high flood and result in loss and damage to human life as well as properties. It may also lead to undermine channel carrying capacity. Therefore to prevent the guide bank from erosion and to make the flow pass in the center of the bridge, submerged vanes are recommended. They would ensure that the main flow passes under the central portion of the bridge and berms are maintained along the sides of the channel to protect the bridge guide bank and the adjacent stream banks.

Hence the following arrangements are given for this study based on simulated result from HEC-RAS and available hydraulic parameters.

Erosion at the abutment can be prevented by designing a vane system that, at all stages, maintains a flow depth along the bank equal to or less than average flow depth in the channel.

This implies that the system at bank full flow must generate a reduction of near-bank flow depth.

6.2 DESIGN PARAMETERS

Table 6.1 Design Parameters

Design parameters	
average width (b)	550m
depth (d_o)	8.5 m
velocity (U_o)	2.5m/s
slope (S)	0.0003
radius of curvature(r)	1500m
Grain diameter of bed material(D)	0.08mm

6.3 CALCULATIONS

Channel resistance parameter (m) = $kU_o/\sqrt{(gSd_o)}$, where k is von Karman constant $\cong 0.4$

$\therefore$ m = $0.4\times2.5/\sqrt{(9.81\times0.0003\times8.5)} = 6.323$

Hence adopted value of m for design is takes to be 4.

Darcy Weisbach friction factor $f = 8k^2/m^2 = 8\times0.4^2/4^2 = 0.08$

Sediment Froude number is $F_D = U_o/\sqrt{(gD)} = 2.5/\sqrt{(9.81\times0.08/1000)} = 89.24$

Channel width to radius ratio (b/r) = 550/1500 = 0.367

$F_D(b/r) = 32.75$

Here the calculated values of m and F_D (b/r) are more than that can be read from the graph, so new values of m and F_D(b/r) are adopted as m = 4 and F_D (b/r) = 5,

Now we read the value of d_m/d_o from the figure 7.1

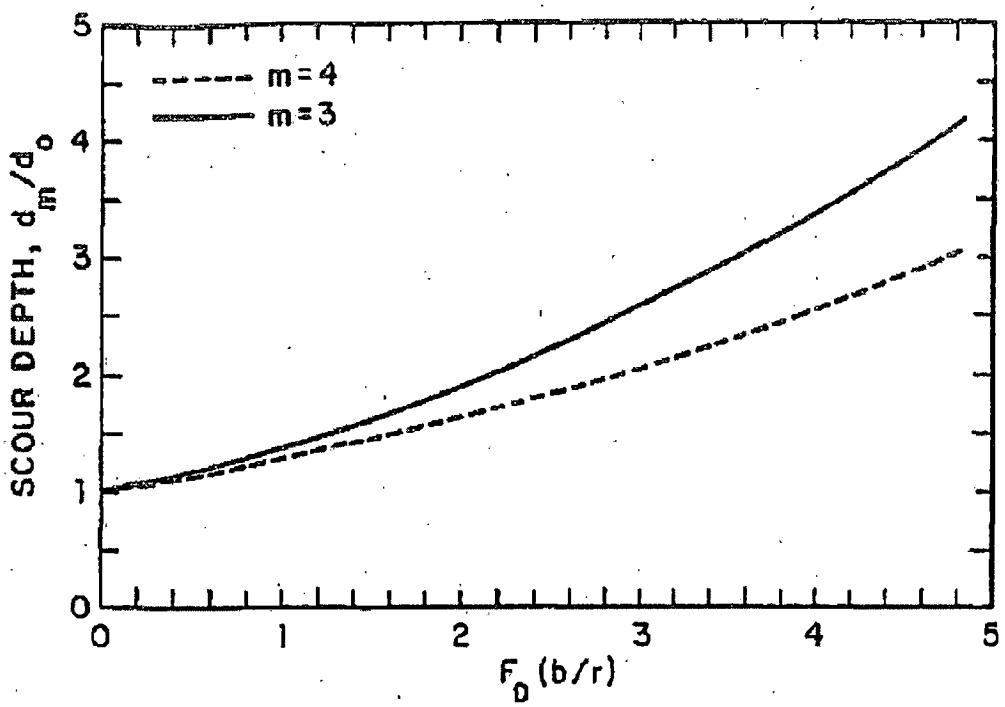

FIG:6.1 Scour Depth at Outer Bank in River Curve

The ratio d_m/d_o is coming to be around 4. To prevent such a scour hole from forming, an array of 3 vanes is needed.

If we assume the following for the purpose of our design:

$T/d_o = 0.7$

$H_o/L = 0.3$ (L = vane length)

Angle of attack, $\alpha = 20°$

Lateral spacing between two vanes in an array, $\delta_n = 3H_o$

Spacing between two arrays, $\delta_s = 30H_o$

$d_o/b = 0.03$,

A vane system with three vanes in each array yields $(d_m - d_v)/d_m = 0.55$ (F_D is assumed 25 as it is maximum value) from the figure 7.2

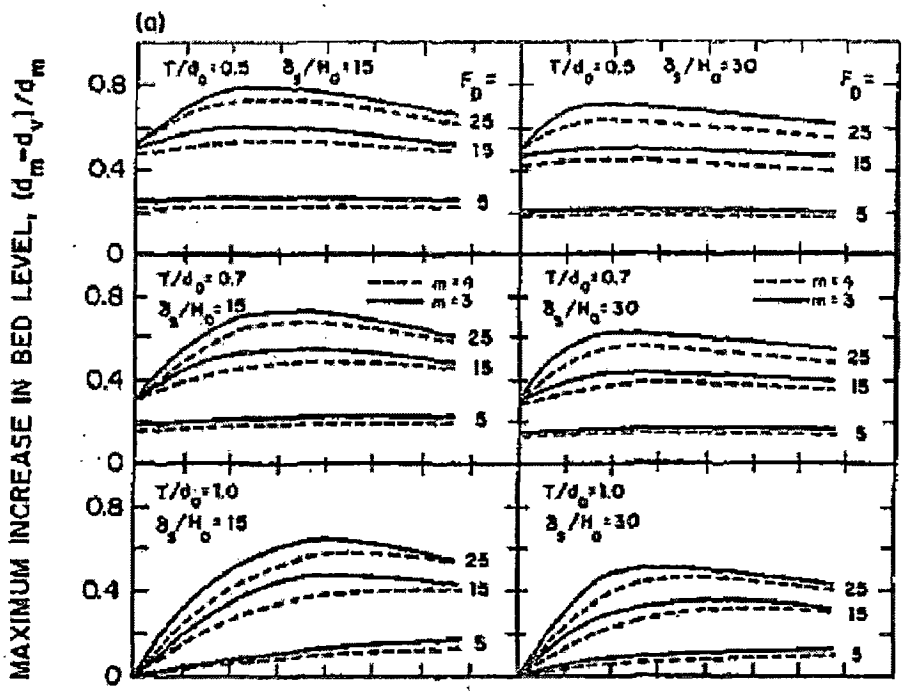

Fig: 6.2 Computed Vane-Induced Maximum Increase in Bed Level along Bank with Three Vanes per Array

Hence $d_v = 1.8\ d_o$, i.e. vane induced depth d_v for the cross-section is 80% larger than c/s average depth d_o (without vanes). Hence no further increase of α is required to increase the value of d_v.

Now let the height of vane $H_o = 0.2\ d_o = 0.2 \times 8.5\ m = 1.7\ m$

$\therefore L = 1.7/0.3 = 5.67\ m \cong 5.5\ m$

$\therefore \delta_n = 3H_o = 5.1\ m$ or less

$\therefore \delta_s = 30H_o = 51$ m or less

6.4 FINAL DESIGN SPECIFICATIONS FOR SUBMERGED VANES

Table: 6.2 Submerged vane dimensions

No	Parameter	Dimension
1	Number of vanes per array	3
2	Vane height (Ho)	1.7m
3	Vane length (L)	5.0m
4	Angle of attack (α)	20 degree
5	Lateral spacing	5 m
6	Array spacing	40 to 50 m

6.5 CONCLUSION

The proposed river channel rectification is given in Table 6.2.

REFERENCES

1. Ackers, P. and White, W. R. (1973), —Sediment Transport: New Approach and Analysis□, *Journal of Hydraulic Engineering,* ASCE Vol. 99 No. HY.11.

2. American Society of Civil Engineers. 1982. "Modelling Hydraulic Phenomena: A Glossary of Terms," *Journal of Hydraulic Engineering*, Vol 108, No. 7, pp. 845-852.

3. Amin, M.I. and Murphy, P. J. (1981), —Two Bed Load Formulas□. *Journal of Hydraulic Engineering, Proc.* ASCE, Vol. 107, No. HY-8.

4. Bagnold,R.A. (1966), —An approach to the sediment transport problem from general physics□, Geological survey professional paper 422-1 (USA).

5. Brunner Gary W. (2002), —HEC-RAS, River Analysis System Hydraulic Reference Manual□ _The U.S. Army Corps of Engineers' (HEC) 609 Second Street Davis, CA 95616-4687.

6. Cao Z. and Carling P. A. (2002), —Mathematical modelling of alluvial rivers: reality and myth. Part 1: General review□ *Proceedings of the Institution of Civil Engineers*, Water & Maritime Engineering 154, Issue 3 Pages 207-219.

7. Cao Z. and Carling P. A. (2002), —Mathematical modelling of alluvial rivers: reality and myth. Part 2: General review□ *Proceedings of the Institution of Civil Engineers*, Water & Maritime Engineering 154, Issue 4 Pages 297-307.

8. Correia L. R. P., Krishnappan B.G. and Graf W. H. (1992), —Fully coupled unsteady mobile boundary flow model□. *Journal of Hydraulic Engineering*, ASCE, 1992, 118, No. 3, 476–494.

9. Chang, H.H. —Modelling of River Channel Changes□, *Journal of Hydraulics Division*, ASCE, Vol. 110, No. 2, February, 1984.

10. Chang ,H.H.and Hill,J.C. (1976), —Computer Modelling of Erodible Flood Channels and Deltas, Model for erodable channel□ J. Hydraulic Division,ASCE,102(HY10),pp.1461-1477 223

11. DeVries M. (1973), —River bed variations—aggradation and Degradation□. *Proceedings of an International Seminar on the Hydraulics of Alluvial Streams*, IAHR, Delft, 1973, pp. 1–10.

12. Chen, Y.H. (1973), —Mathematical Modelling of water and Sediment Routing in Natural Channels , Dissertation presented to the department of Civil Engineering , Colorado State University , Fort Collins, Colorado, in partial fulfilment of the requirements for the degree of Doctor of Philosophy.

13. Cunge, J. A., Holly, F. M., and Vervey, A. (1980), —Practical Aspects of Computational River Hydraulics , Pitman, London.

14. Dass, P. (1975), —Water and Sediment routing in non- uniform channels Doctoral Dissertation submitted to Colorado State University, Fort Collins, Colorado.

15. Einstein H. A. (1950), —The Bed –Load Function for Sediment Transportation in Open Channel Flows USDA,Tech. Bull. No. 1026.

16. Emerson, D.G., and Dressler, V.M., (2002), —Historic and unregulated monthly stream-flow for selected sites in the Red River of the North Basin in North Dakota,

Minnesota, and South Dakota , 1931-99: U.S. Geological Survey Water-Resources Investigations Report 02-4095, 271 p.

17. Engelund, F., (1966), —Hydraulic Resistance of Alluvial Streams , *Journal of Hydraulics Division*, ASCE, Vol. 92, No. HY.

18. Engelund,F. and E. Hansen. (1967), —A Monogram on Sediment Transport in Alluvial Streams , Teknisk Forlag, Denmark.

19. French, R. H. (1985). —Open-Channel Hydraulics , McGraw-Hill.

20. Garbrecht, J., Kuhnle, R. and Alonso, C. (1995). —A sediment transport capacity formulation for application to large channel networks. *J. of Soil and Water Conservation*, 50(5), pp.527-529

21. Garde, R. J. (1982), —Longitudinal profile on an alluvial Stream Engineering Geoscience Ed. B.B.S. Singhal . Sarita Prakashan, New Delhi.

22. Garde R.J. and Ranga Raju K.G. (2000), —Mechanics of Sediment Transportation and Alluvial Stream Problems (3e), New Age International Publishers , pp. 14-178 , 271-308,366-384 381-406 , 614-644.

23. Gomez B. and Church M. (1989), —An assessment of bed load sediment transport formulae for gravel bed rivers. *Water Resource Research*, 1989, 25, No. 6, 1161–1186.

24. Goswami, D.C., (1985), —Brahmaputra River, Assam, India: Physiography, Basin Denudation, and Channel Aggradation , Water Resources Research, V-21, pp. 959-978

25. Graf W.H (1971). —Hydraulics of sediment transport , McGraw-Hill, New York.

26. Guenthner, R.S., Weigel, J.F., and Emerson, D.G.,(1990), —Gaged and estimated monthly streamflow during 1931-84 for selected sites in the Red River of the North Basin in North Dakota and Minnesota□, U.S. Geological Survey Water-Resources Investigations Report 90-4167, 230 p.

27. Hack, J.J (1962) —Study of Longitudinal Stream Profiles in Virginia and Maryland□, USGS Prof. Paper 500-A.

28. —HEC-RAS River Analysis System User's Manual Version 4.1□ (2010), US Army Corps Of Engineers Institute of Water Resources, HEC, CA- 95616.

29. Hinds, Julian. (1928), "The Hydraulic Design of Flume and Siphon Transitions," Transactions of the American Society of Civil Engineers, vol. 92, New York, NY.

30. Julian, P.Y. (2002). —River Mechanics□, Physical models, pp-334-350, CAMBRIDGE.

31. Karamisheva (2006), —Sediment transport formulae for compound channel flow□, proceeding of institution of civil engineering, Water Management 159, Issue WM3 pp.183-193.

32. King, Horace W. and Brater, Ernest F. (1963), —Handbook of Hydraulics□, McGraw-Hill Book. Company, Inc., New York, NY.

33. Laursen,E.M,(1958), —Total Sediment Load of Streams.□ *Journal of Hydraulic Engineering.* ASCE,Vol.84, N0.HY- 1.

34. Lyn D. A. (1987), —unsteady sediment transport modelling□, *Journal of Hydraulic Engineering*, ASCE, 1987, 113, No. 1, 1–15.

35. Meyer-Peter, E and R. Müller.(1948), —Formulas for Bed Load Transport□, *Proc. IAHR*,2nd Congress , Stockhom.

36. Mike by Danish Hydraulic Institute (DHI) online material (2011). < http://www.mikebydhi.com/>

37. Odgaard, A. J., and Wang, Y. (1991). "Sediment management with submerged vanes. I: Theory." J. *Journal of Hydraulic Engineering*, ASCE, 117(3), 267-283.

38. Odgaard, A. J., and Wang, Y. (1991). "Sediment management with submerged vanes. II: Application.", *Journal of Hydraulic Engineering*, ASCE, 117(3), 283-302.

39. Sarma J. N. (2005), —Fluvial process and morphology of the Brahmaputra River in Assam, India□, Science Direct, Geomorphology 70 (2005) p-226– 256.

40. Shankua R.N (2006), —ANN based Spatio-Temporal Morphological Model of the river Brahmaputra□, Ph.D Thesis I.I.T Roorkee.

41. Sinha, R. (1998), —On the controls of fluvial hazards in the north Birhar Plains, eastern India□. *Geohazards in Engineering Geology.* Geological Society, London (15), pp 35-50.

42. Sinha Rajiv (2005), —Why do Gangetic Rivers aggrade or degrade?□ Current Science, VOL. 89, No. 5. 225

43. Rouse, H. (1965). __Critical analysis of open-channel resistance.“ *J. Hydraul. Div.,* ASCE., 91(HY4), 1–25.

44. Ryskin, G., and Leal, L.G (1983), —Orthogonal mapping□, J. Comput. Phys. 1983; 50(1):71-100.

45. Tassi, P. (2007). —Numerical Modelling of River Processes: Flow and River Bed Deformation□ doctoral dissertation, University of Twente, Enschede, The Netherlands.

46. TELEMAC Modelling System (1998), —2D Hydrodynamics TELEMAC-2D software, v.4.0, User‘s Manual□, EDF. Electricit´e de France, D´epartement Laboratoire National d‘Hydraulique.

47. Thomas, W. A., and McAnally, W. H. (1985). "Open-Channel Flow and Sedimentation TABS-2," User‘s Manual, US Army Engineer Waterways Experiment Station, Instruction Report HL-85-1, Vicksburg, MS.

48. Thompson, J.F., Thames, F.C., and Mastin, C.W.(1977), —TOMCAT—A code for numerical generation of boundary-fitted curvilinear coordinate system on fields containing any number of arbitrary two-dimensional bodies,□ *J. Comput. Phys.* 1977; 24:274-302.

49. Toffaleti, F. B. (1969), —Definitive Computations of Sand Discharge in rivers□, *Journal of Hydraulic Engineering, Proc.* ASCE,Vol.95,No.HY-1.

50. US Army Corps of Engineers, Hydrologic Engineering Center. 1982b. "Two-Dimensional Flow Modeling," *Proceedings of the First National US Army Corps of Engineers*-Sponsored Seminar on Two-Dimensional Flow Modeling.

51. U.S. Army Corps of Engineers, Hydrologic Engineering Centre (HEC), (1990a), "HEC-2, Water Surface Profiles User's Manual," Davis, CA.

52. U.S. Army Corps of Engineers, (1993), —Engineering and Design RIVER HYDRAULICS Engineers manual□ Washington, DC.

53. Warner (2002), —HEC-RAS, River Analysis System Applications Guide□, US Army Corps of Engineers Hydrologic Engineering Centre (HEC) 609 Second Street Davis, CA 95616-4687.

54. Wiche, G.J., Benson, R.D., and Emerson, D.G.(1989),□ Streamflow at selected gaging stations on the James River in North Dakota and South Dakota, 1953-82, with a section on climatology□, U.S. Geological Survey Water-Resources Investigations Report 89-4039, 99 p.

55. Yen, B.C. (2002).□ Open channel flow resistance□. J. Hydraul. Eng. 128 (1), 20–39.

56Wu W., Rodi W. and Wenka T. (2000), —3D numerical modelling of flow and sediment transport in open channels□, *Journal of Hydraulic Engineering*, ASCE, 2000, 126, No. 1, 4–15.

57. Yang, C.T. (1973), —Incipient Motion and Sediment transport□. JHD, Proc. ASCE, Vol.99, No HY-10.

58. Yang C. T. and Wan, S., (1991), "Comparisons of Selected Bed-Material Load Formulas," *Journal of Hydraulic Engineering,* ASCE Vol. 117, No. 8, pp. 973-989.

59. Yen, B.C. (1991). —Hydraulic resistance in open channels.□ In: Yen, B.C. (Ed.), Channel flow resistance: Centennial of Manning's formula. Water Resources Publications. Littlelton, USA, pp. 1–135.

APPENDIX

CROSS-SECTION WISE TEMPORAL THALWEG CHANGES OF BASI REACH BY ACKER-WHITE PREDICTOR

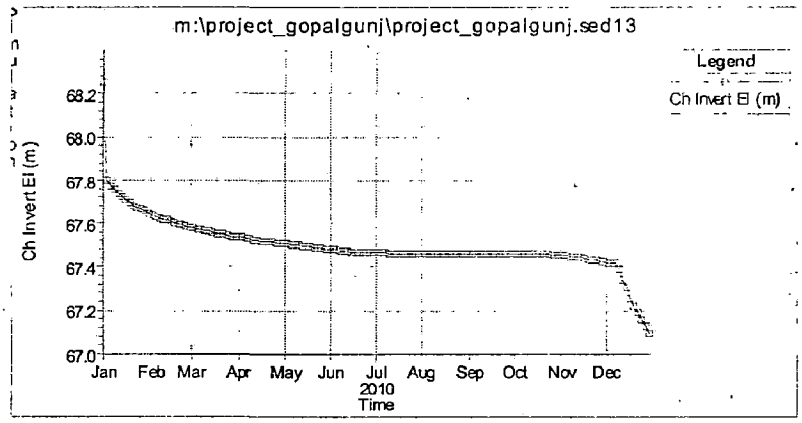

CROSS SECTION 29

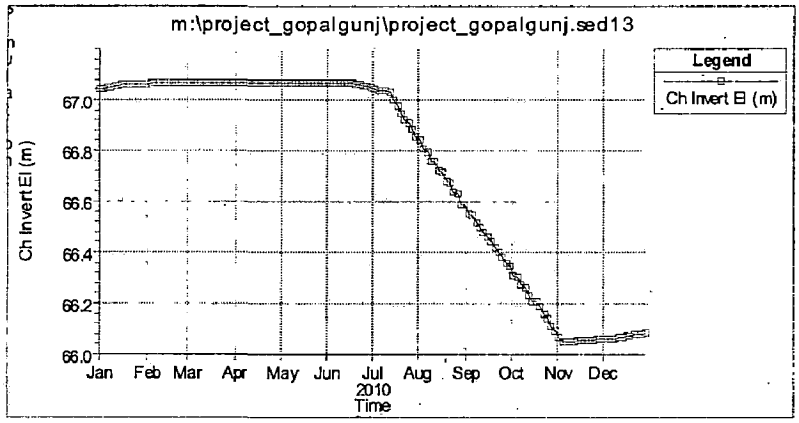

CROSS SECTION 28

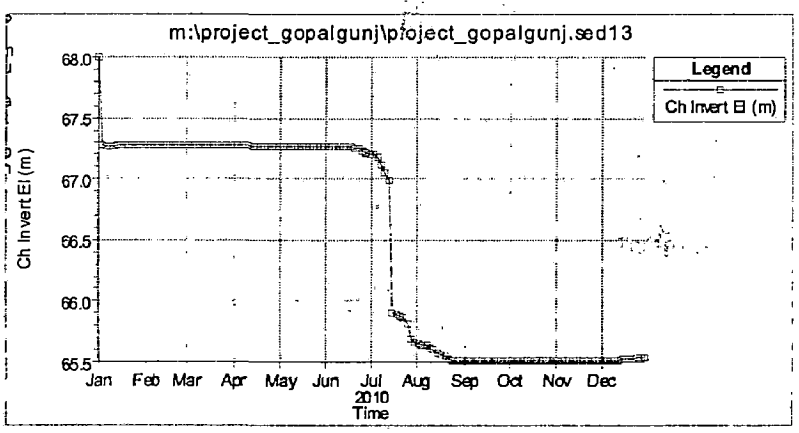

CROSS SECTION 27

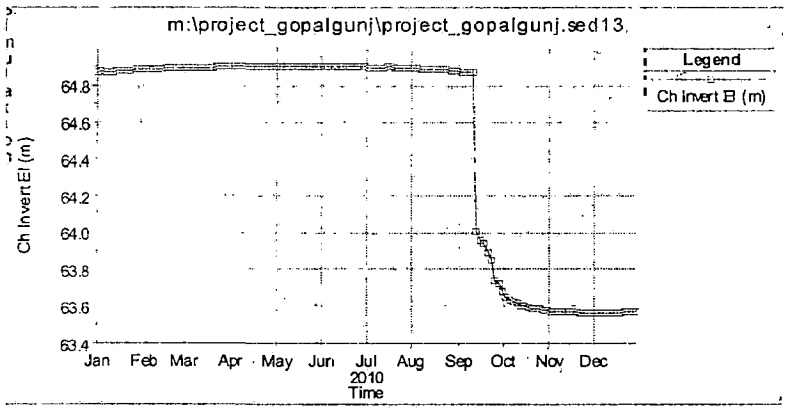

CROSS SECTION 26

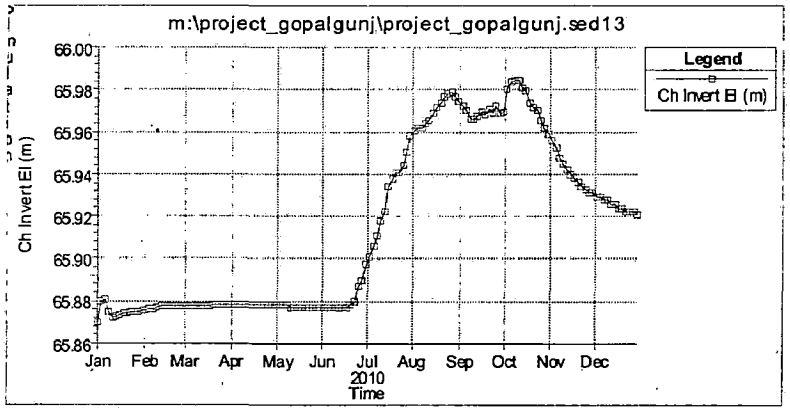

CROSS SECTION 25

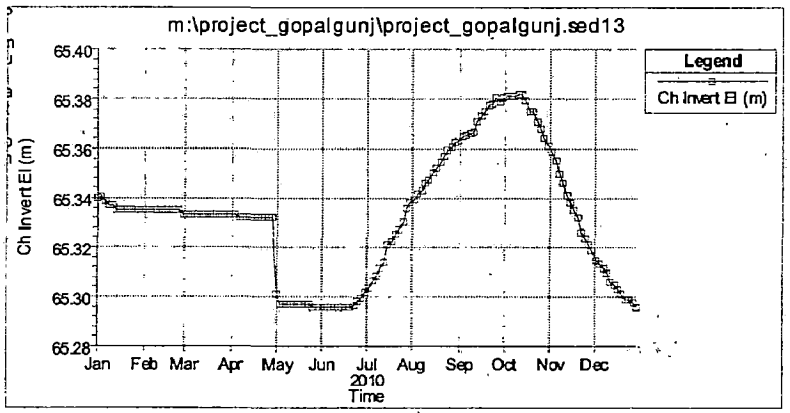

CROSS SECTION 24

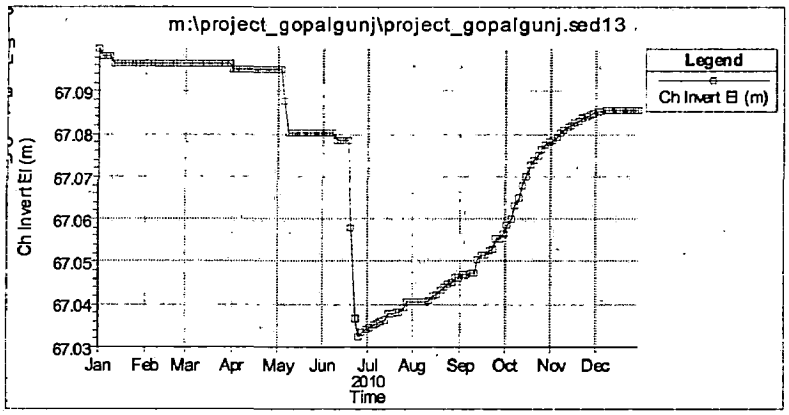

CROSS SECTION 23

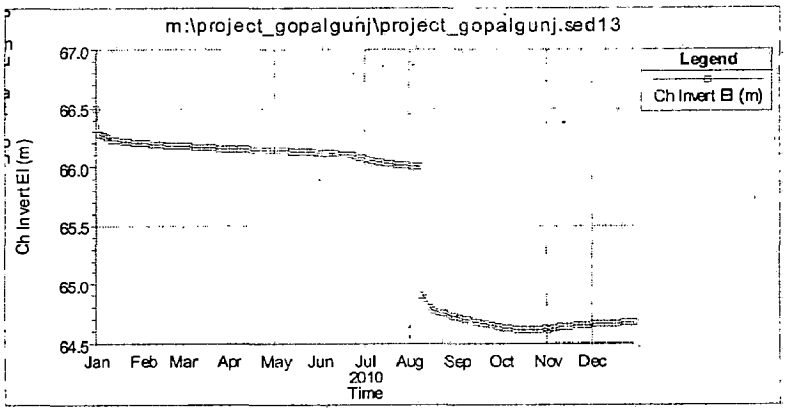

CROSS SECTION 22

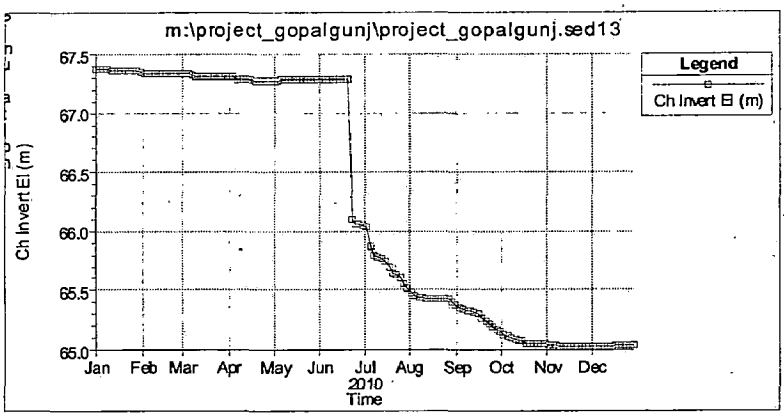

CROSS SECTION 21

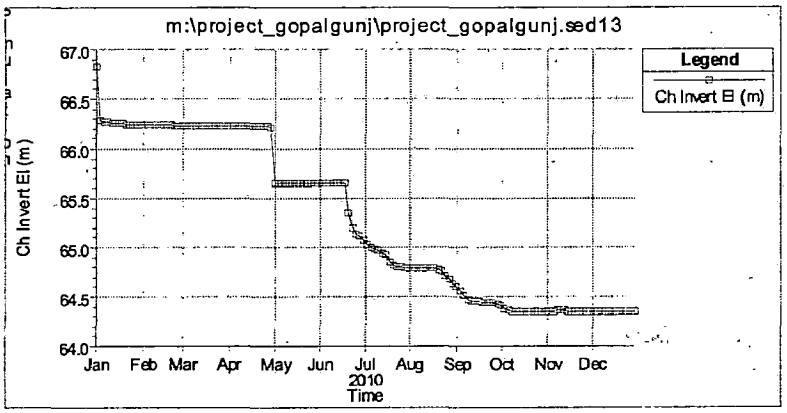

CROSS SECTION 20

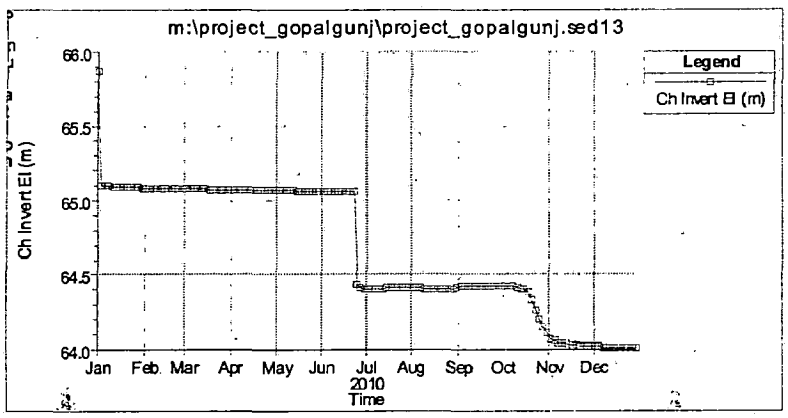

CROSS SECTION 19

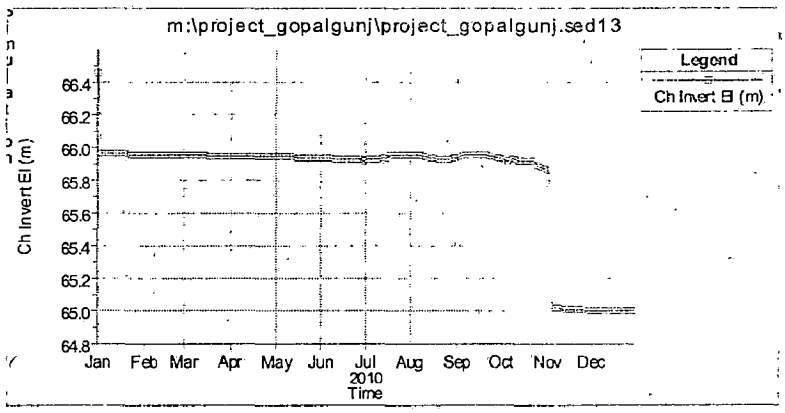

CROSS SECTION 18

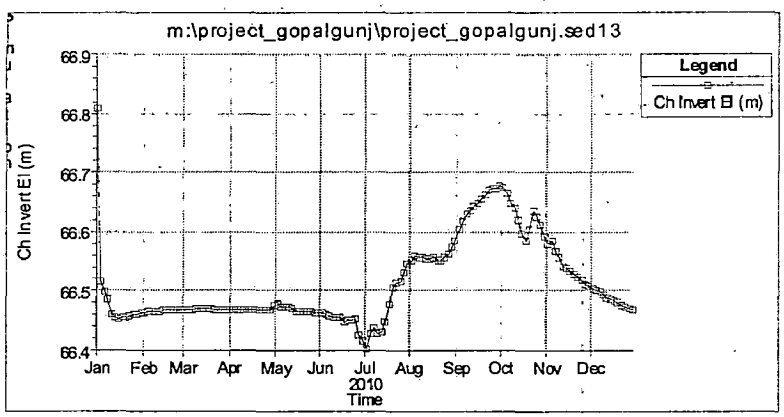

CROSS SECTION 17

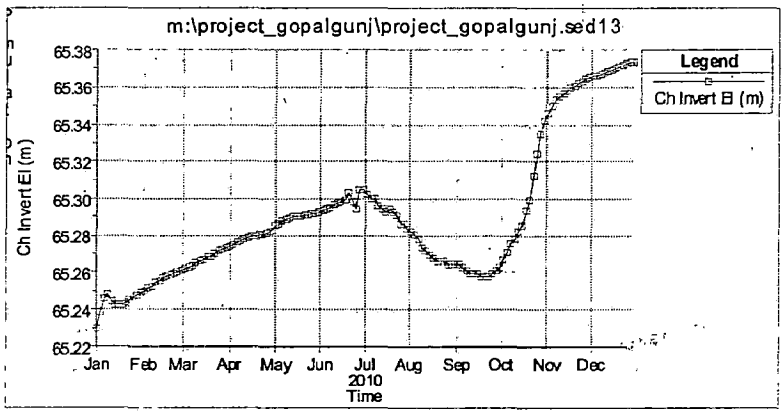

CROSS SECTION 16

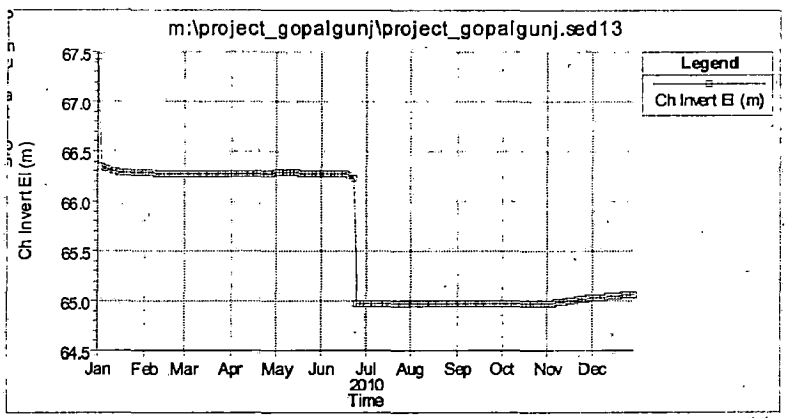

CROSS SECTION 15

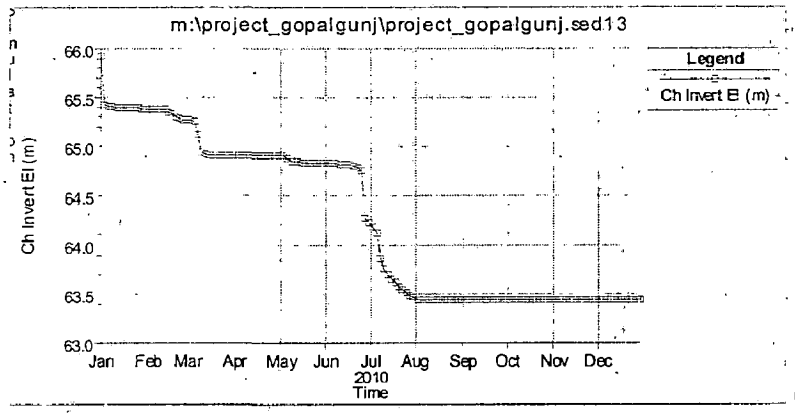

CROSS SECTION 14

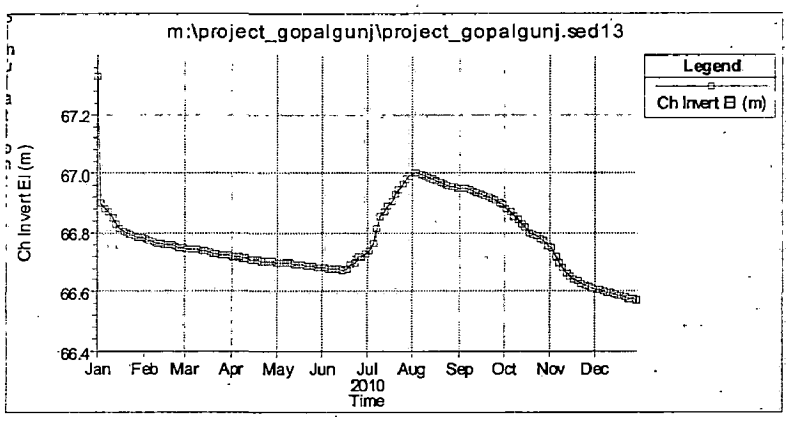

CROSS SECTION 13

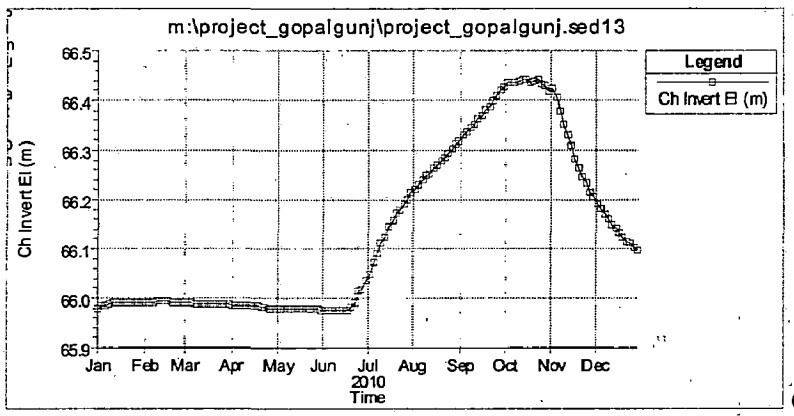

CROSS SECTION 12

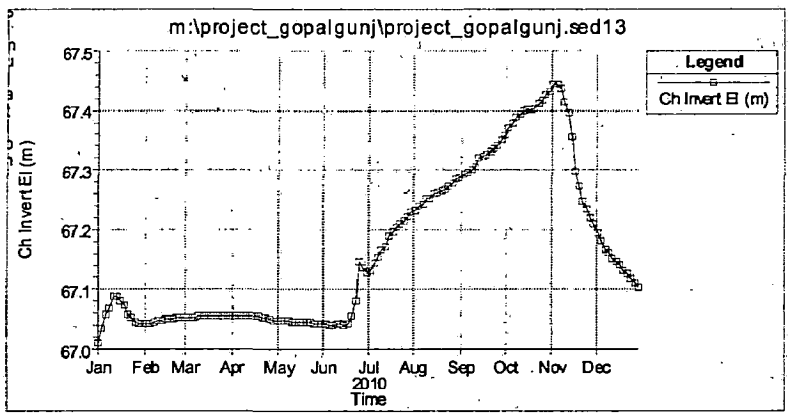

CROSS SECTION 11

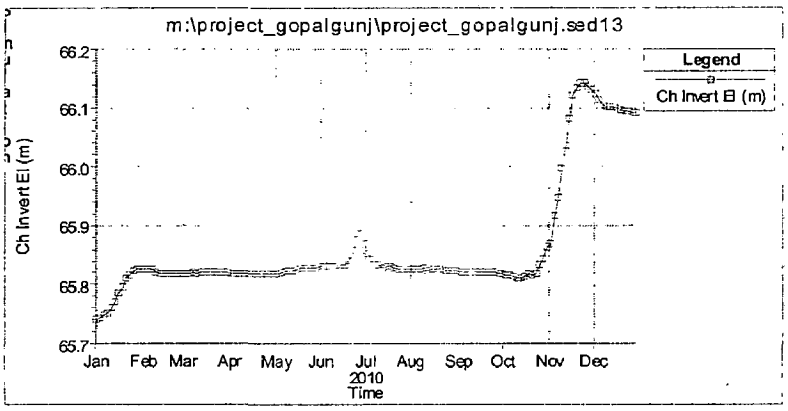

CROSS SECTION 10

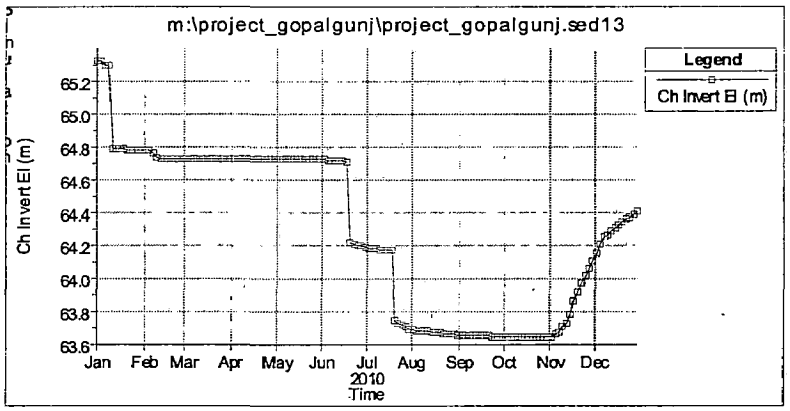

CROSS SECTION 09

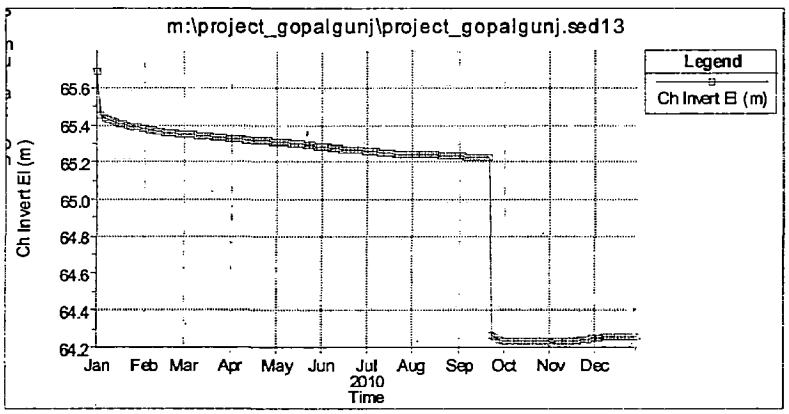

CROSS SECTION 08

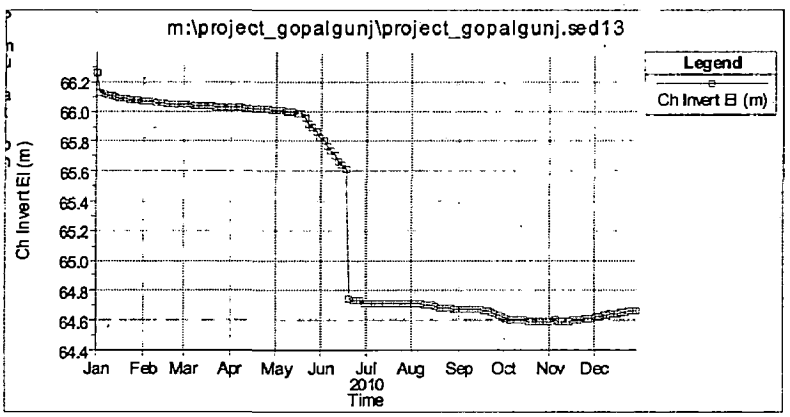

CROSS SECTION 07

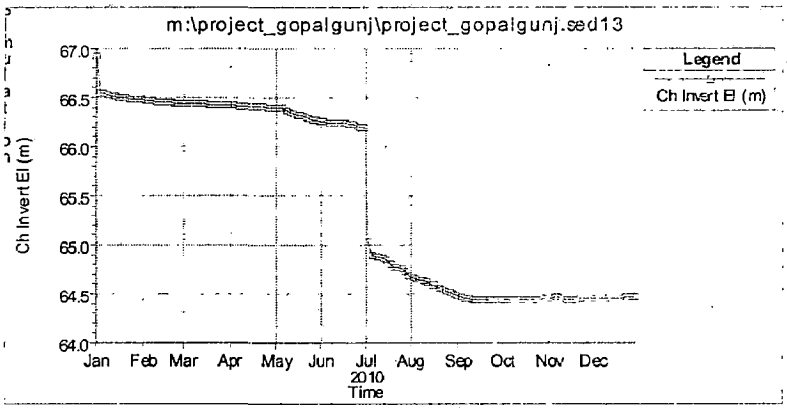

CROSS SECTION 06

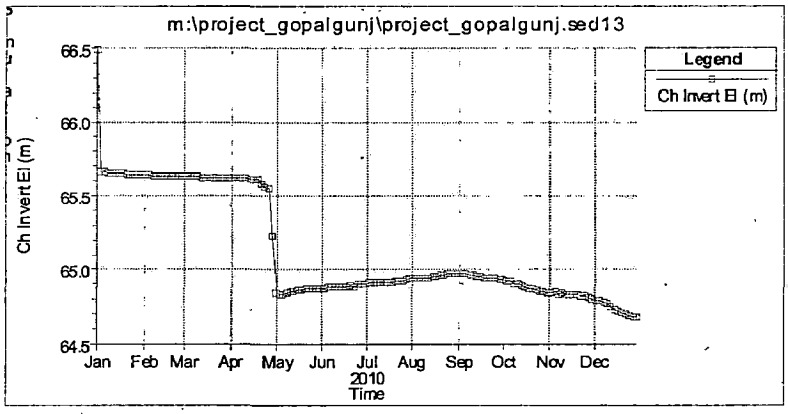

CROSS SECTION 05

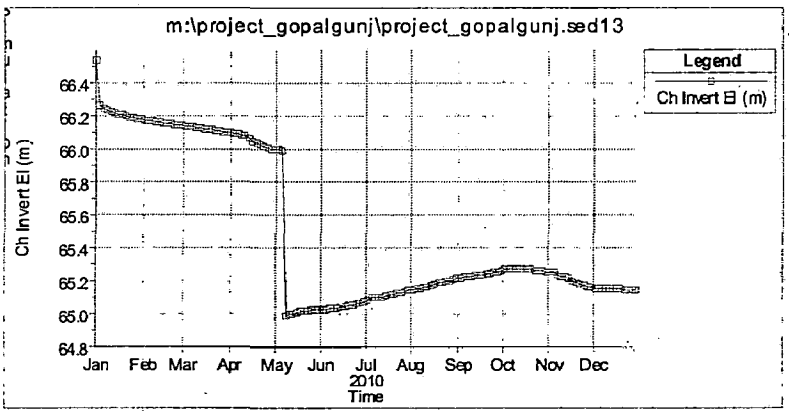

CROSS SECTION 04

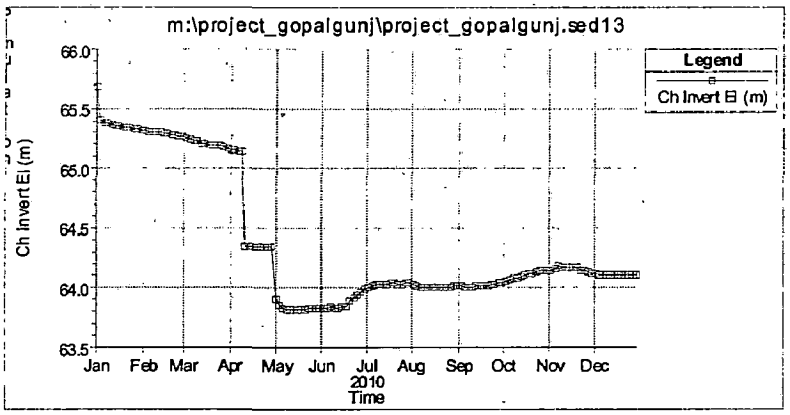

CROSS SECTION 03

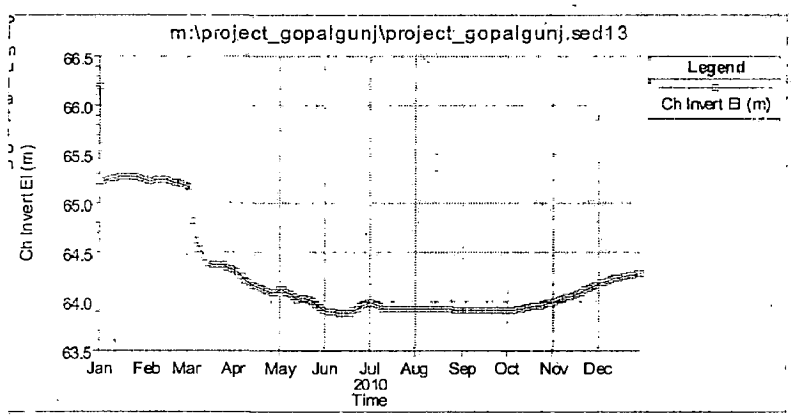

CROSS SECTION 02

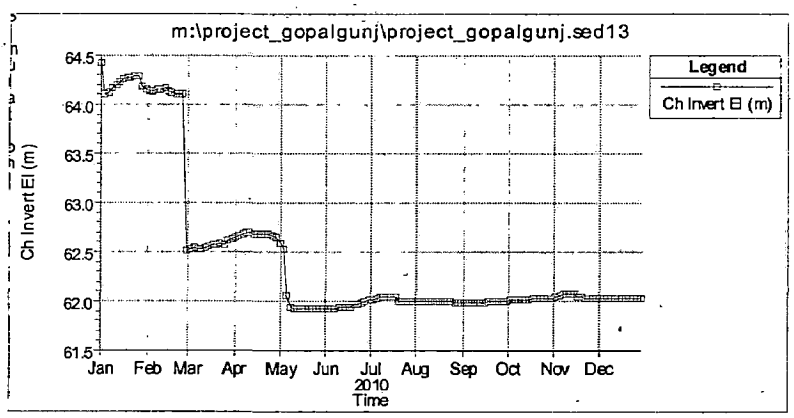

CROSS SECTION 01

CROSS-SECTION WISE TEMPORAL THALWEG CHANGES OF GANDAK REACH BY ACKER-WHITE PREDICTOR

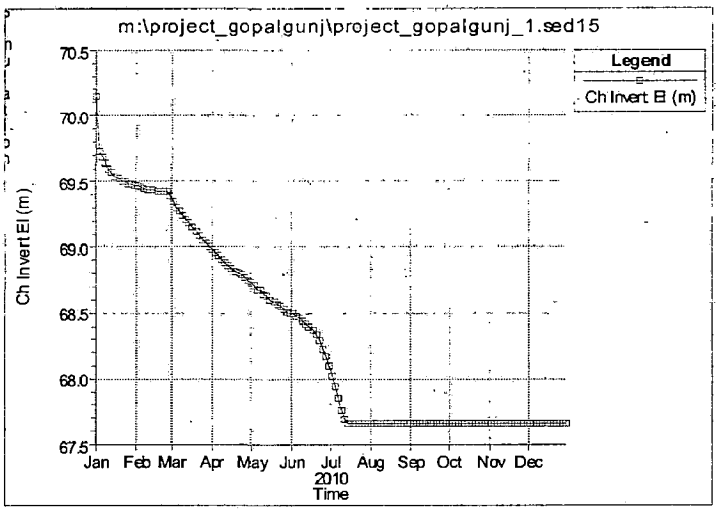

CROSS SECTION 30

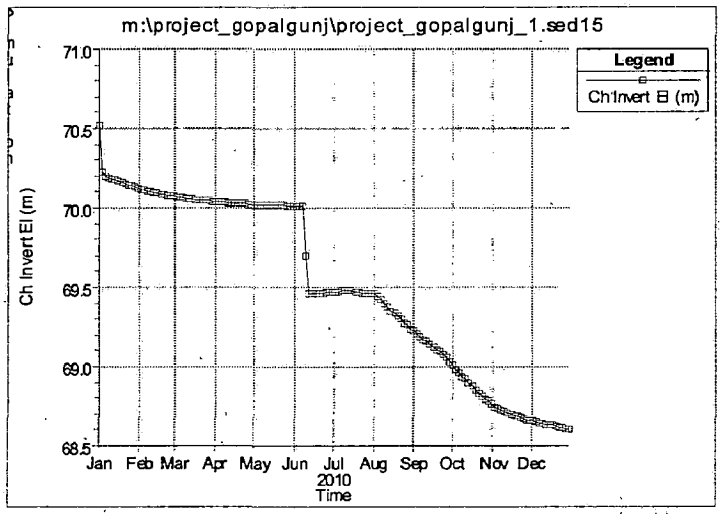

CROSS SECTION 29

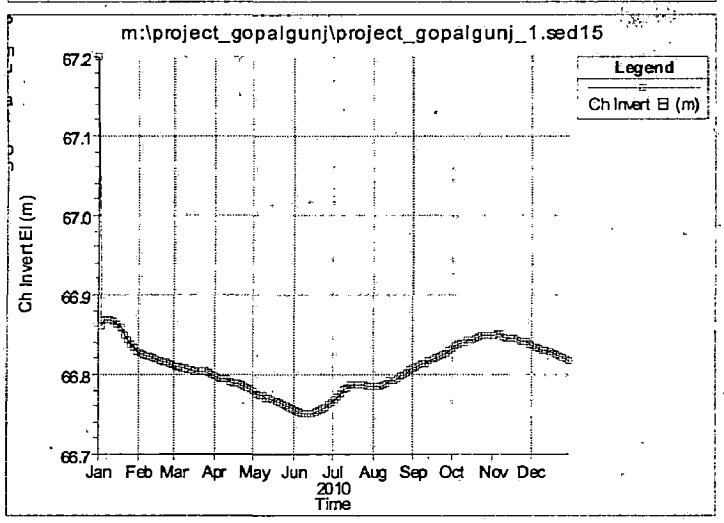

CROSS SECTION 28

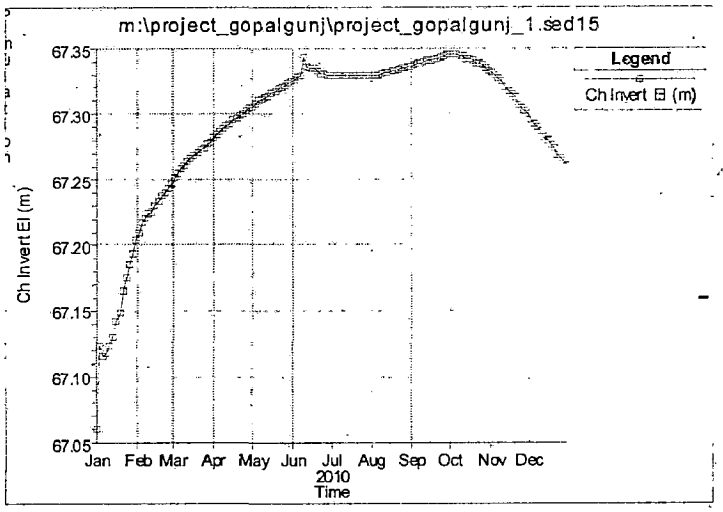

CROSS SECTION 27

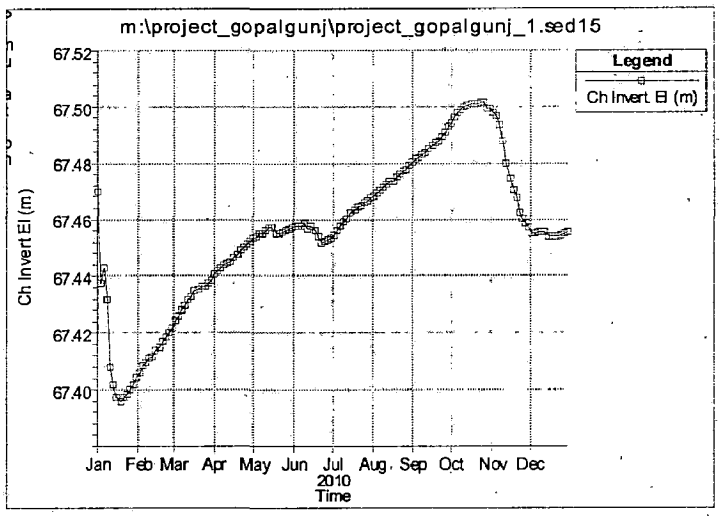

CROSS SECTION 26

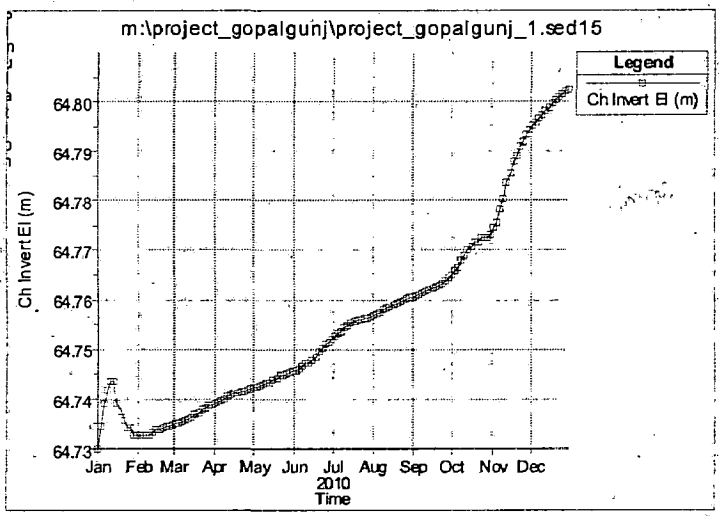

CROSS SECTION 25

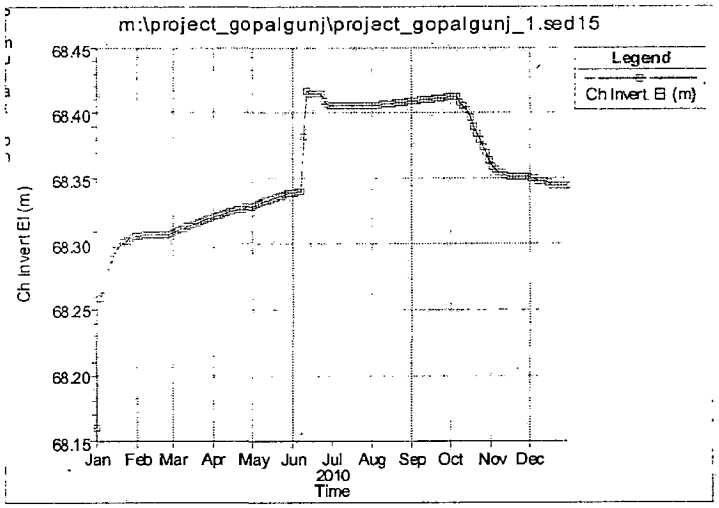

CROSS SECTION 24

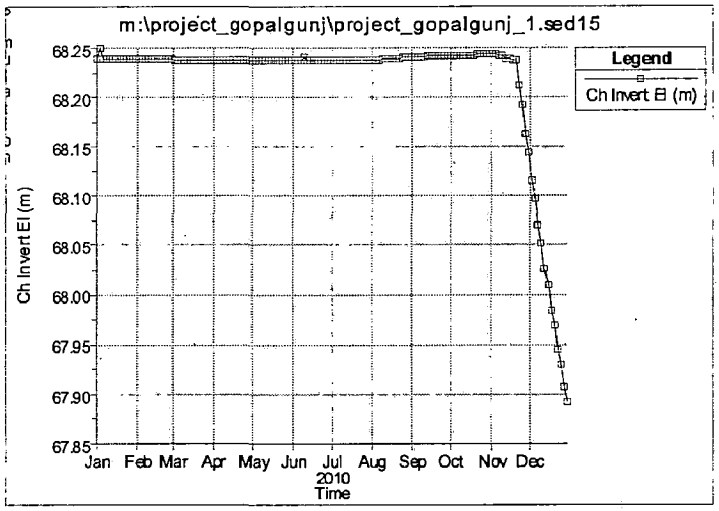

CROSS SECTION 23

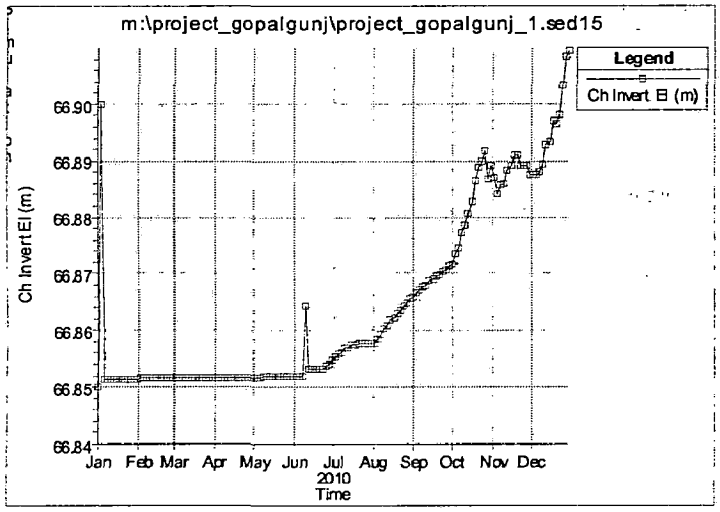

CROSS SECTION 22

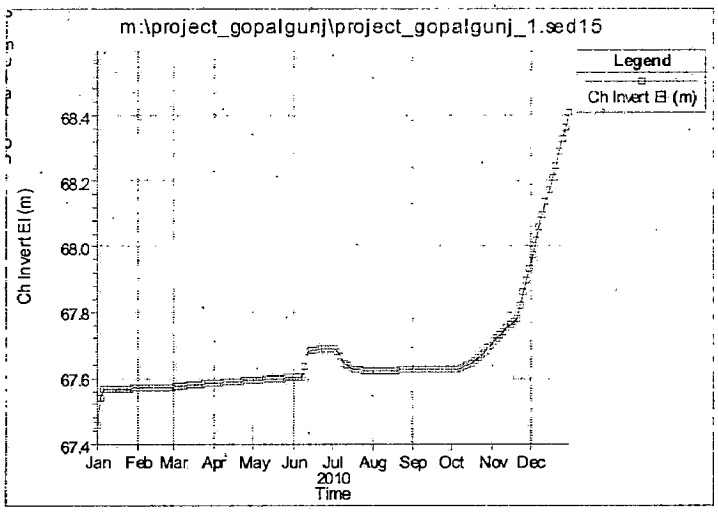

CROSS SECTION 21

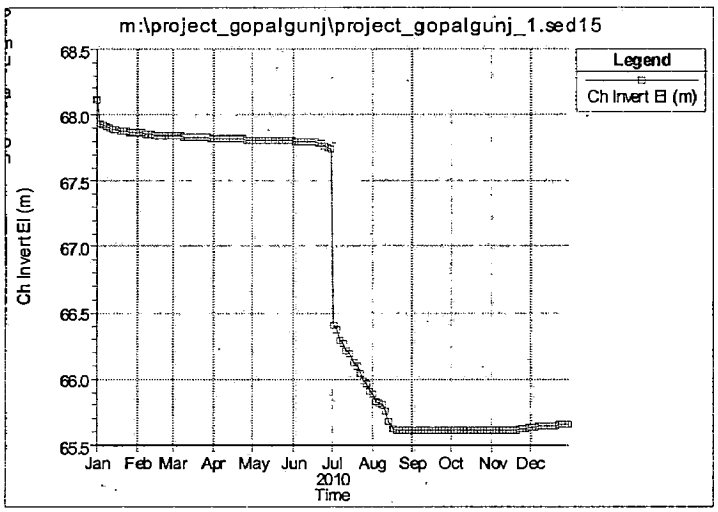

CROSS SECTION 20

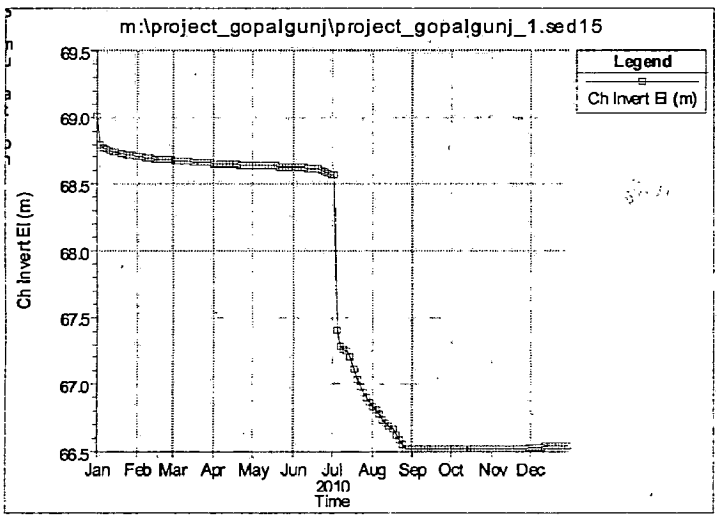

CROSS SECTION 19

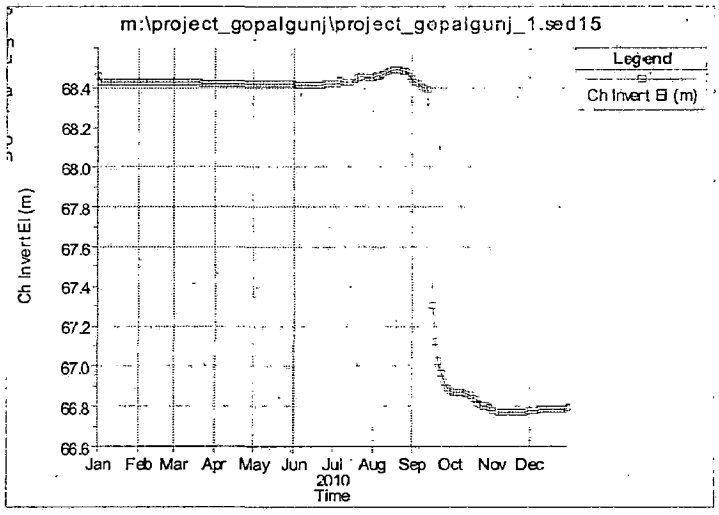

CROSS SECTION 18

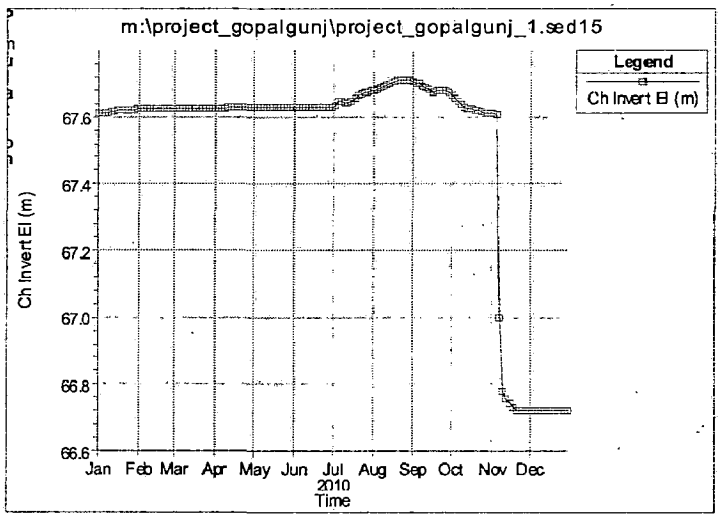

CROSS SECTION 17

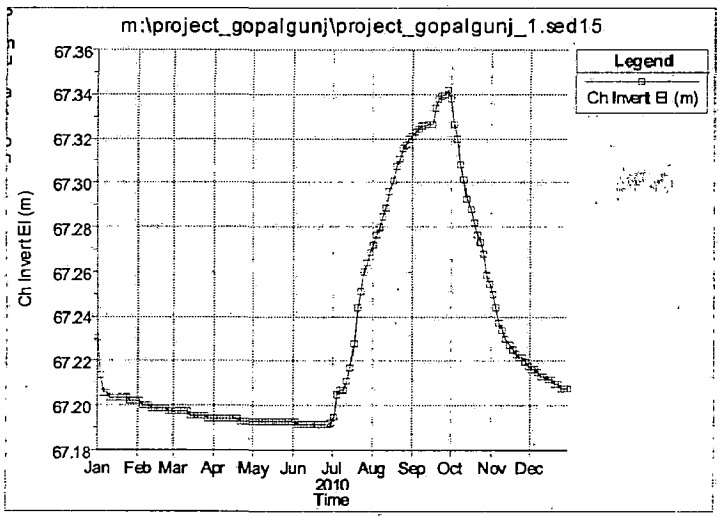

CROSS SECTION 16

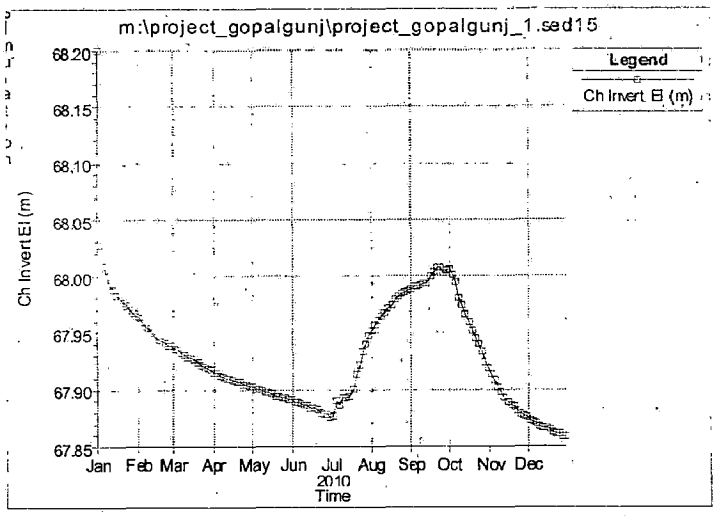

CROSS SECTION 15

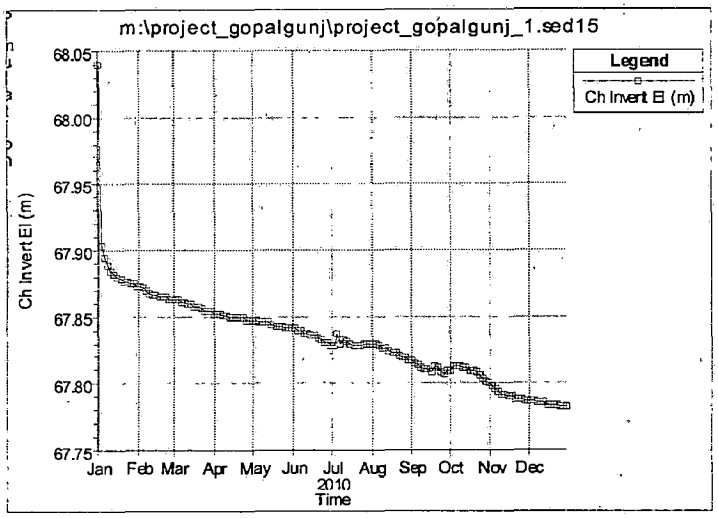

CROSS SECTION 14

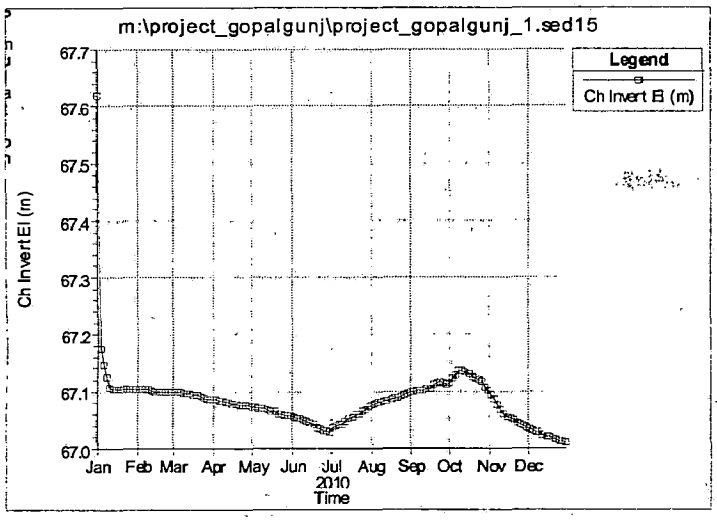

CROSS SECTION 13

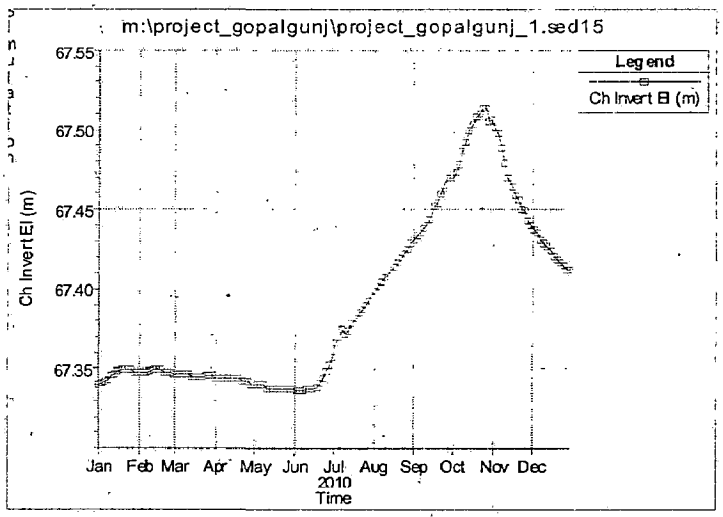

CROSS SECTION 12

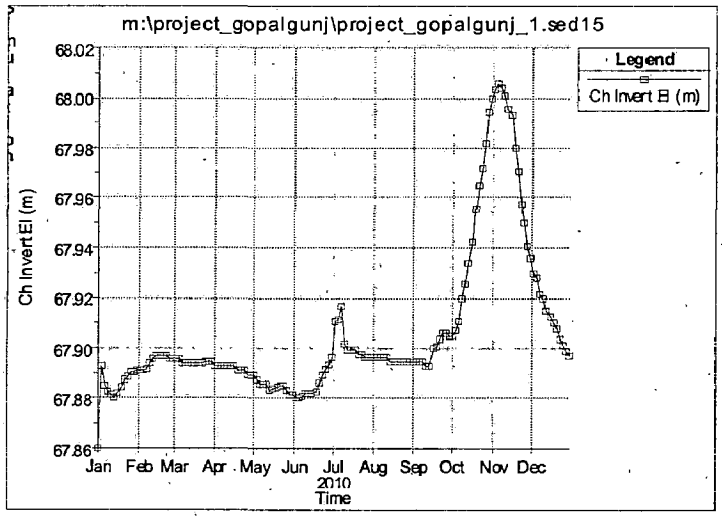

CROSS SECTION 11

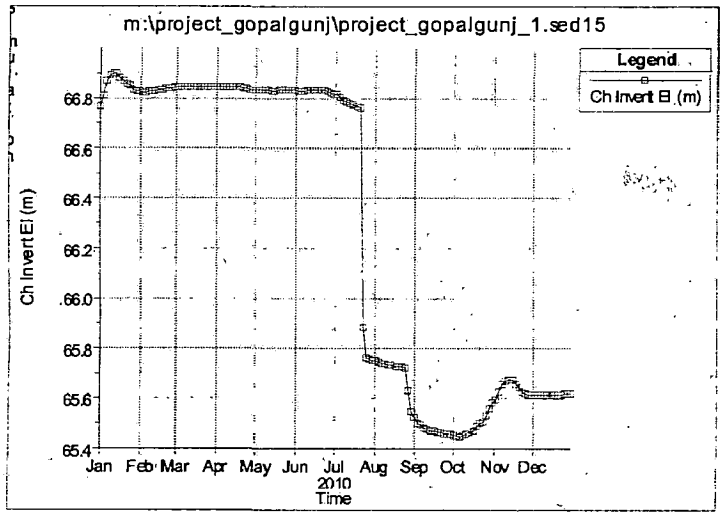

CROSS SECTION 10

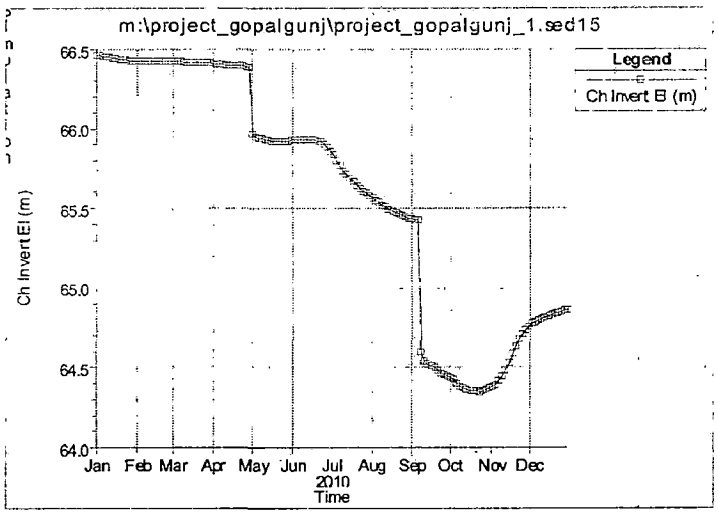

CROSS SECTION 09

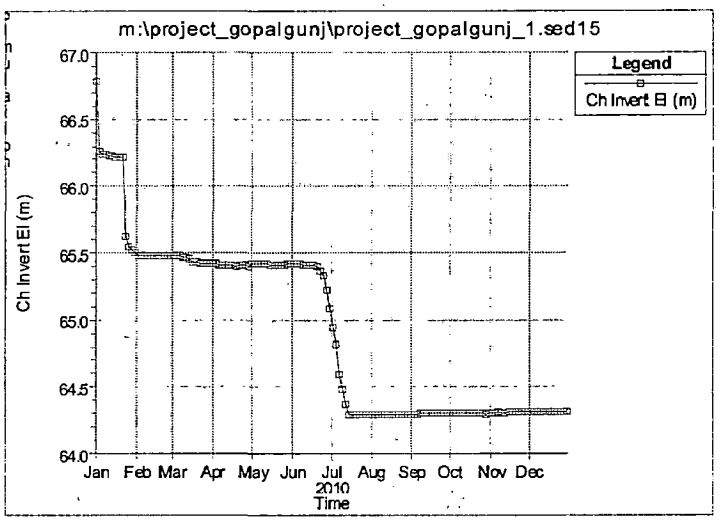

CROSS SECTION 08

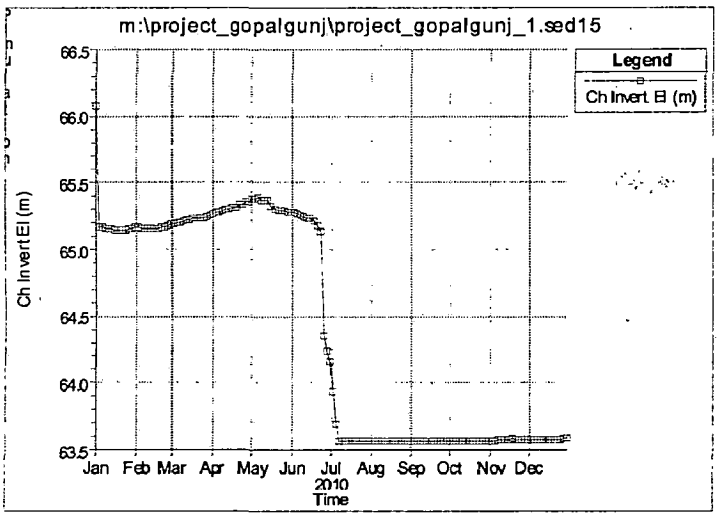

CROSS SECTION 07

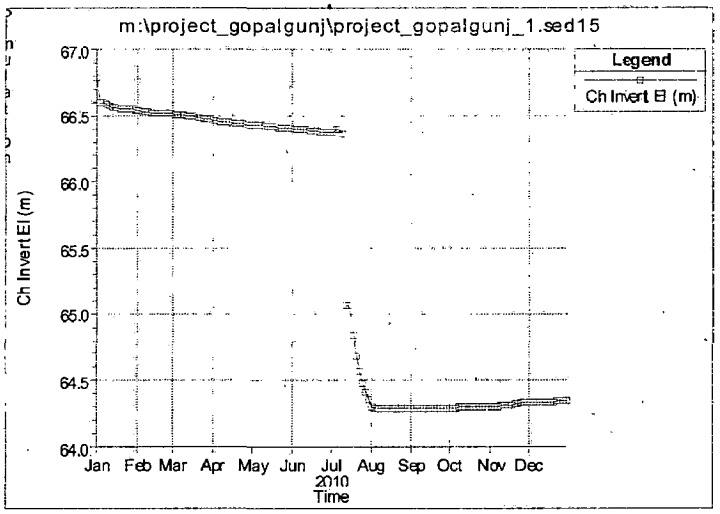

CROSS SECTION 06

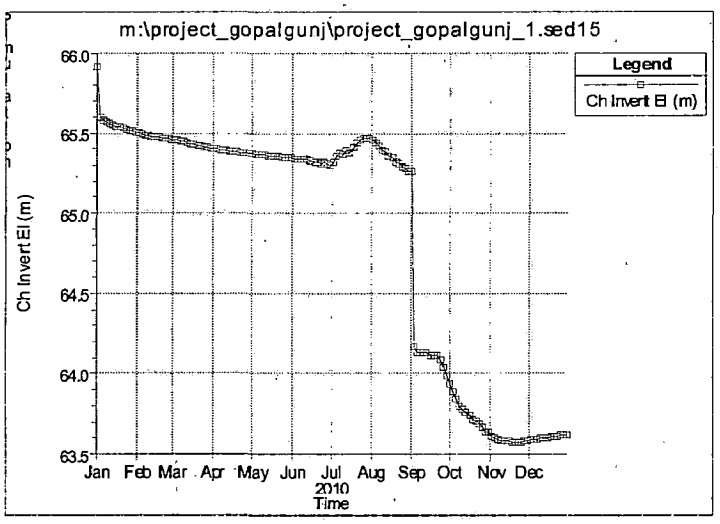

CROSS SECTION 05

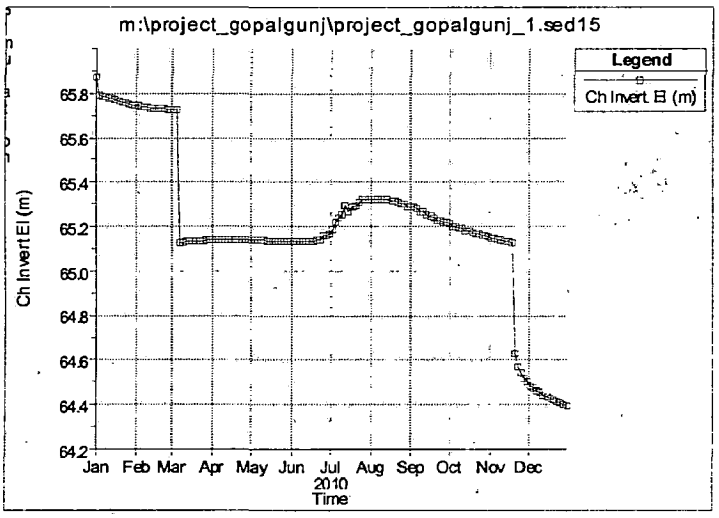

CROSS SECTION 04

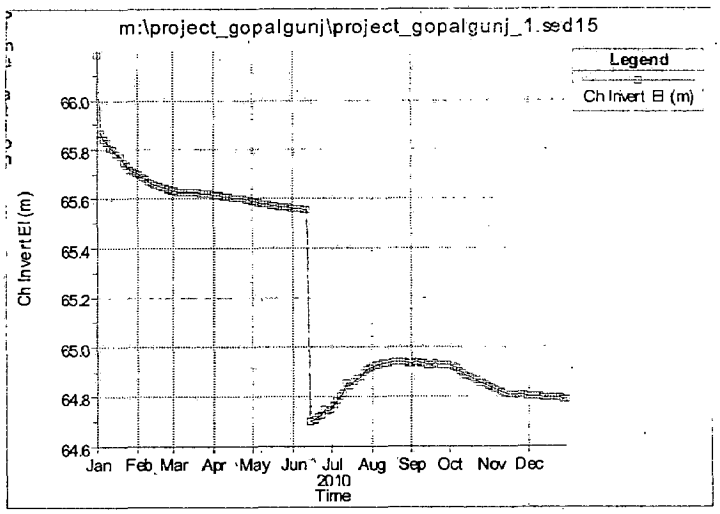

CROSS SECTION 03

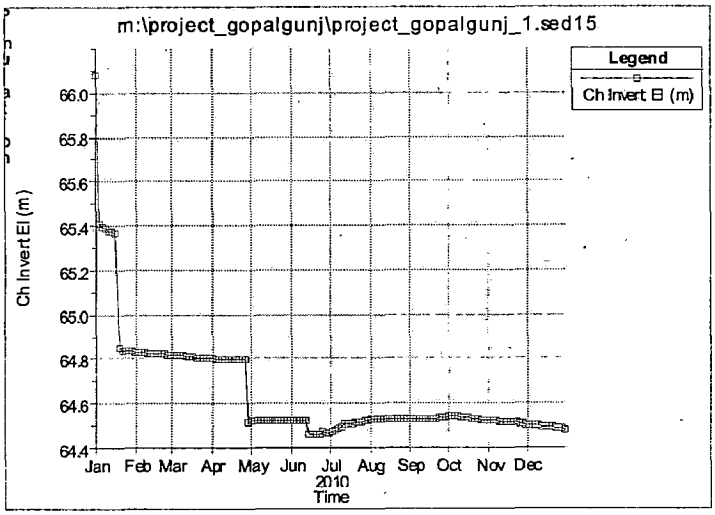

CROSS SECTION 02

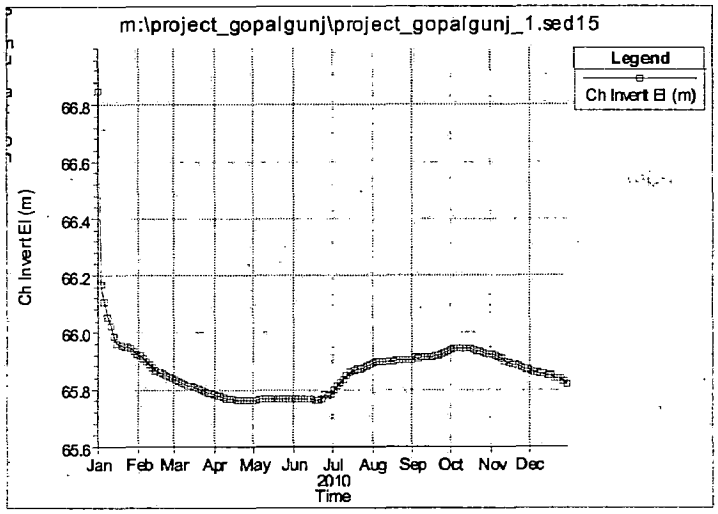

CROSS SECTION 01

CROSS-SECTION WISE TEMPORAL THALWEG CHANGES OF BASI REACH BY YANG PREDICTOR

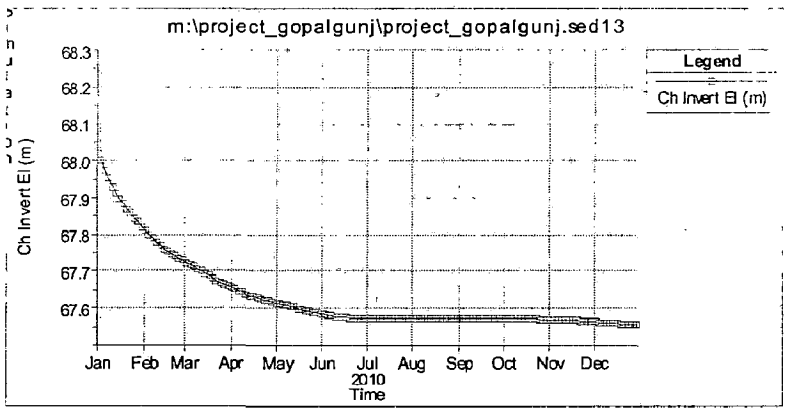

CROSS SECTION 29

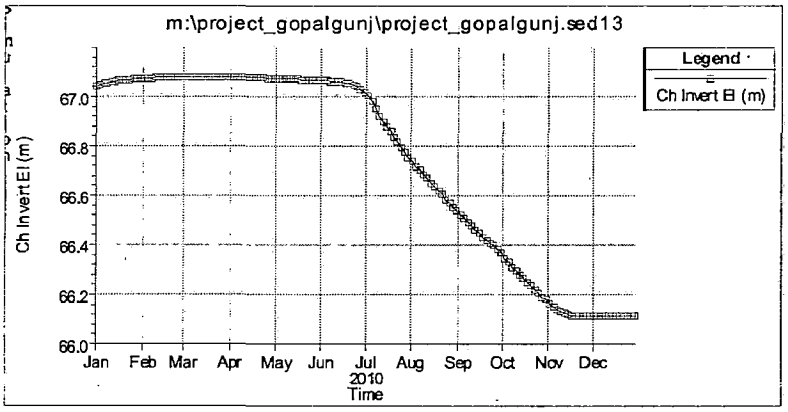

CROSS SECTION 28

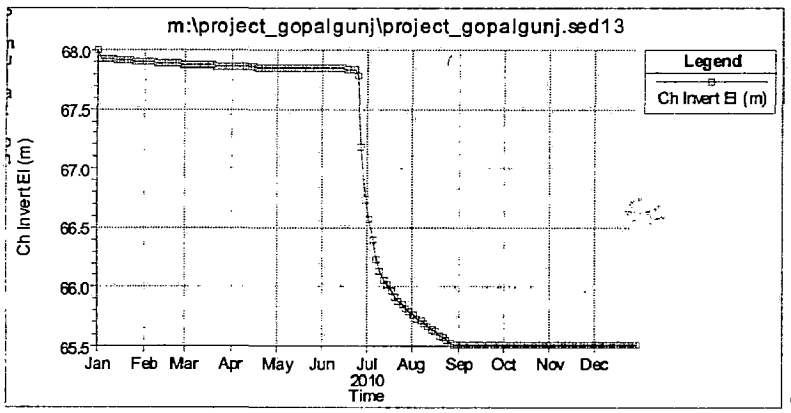

CROSS SECTION 27

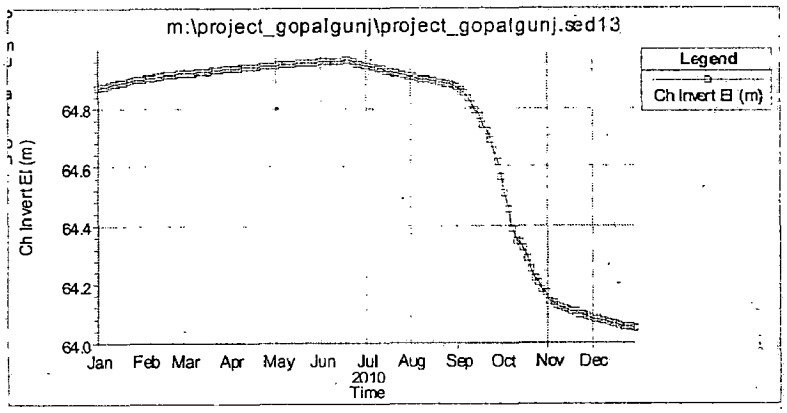

CROSS SECTION 26

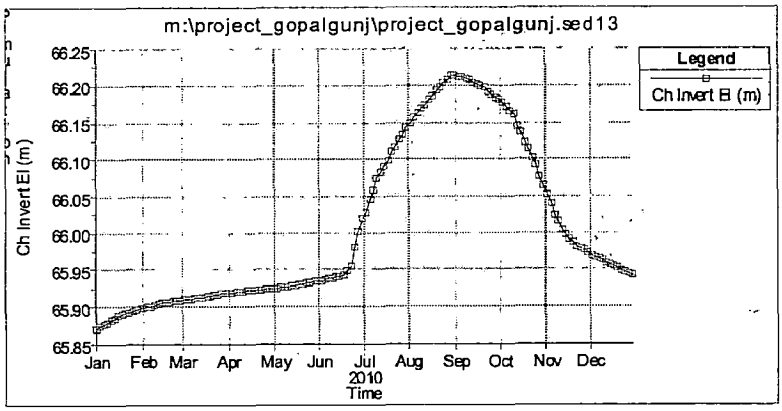

CROSS SECTION 25

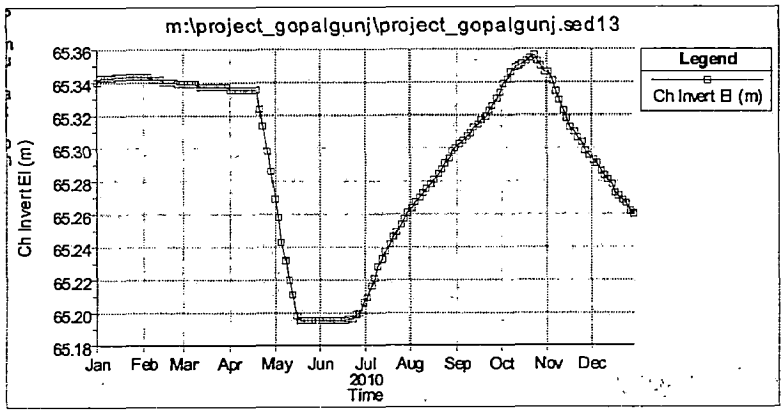

CROSS SECTION 24

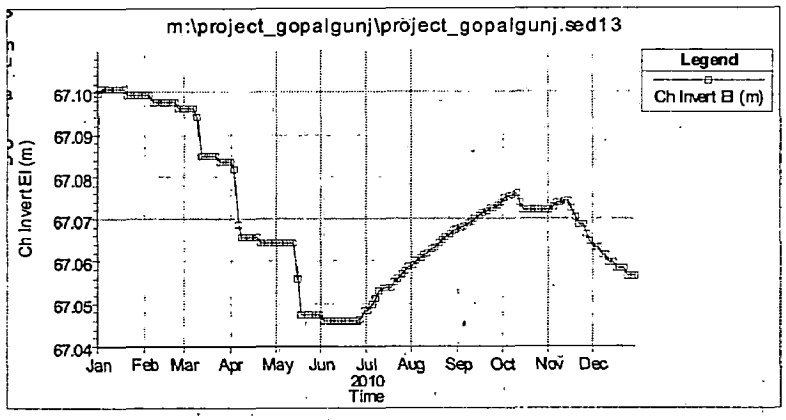

CROSS SECTION 23

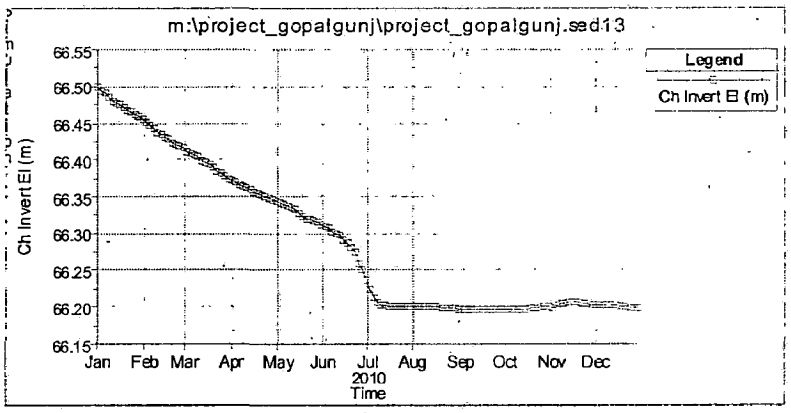

CROSS SECTION 22

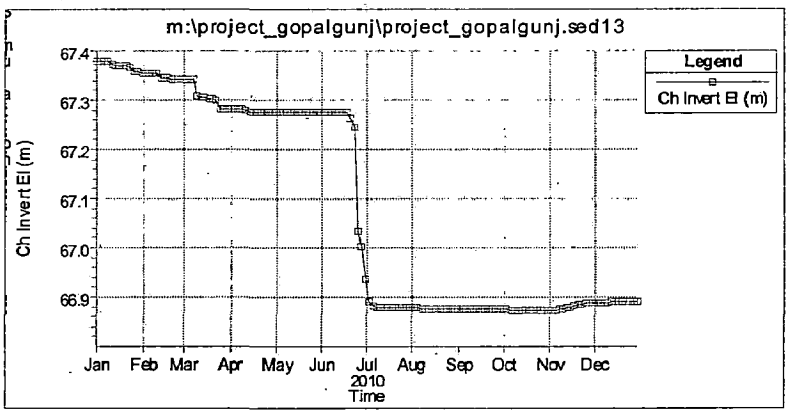

CROSS SECTION 21

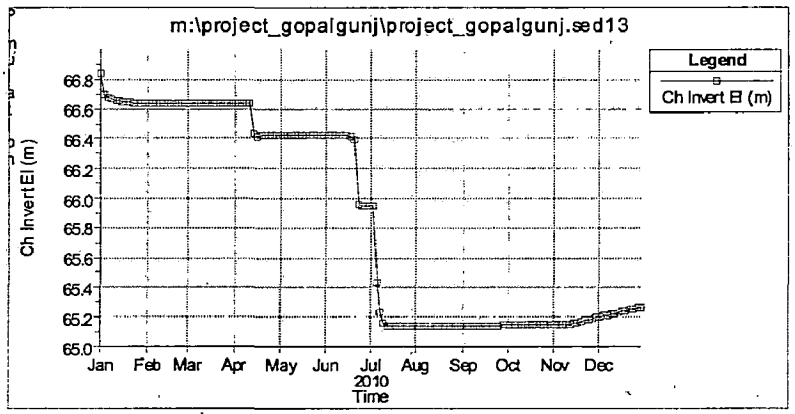

CROSS SECTION 20

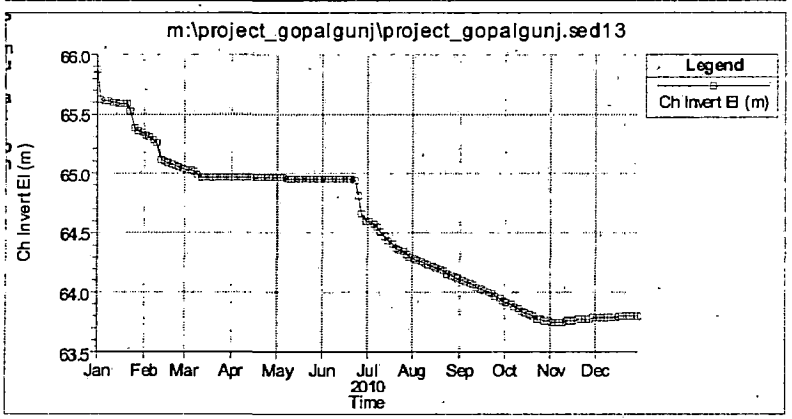

CROSS SECTION 19

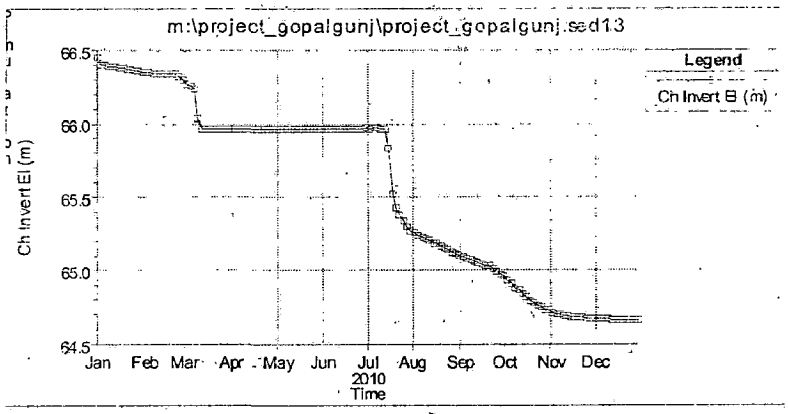

CROSS SECTION 18

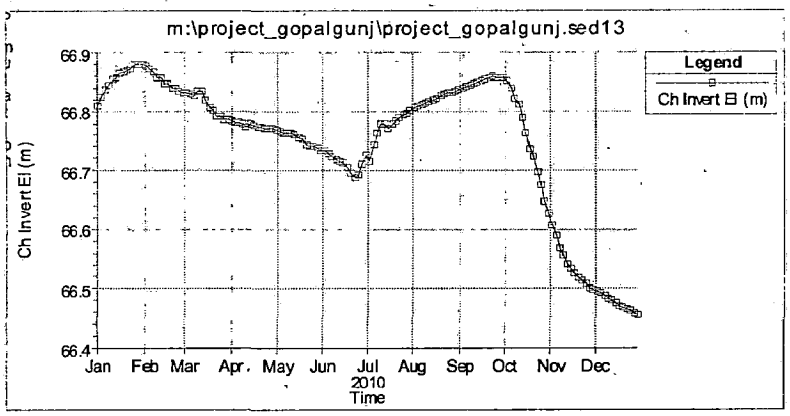

CROSS SECTION 17

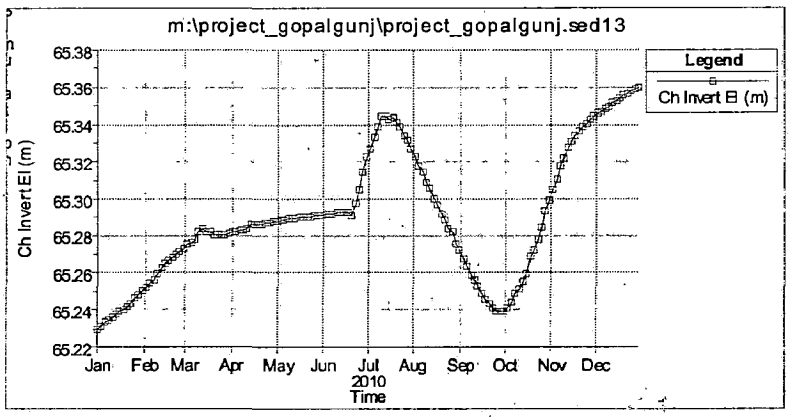

CROSS SECTION 16

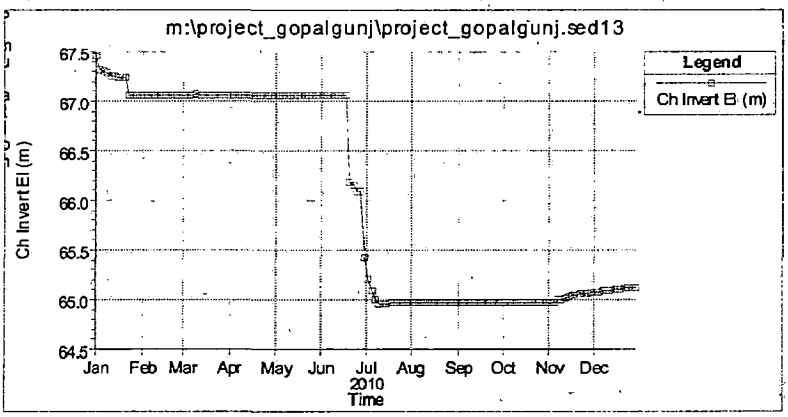

CROSS SECTION 15

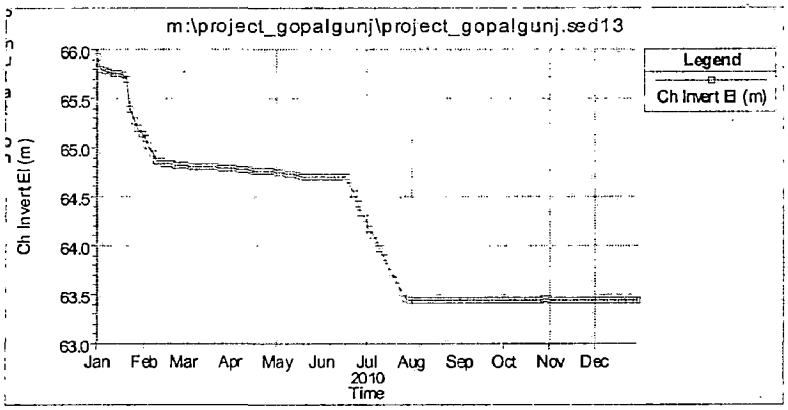

CROSS SECTION 14

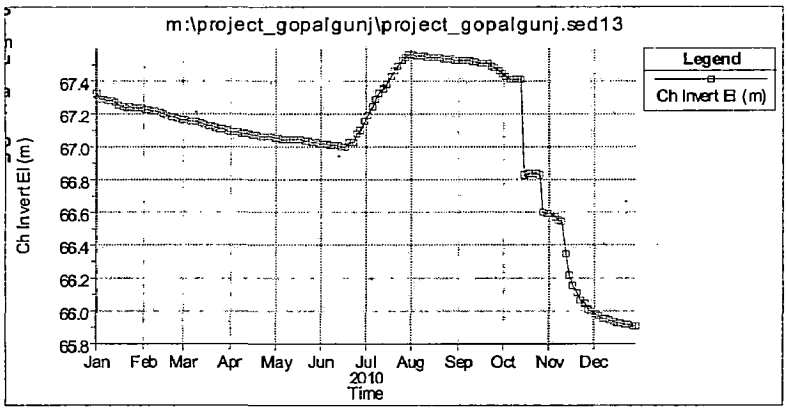

CROSS SECTION 13

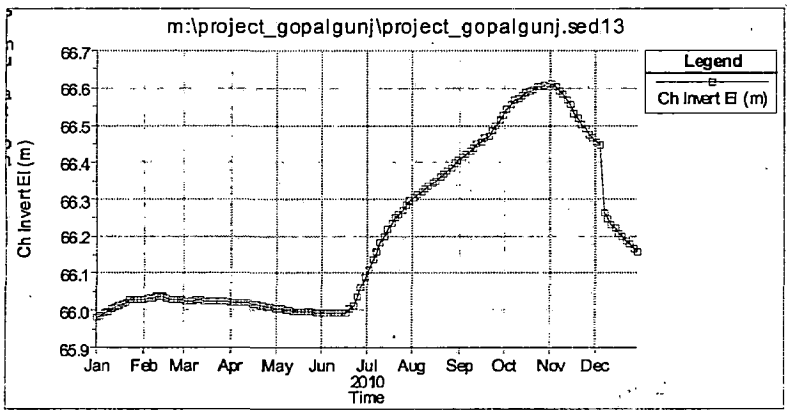

CROSS SECTION 12

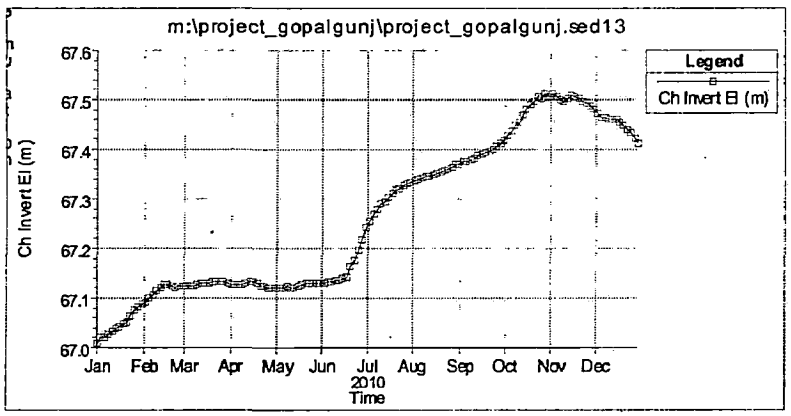

CROSS SECTION 11

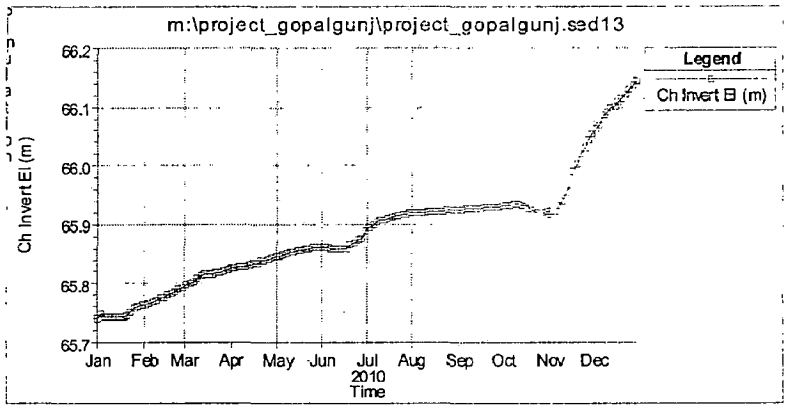

CROSS SECTION 10

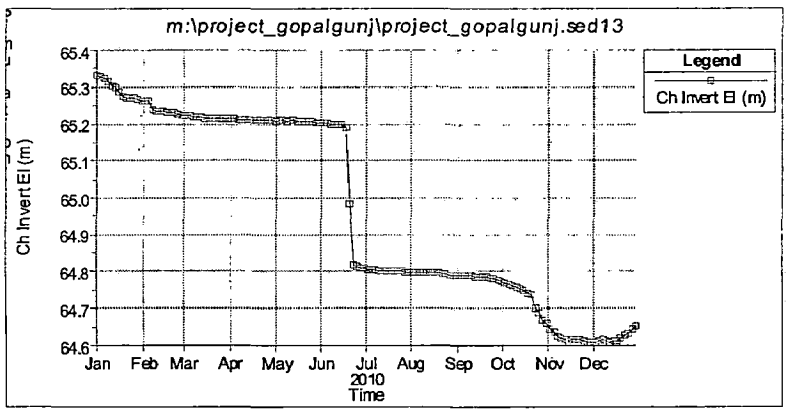

CROSS SECTION 09

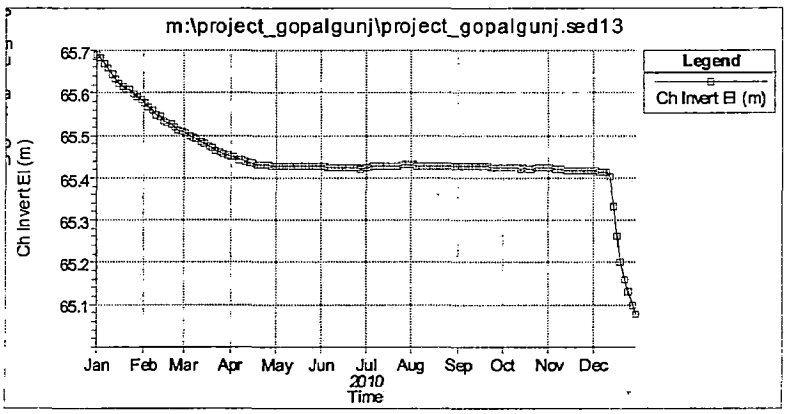

CROSS SECTION 08

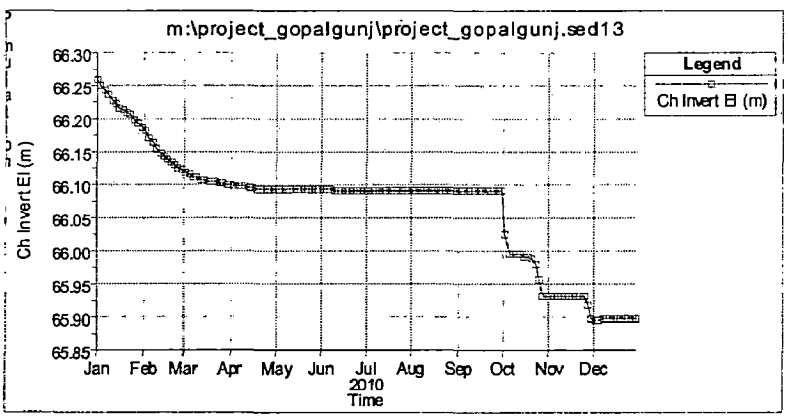

CROSS SECTION 07

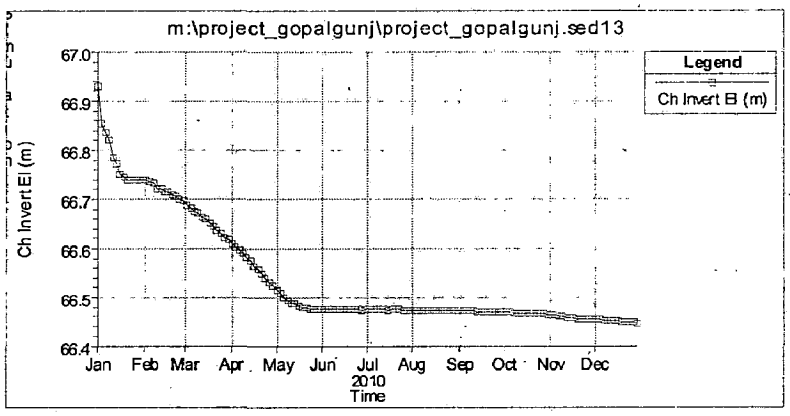

CROSS SECTION 06

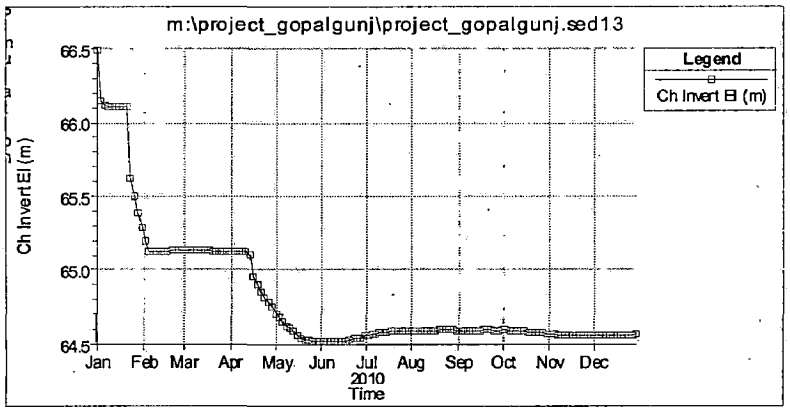

CROSS SECTION 05

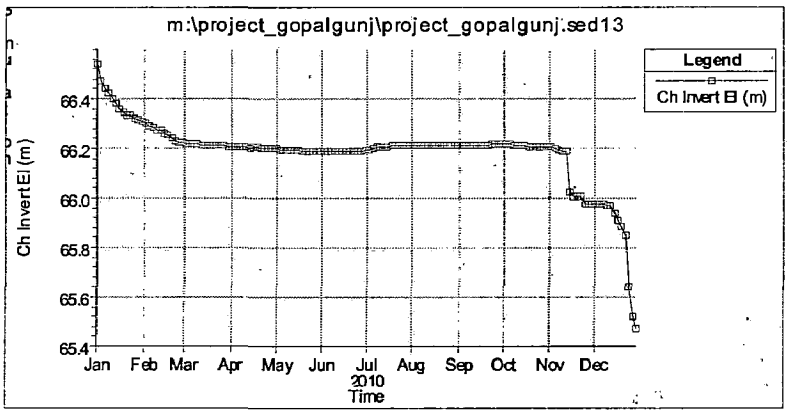

CROSS SECTION 04

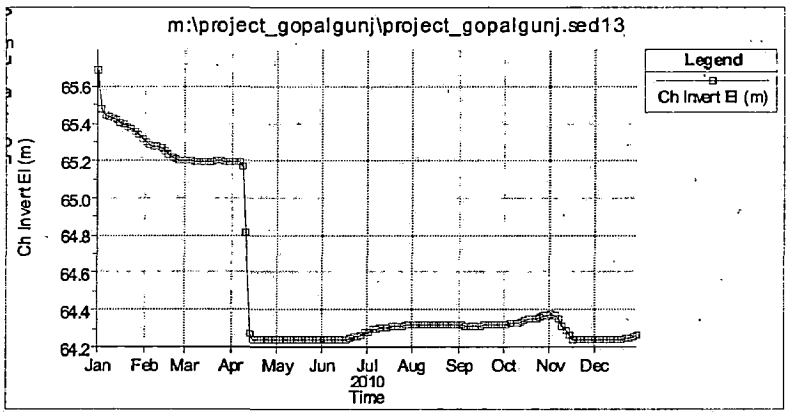

CROSS SECTION 03

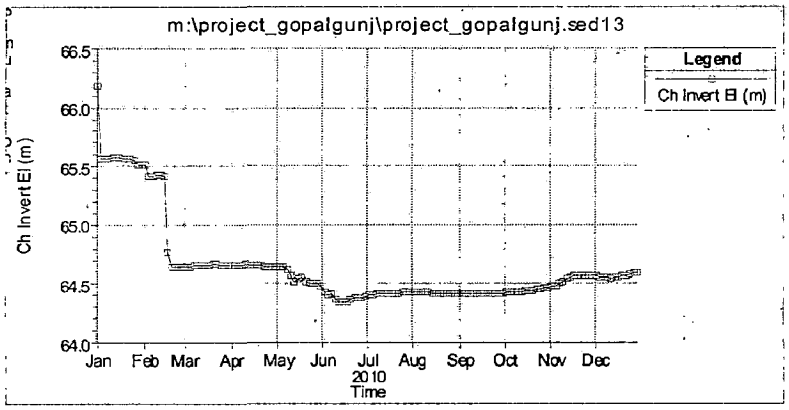

CROSS SECTION 02

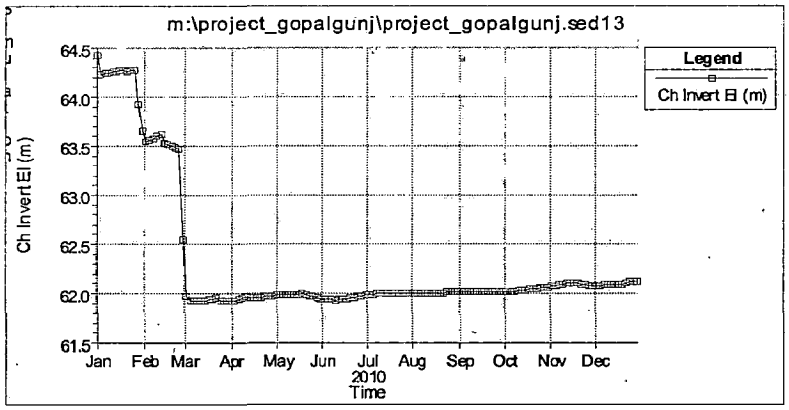

CROSS SECTION 01

CROSS-SECTION WISE TEMPORAL THALWEG CHANGES OF GANDAK REACH BY YANG PREDICTOR

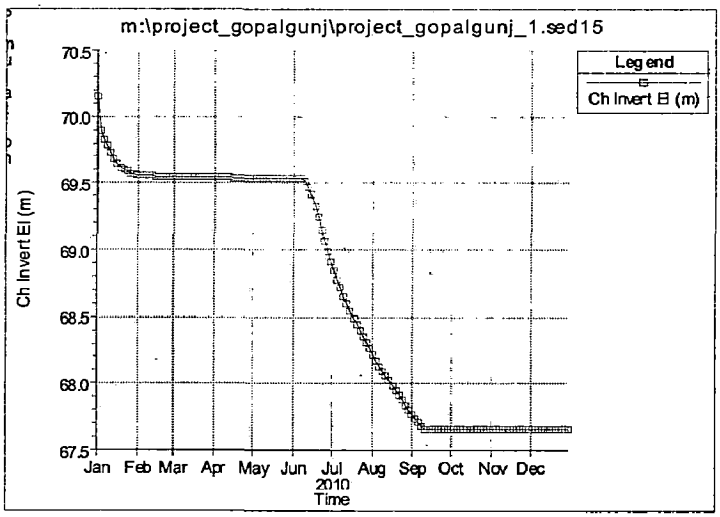

CROSS SECTION 30

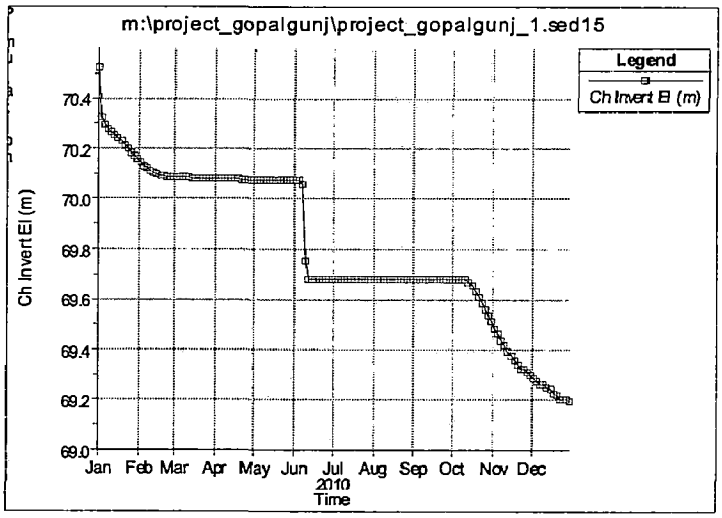

CROSS SECTION 29

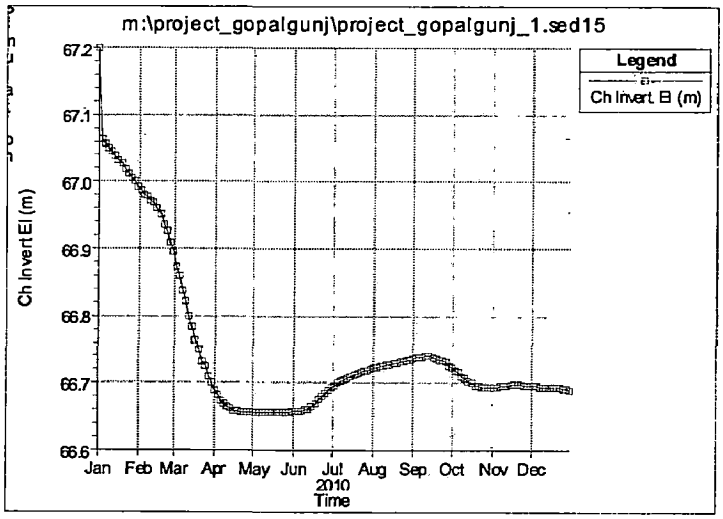

CROSS SECTION 28

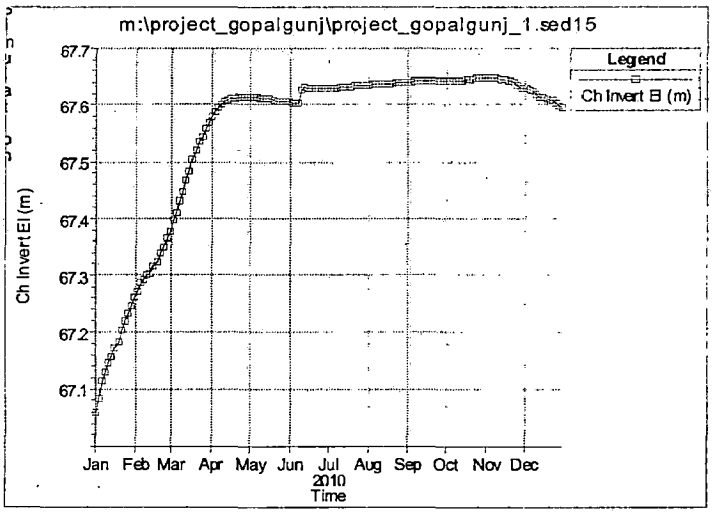

CROSS SECTION 27

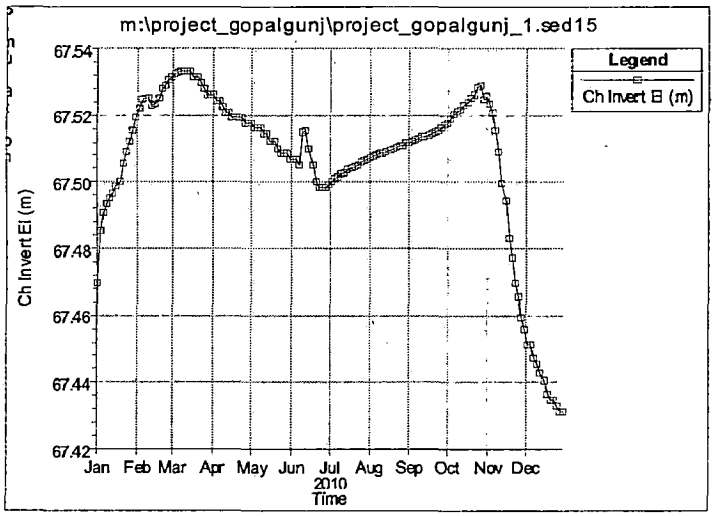

CROSS SECTION 26

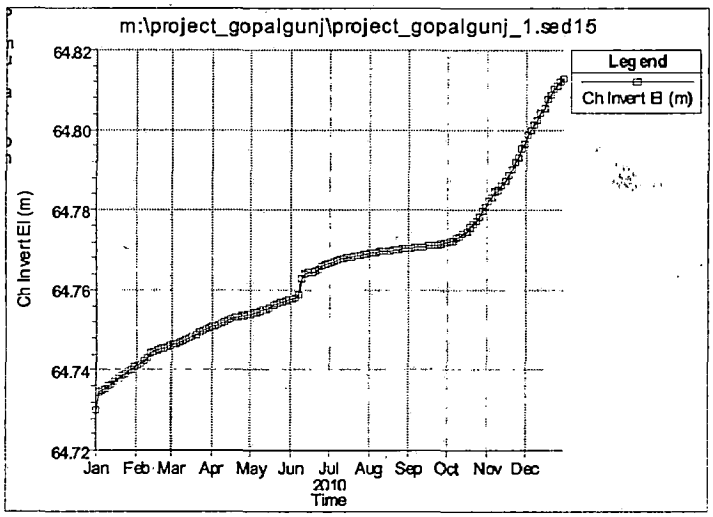

CROSS SECTION 25

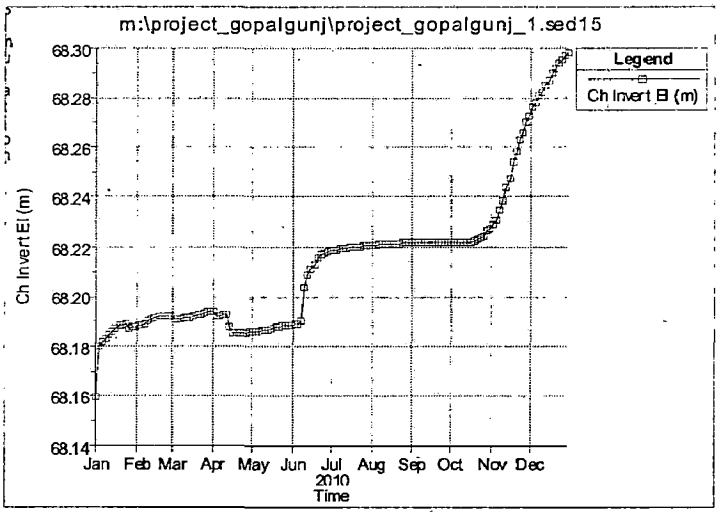

CROSS SECTION 24

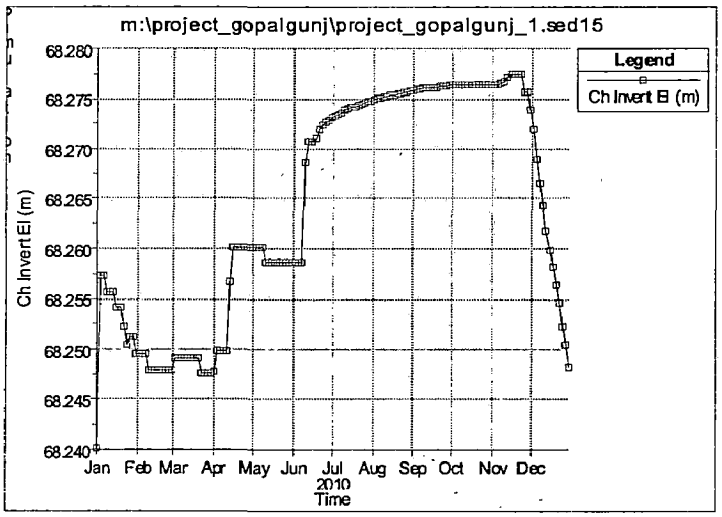

CROSS SECTION 23

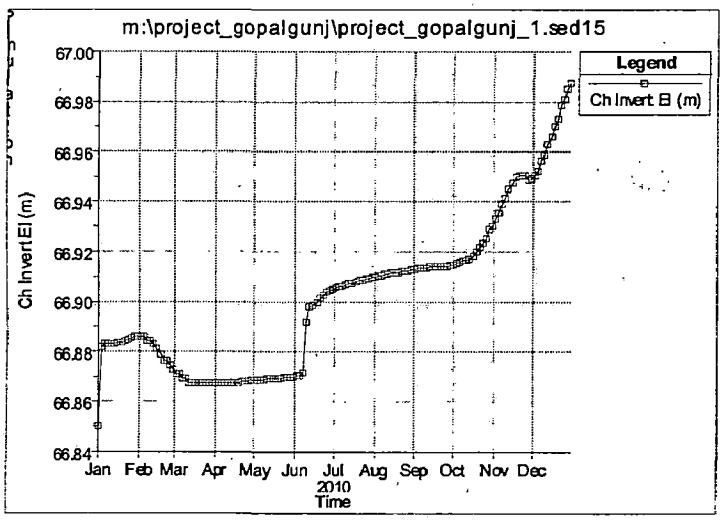

CROSS SECTION 22

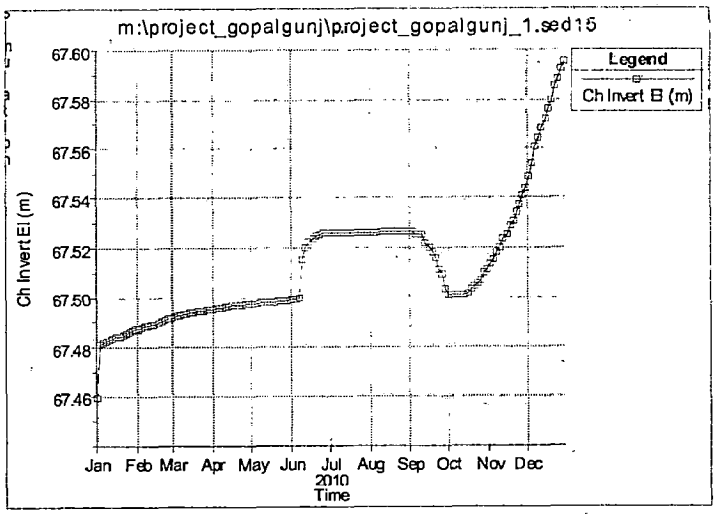

CROSS SECTION 21

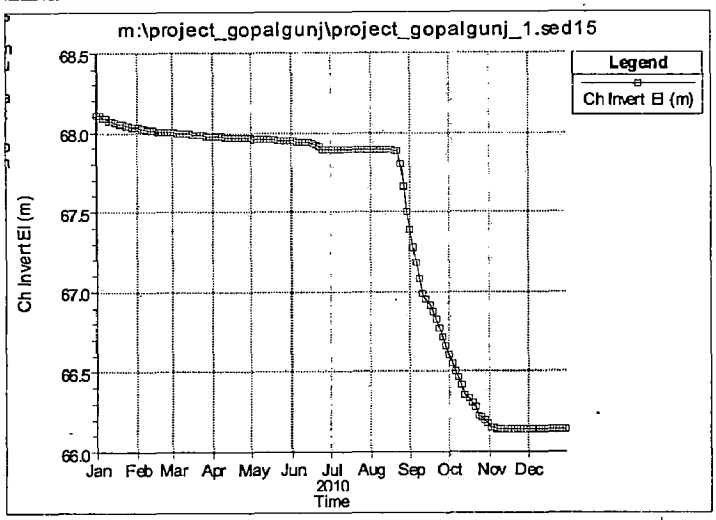

CROSS SECTION 20

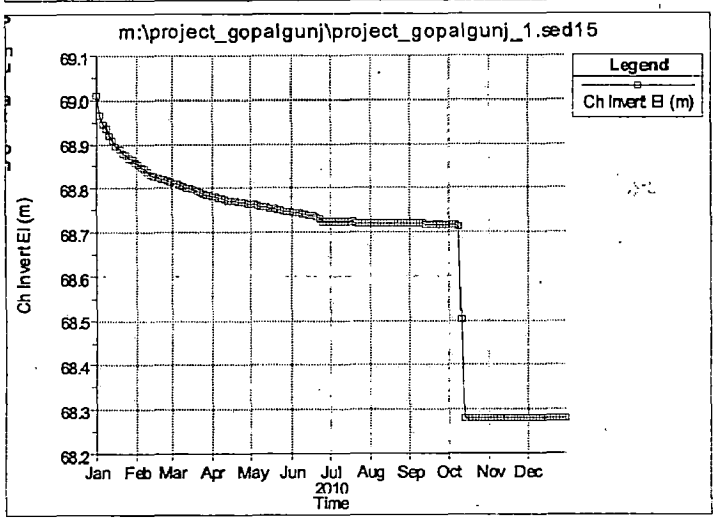

CROSS SECTION 19

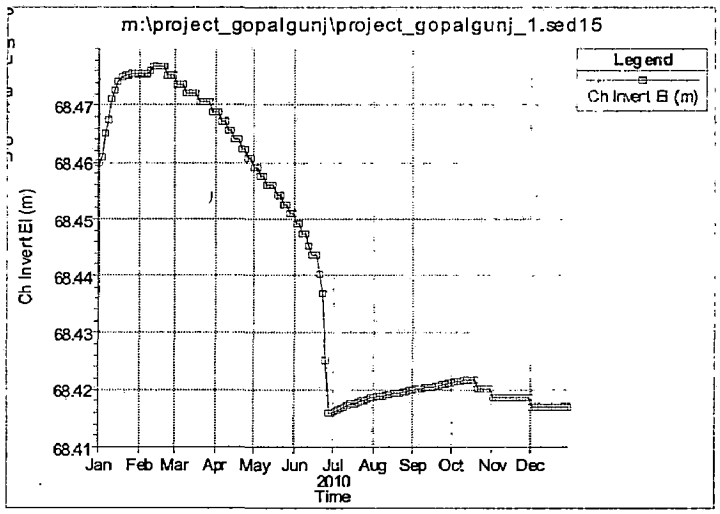

CROSS SECTION 18

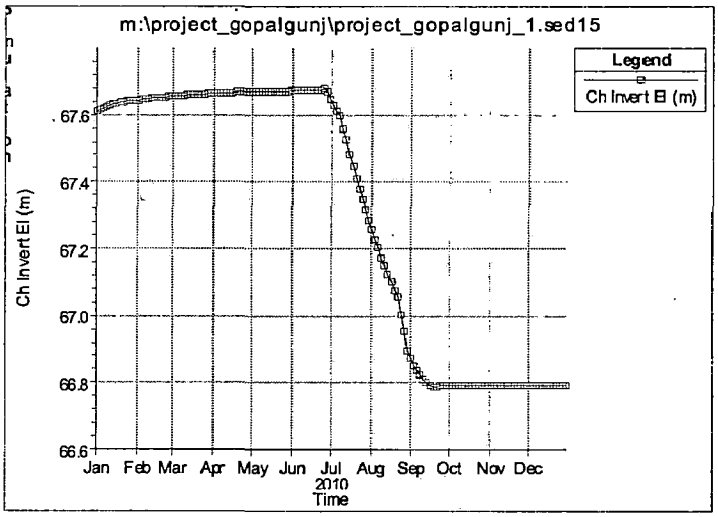

CROSS SECTION 17

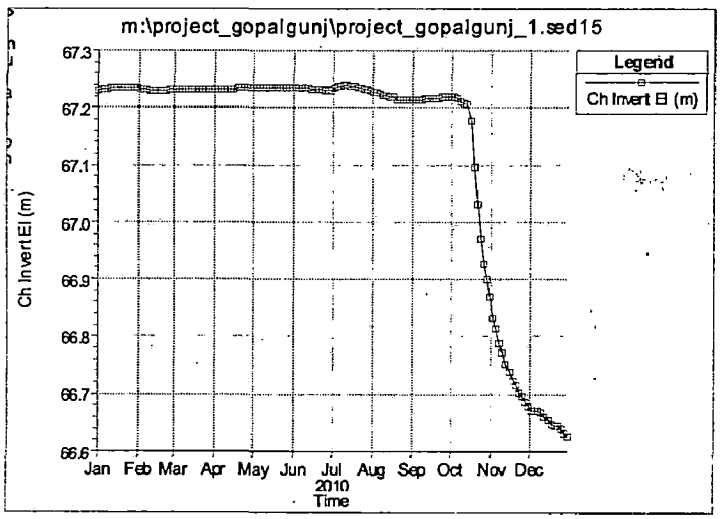

CROSS SECTION 16

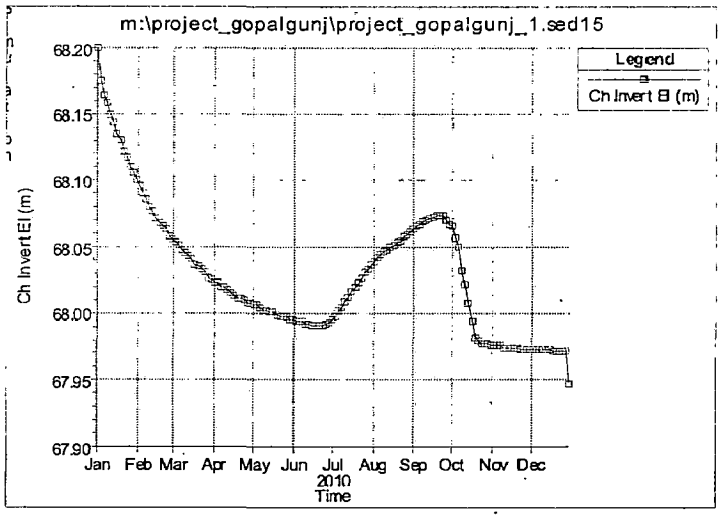

CROSS SECTION 15

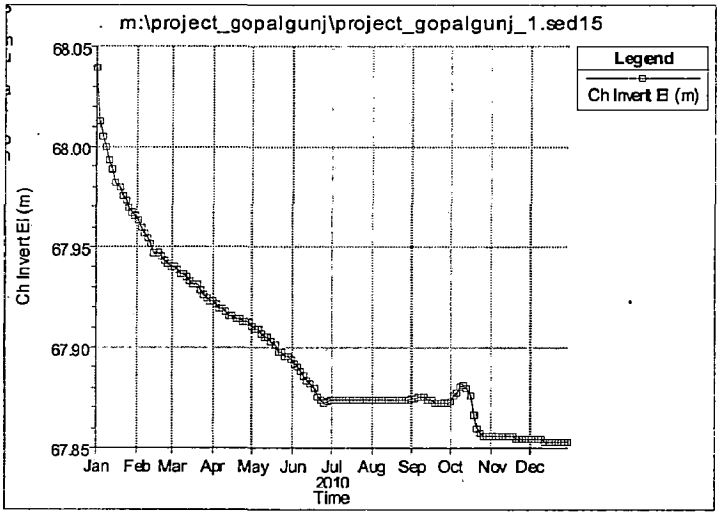

CROSS SECTION 14

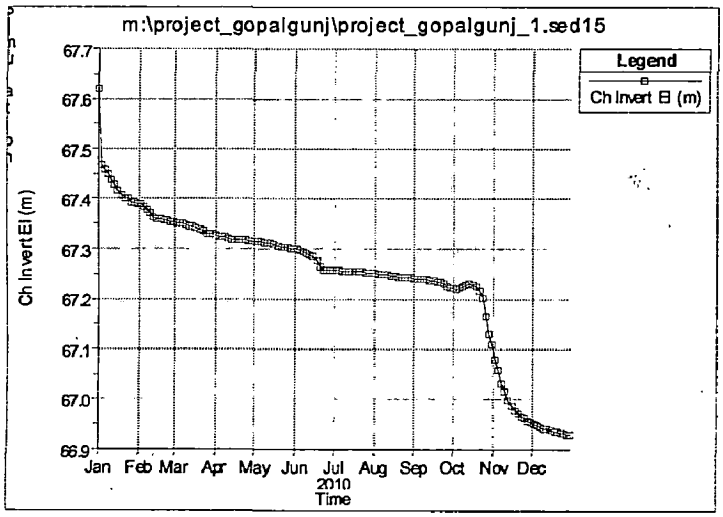

CROSS SECTION 13

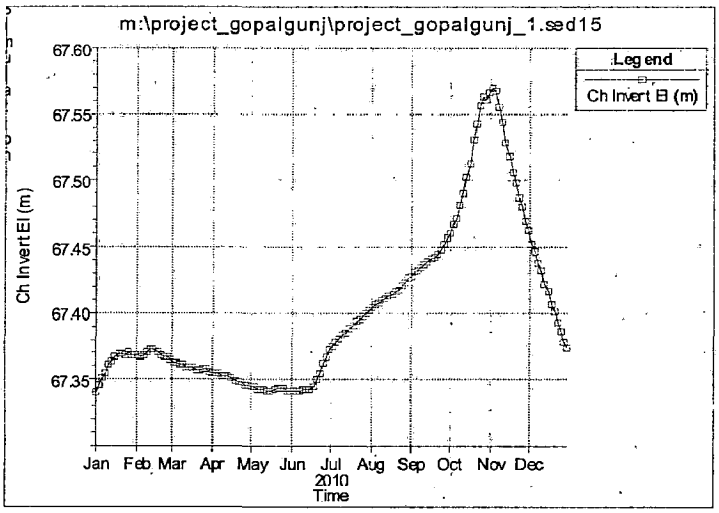

CROSS SECTION 12

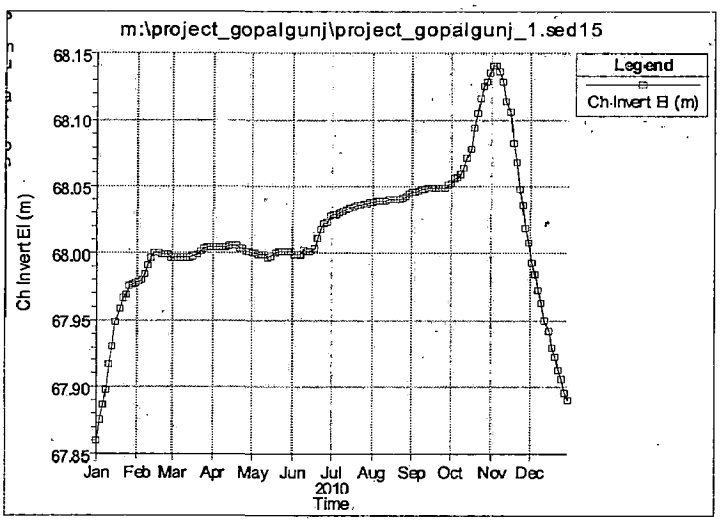

CROSS SECTION 11

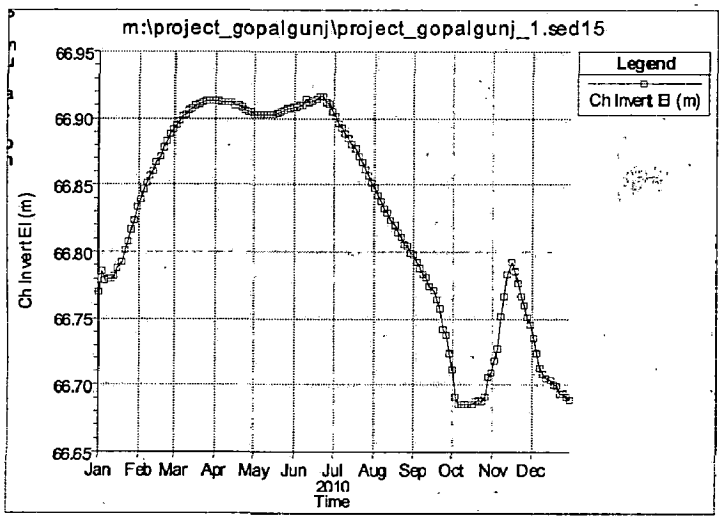

CROSS SECTION 10

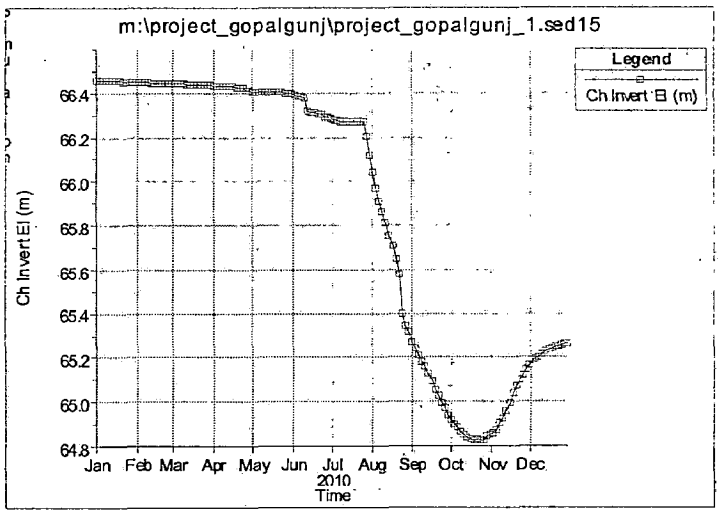

CROSS SECTION 09

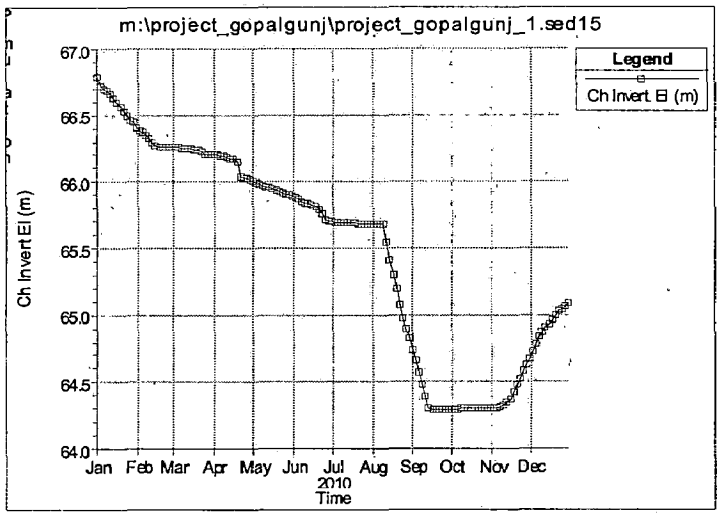

CROSS SECTION 08

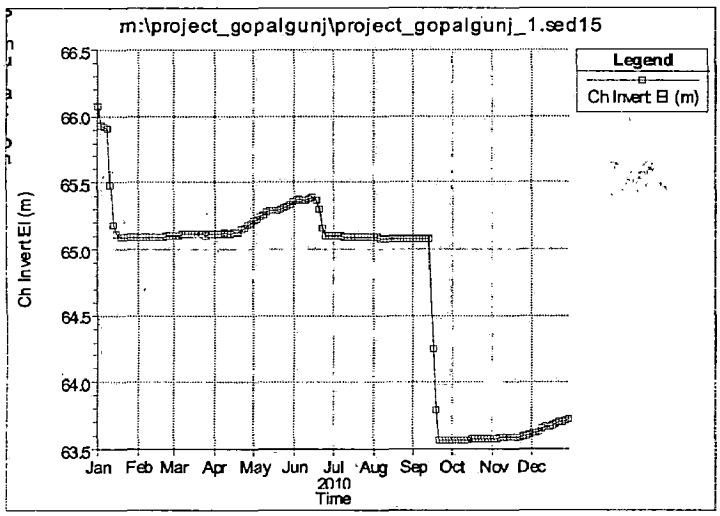

CROSS SECTION 07

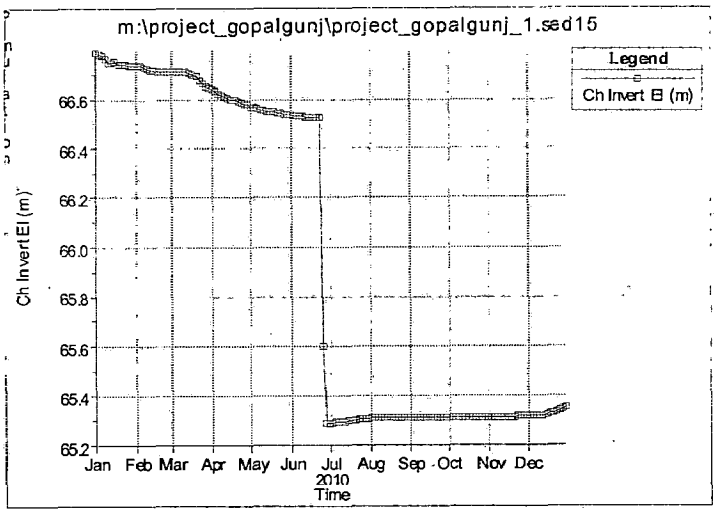

CROSS SECTION 06

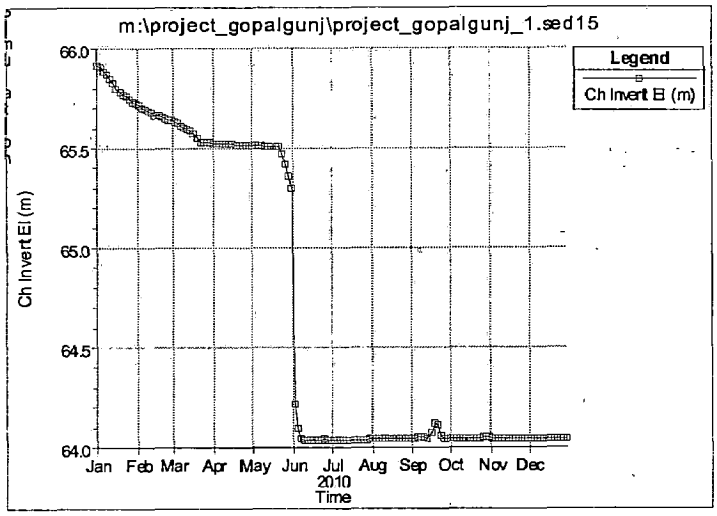

CROSS SECTION 05

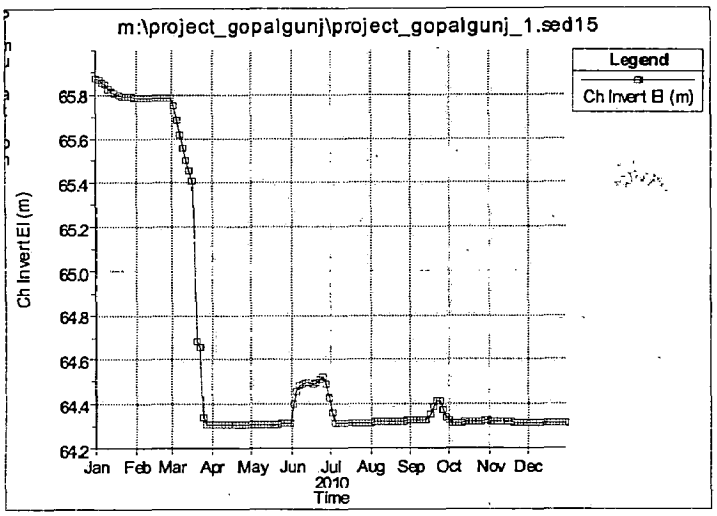

CROSS SECTION 04

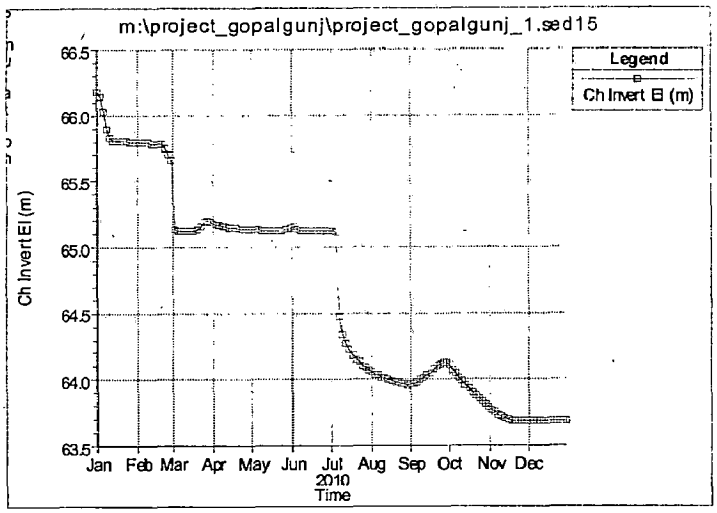

CROSS SECTION 03

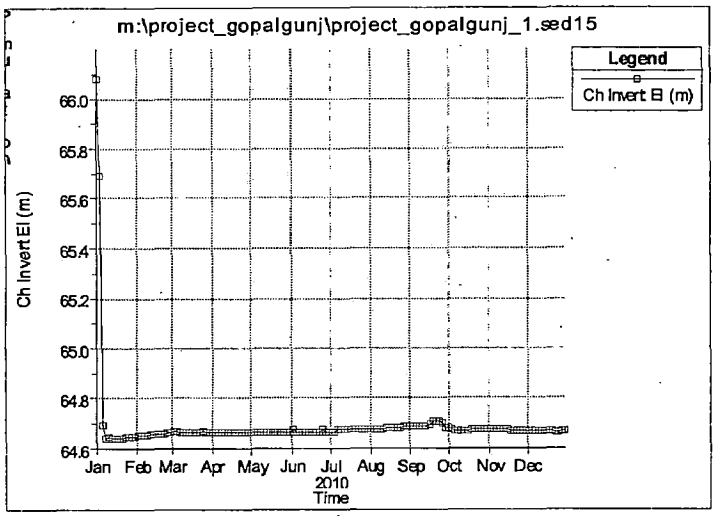

CROSS SECTION 02

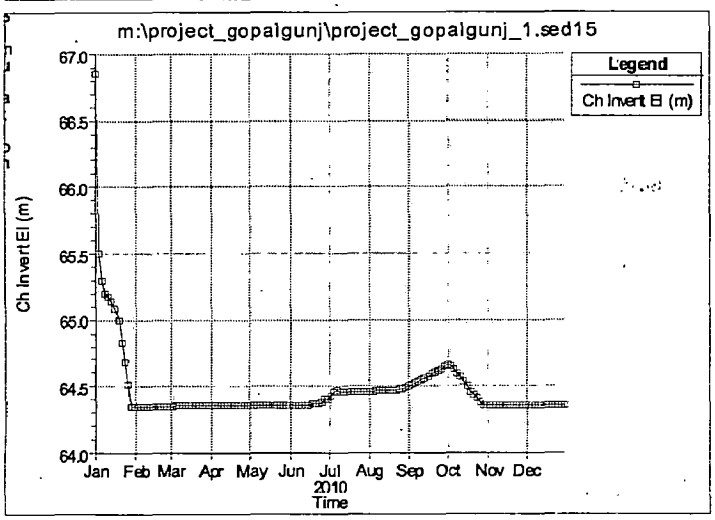

CROSS SECTION 01

CROSS-SECTION WISE TEMPORAL THALWEG CHANGES OF BASI REACH BY ENGELUND-HANSEN PREDICTOR

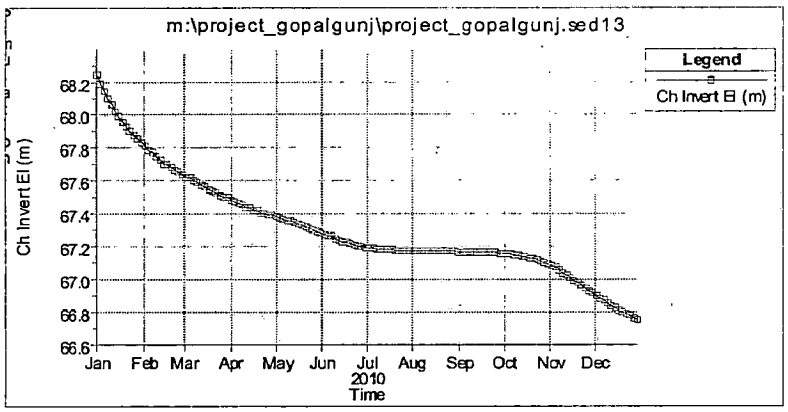

CROSS SECTION 29

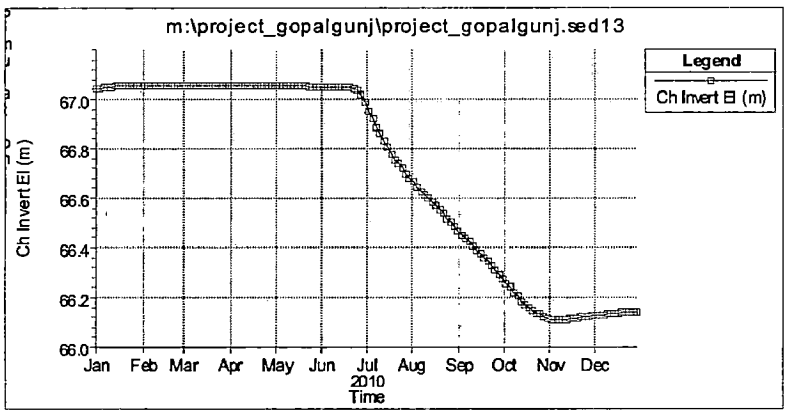

CROSS SECTION 28

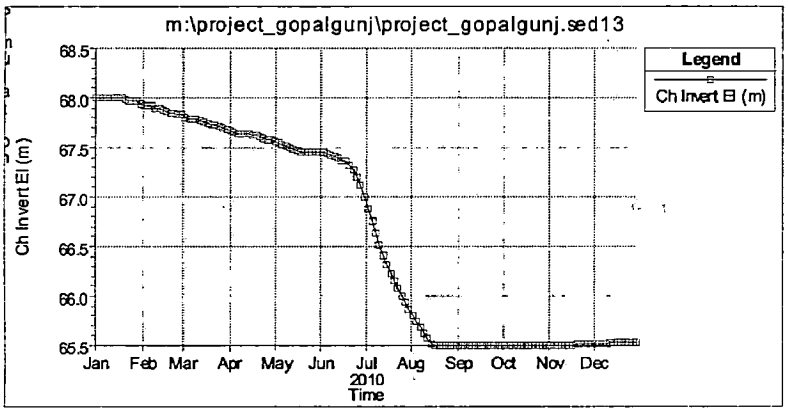

CROSS SECTION 27

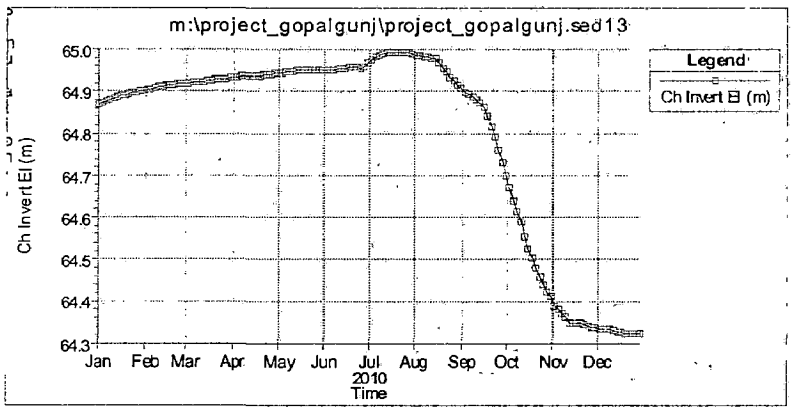

CROSS SECTION 26

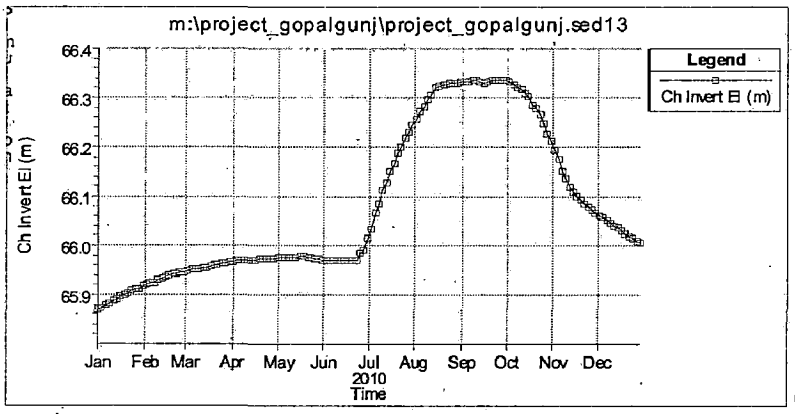

CROSS SECTION 25

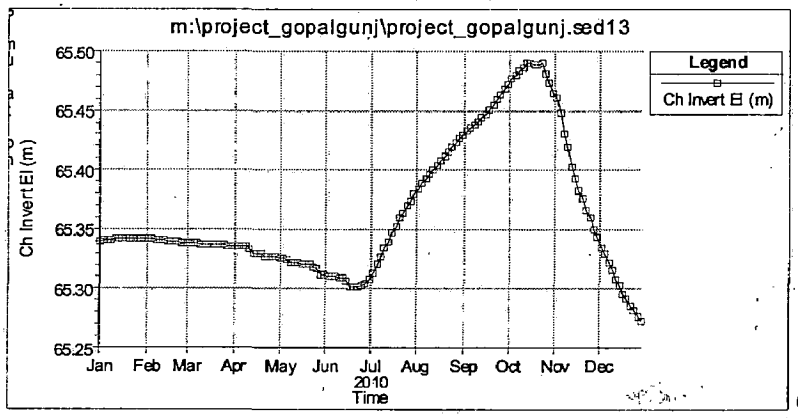

CROSS SECTION 24

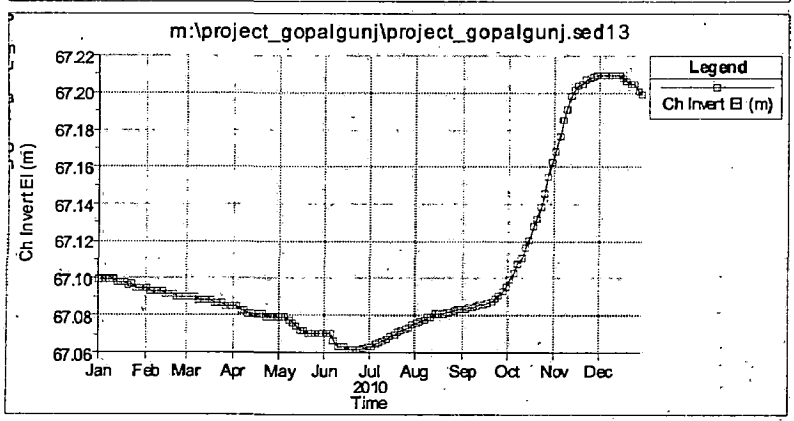

CROSS SECTION 23

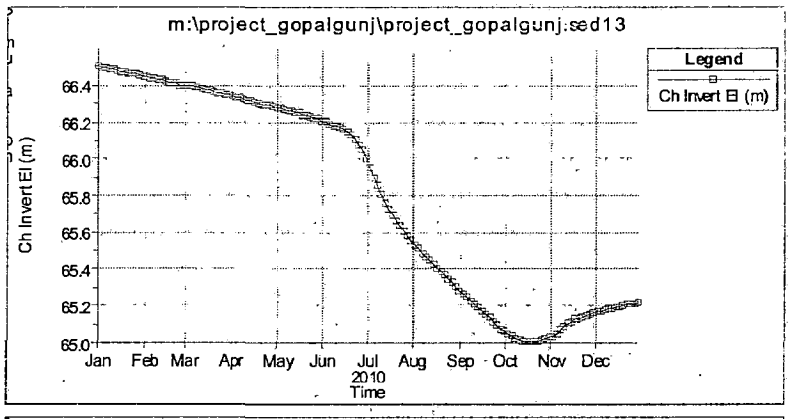

CROSS SECTION 22

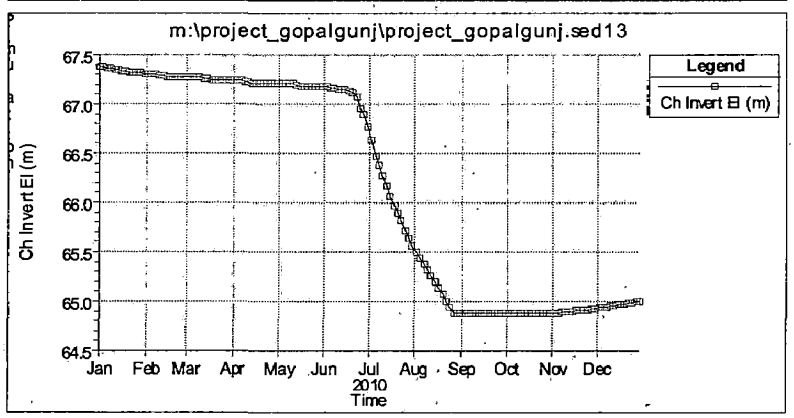

CROSS SECTION 21

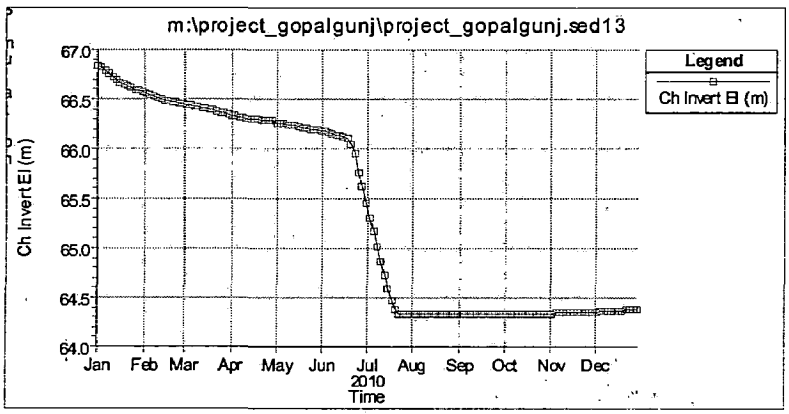

CROSS SECTION 20

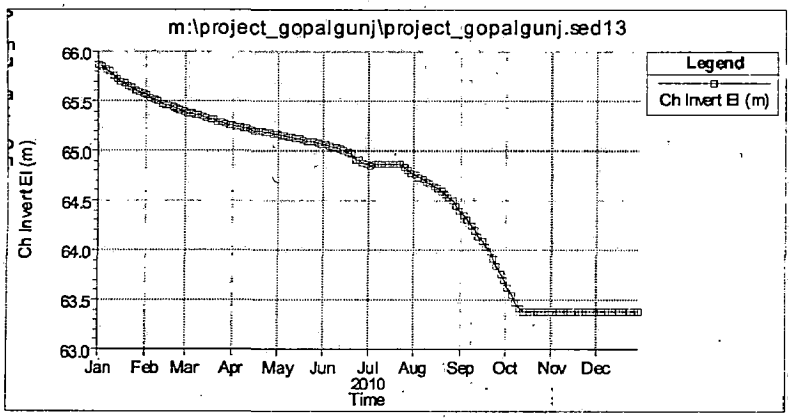

CROSS SECTION 19

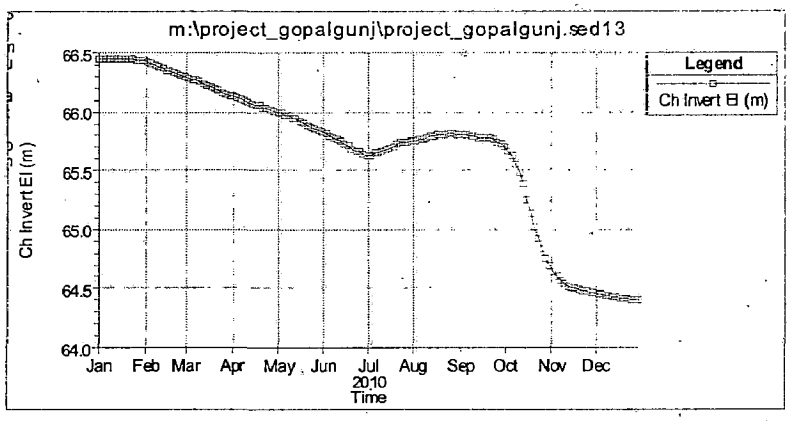

CROSS SECTION 18

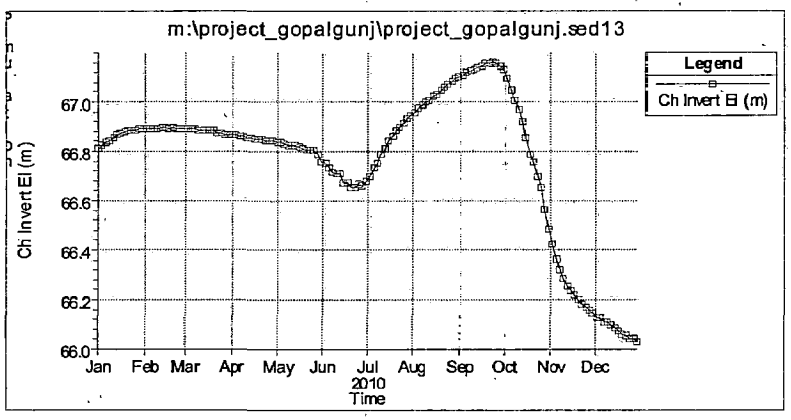

CROSS SECTION 17

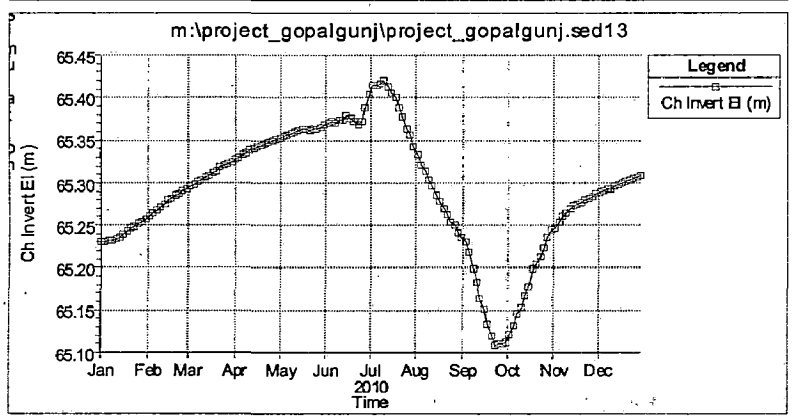

CROSS SECTION 16

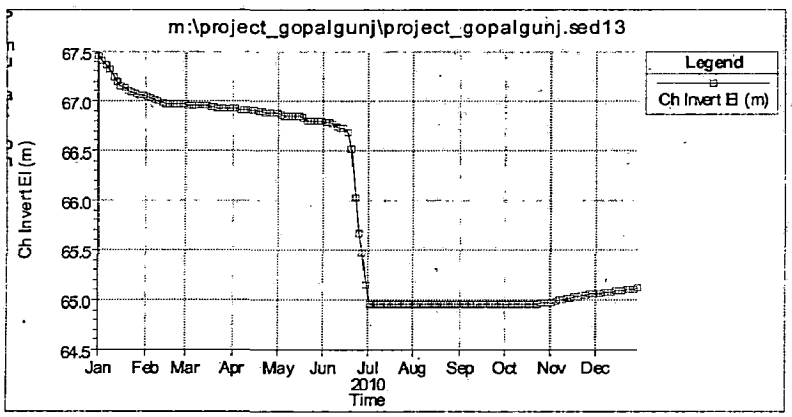

CROSS SECTION 15

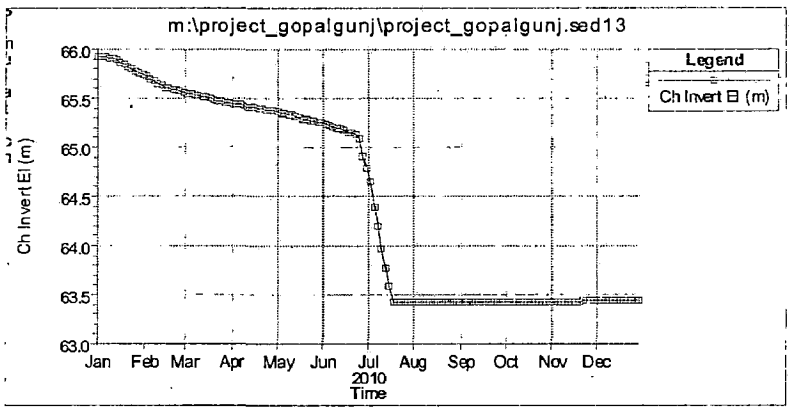

CROSS SECTION 14

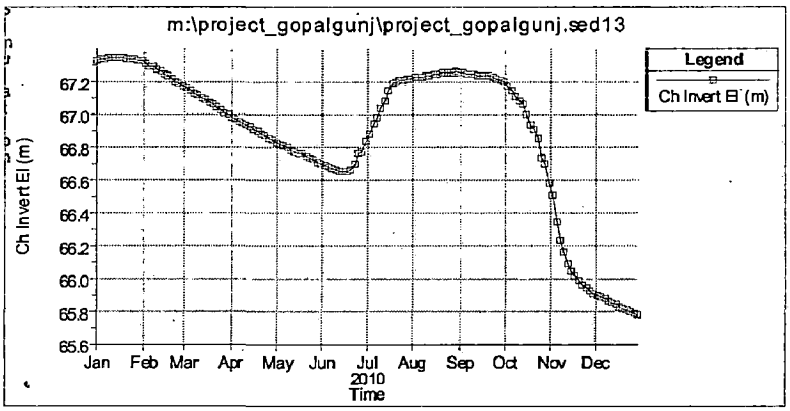

CROSS SECTION 13

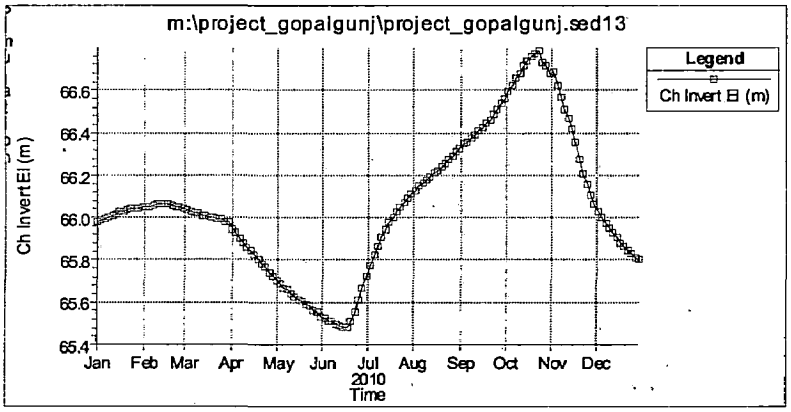

CROSS SECTION 12

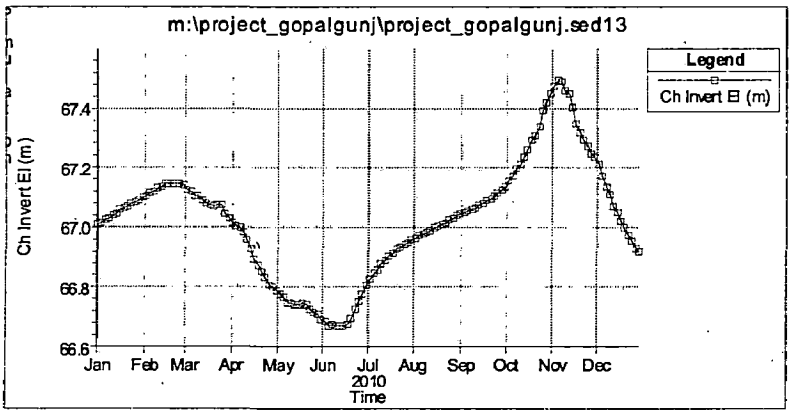

CROSS SECTION 11

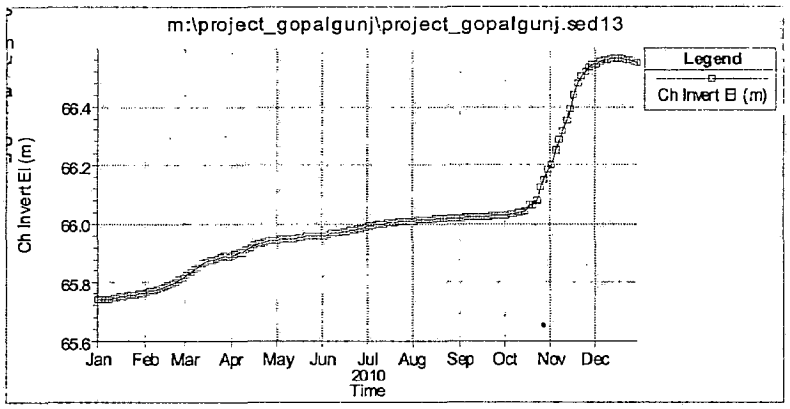

CROSS SECTION 10

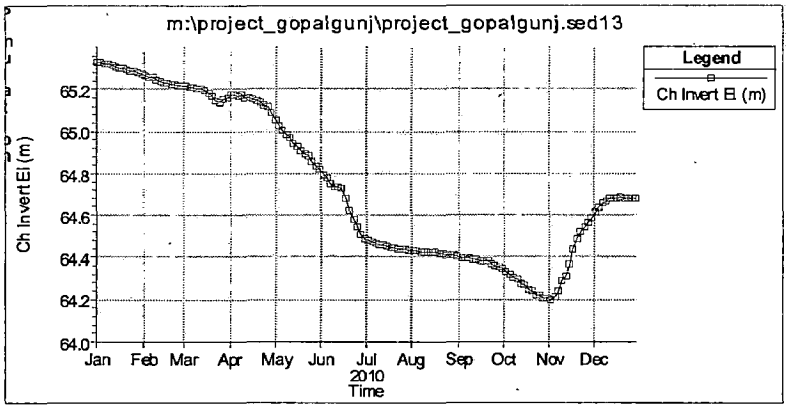

CROSS SECTION 09

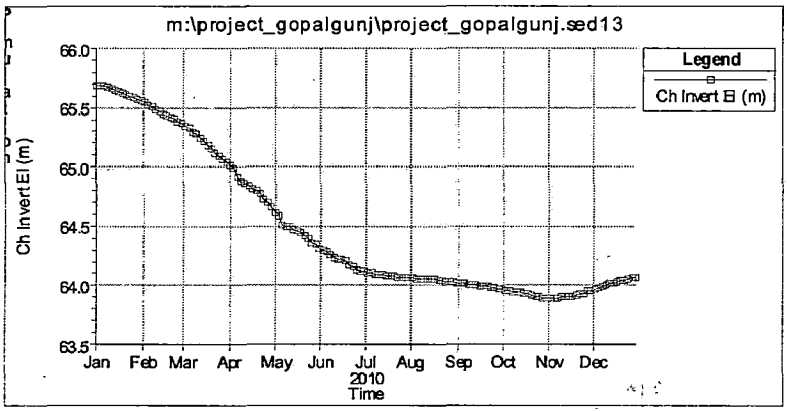

CROSS SECTION 08

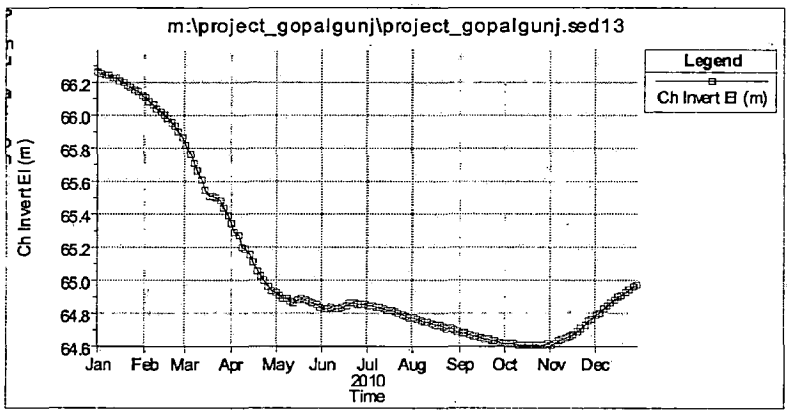

CROSS SECTION 07

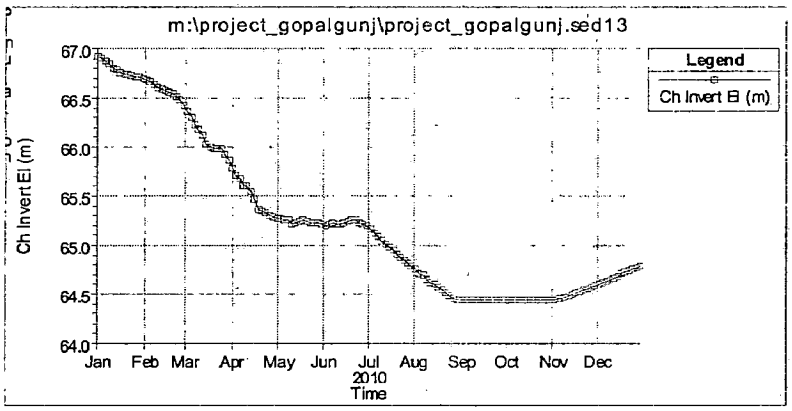

CROSS SECTION 06

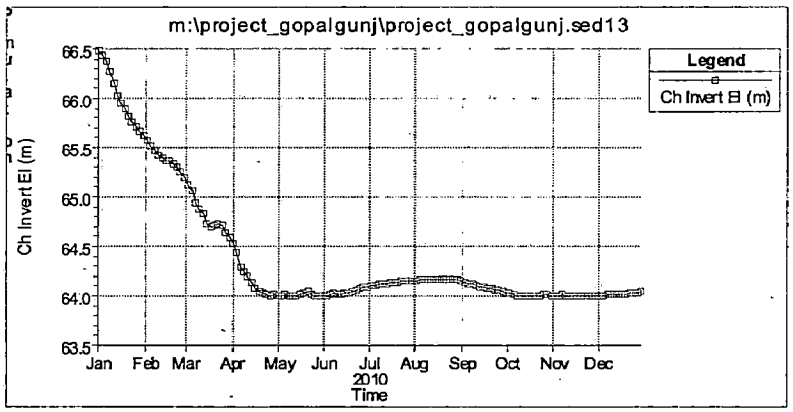

CROSS SECTION 05

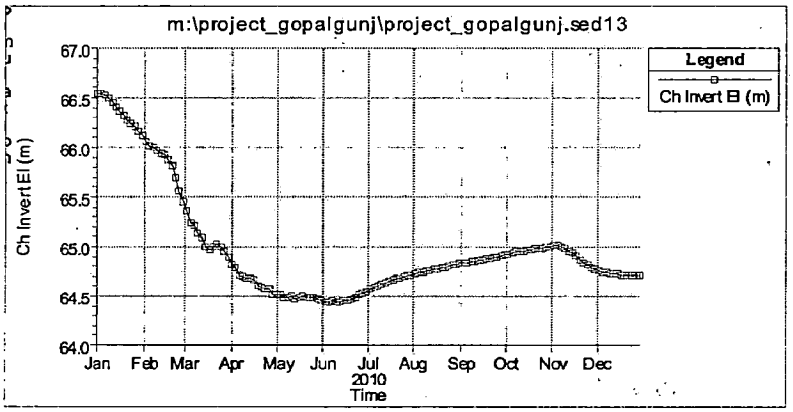

CROSS SECTION 04

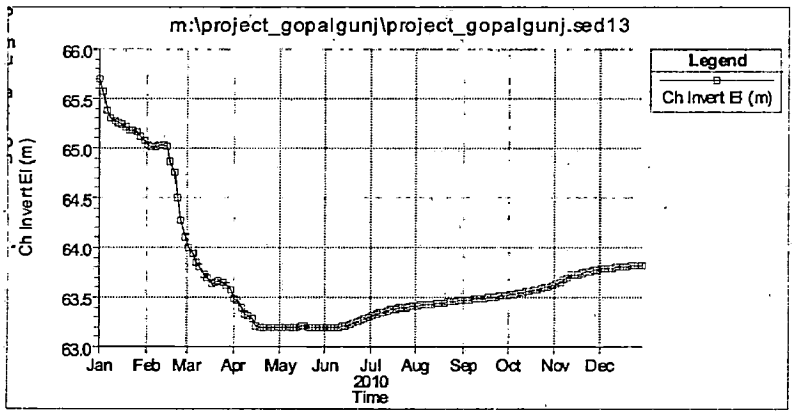

CROSS SECTION 03

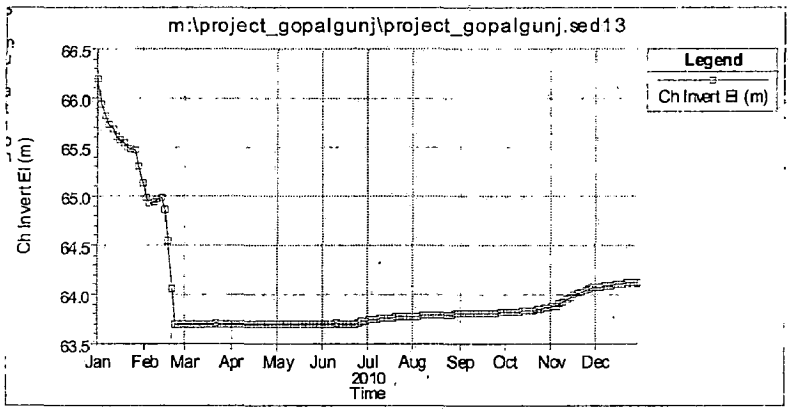

CROSS SECTION 02

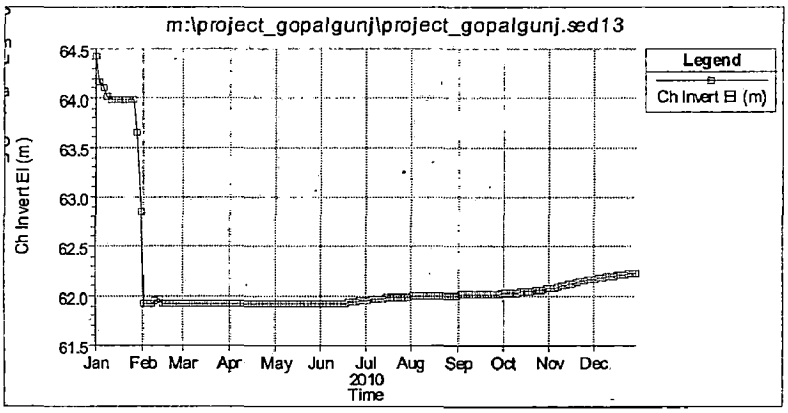

CROSS SECTION 01

CROSS-SECTION WISE TEMPORAL THALWEG CHANGES OF GANDAK REACH BY ENGELUND-HANSEN PREDICTOR

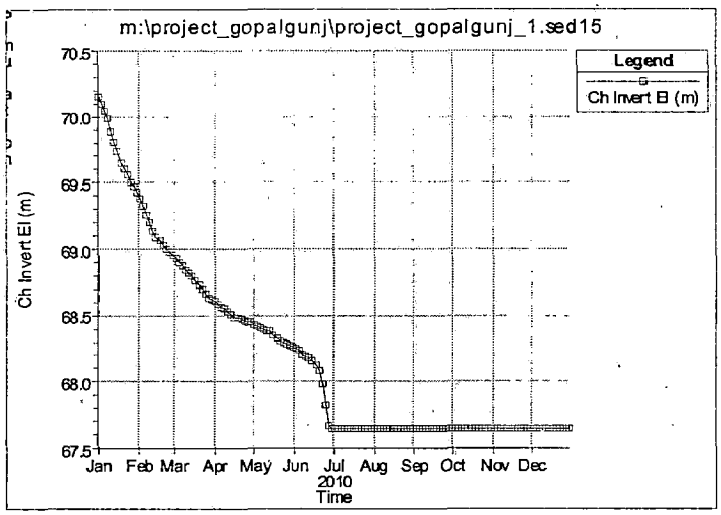

CROSS SECTION 30

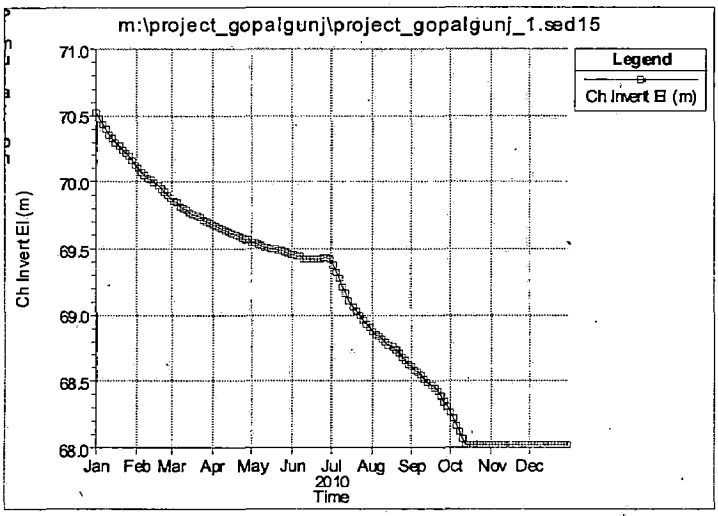

CROSS SECTION 29

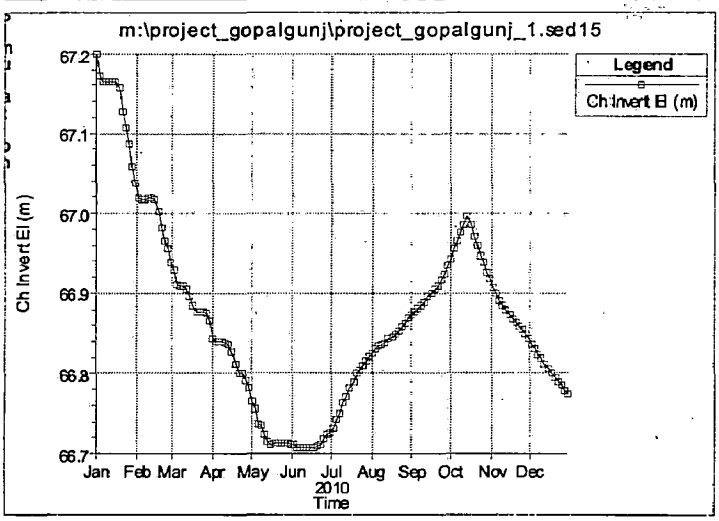

CROSS SECTION 28

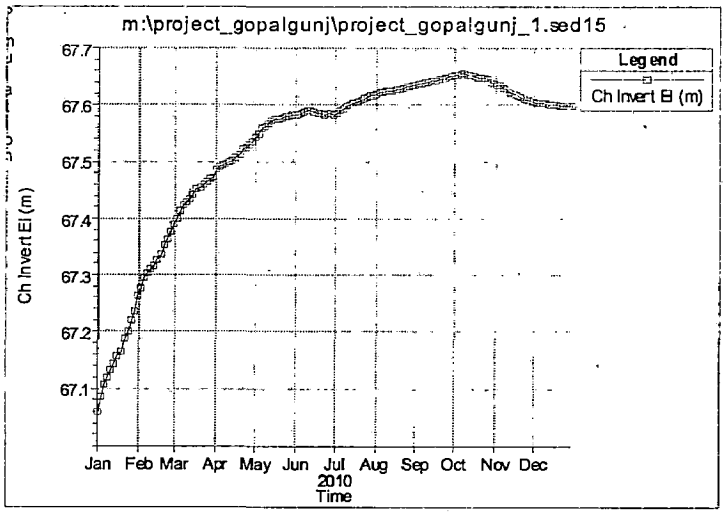

CROSS SECTION 27

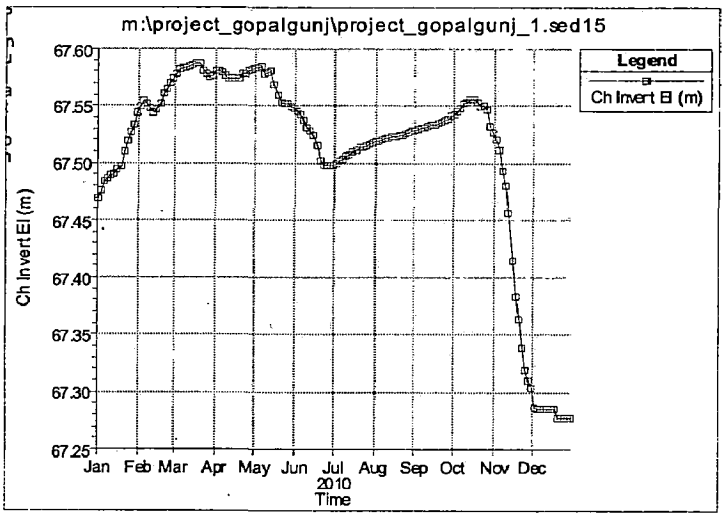

CROSS SECTION 26

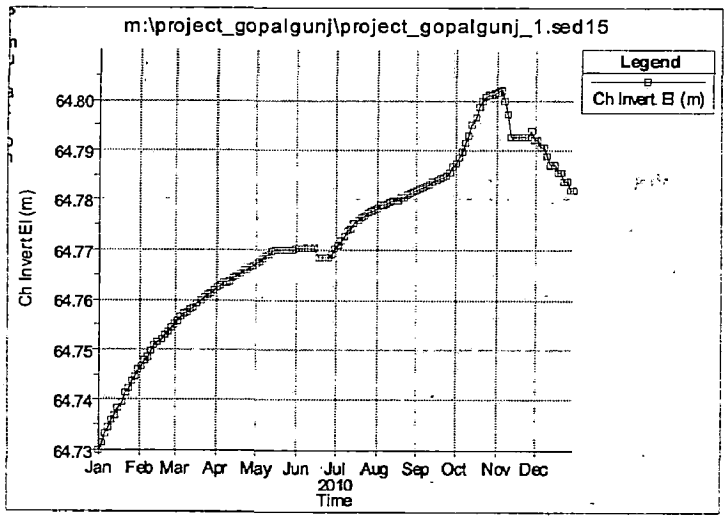

CROSS SECTION 25

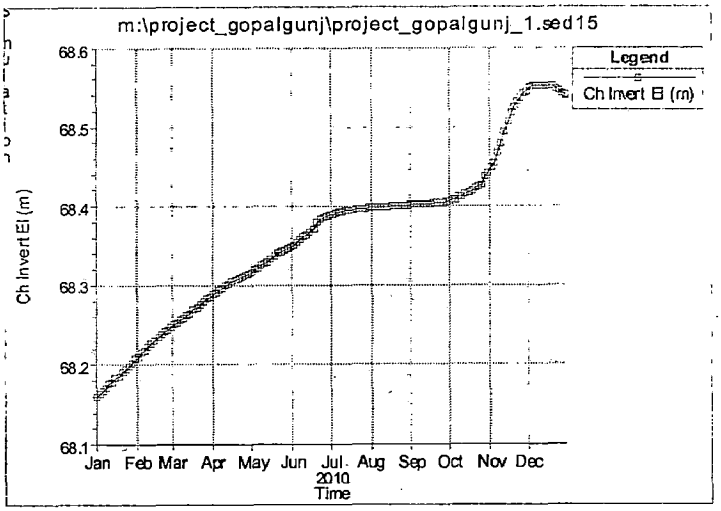

CROSS SECTION 24

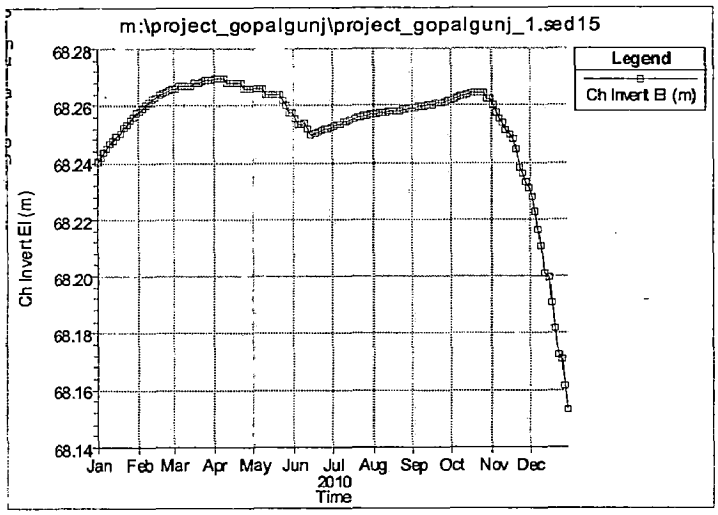

CROSS SECTION 23

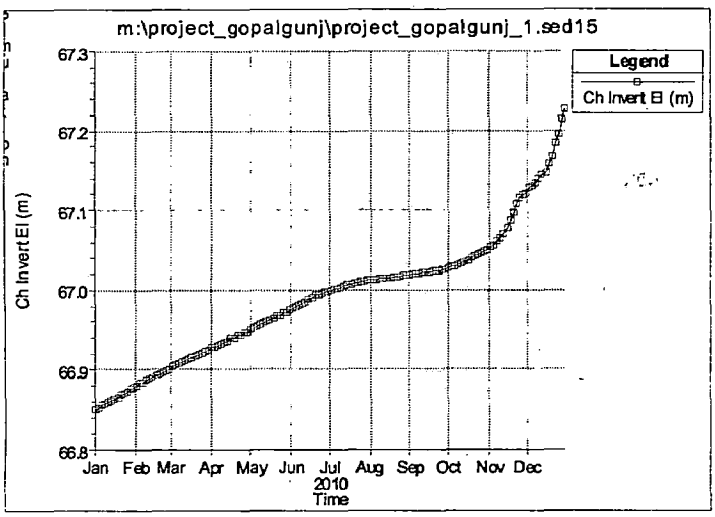

CROSS SECTION 22

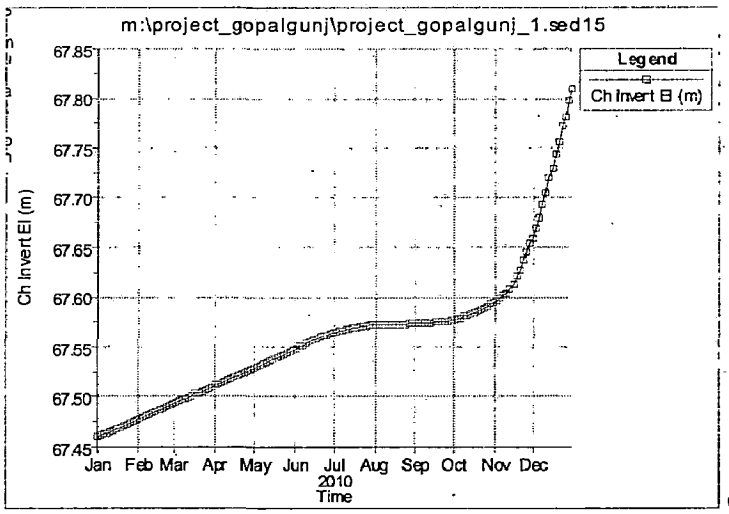

CROSS SECTION 21

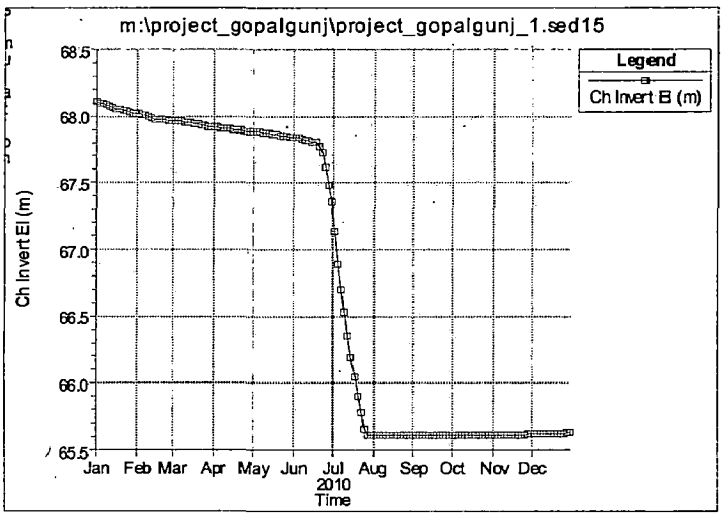

CROSS SECTION 20

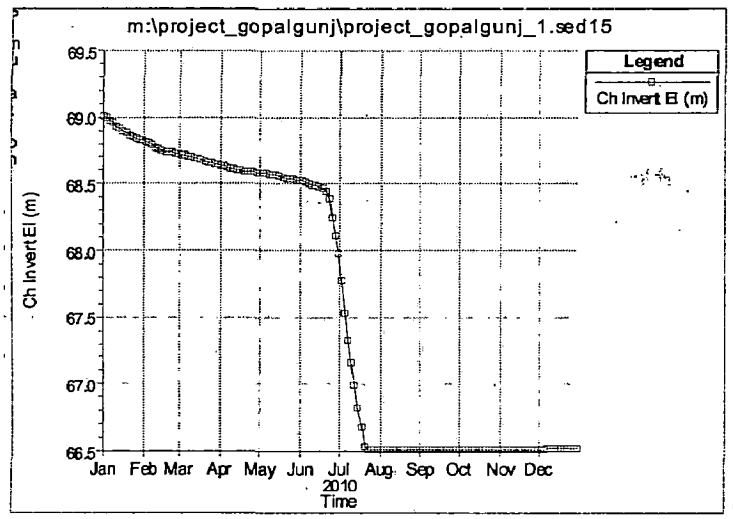

CROSS SECTION 19

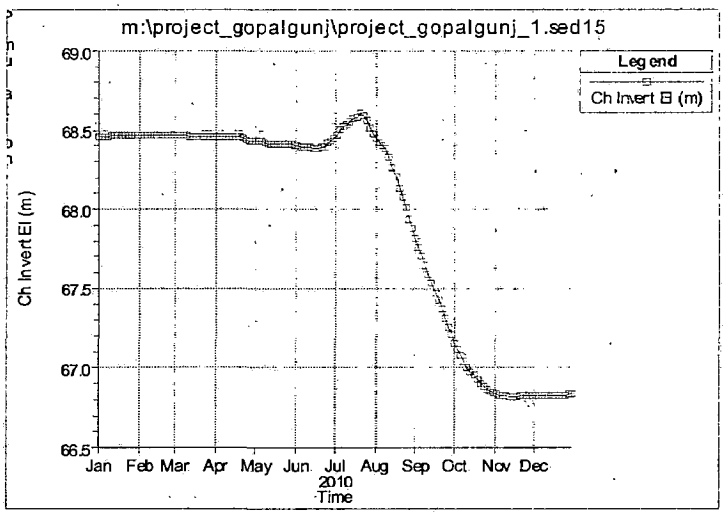

CROSS SECTION 18

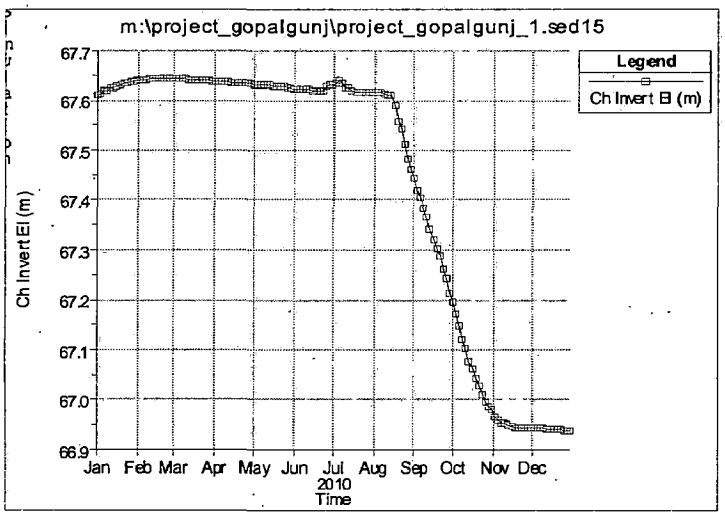

CROSS SECTION 17

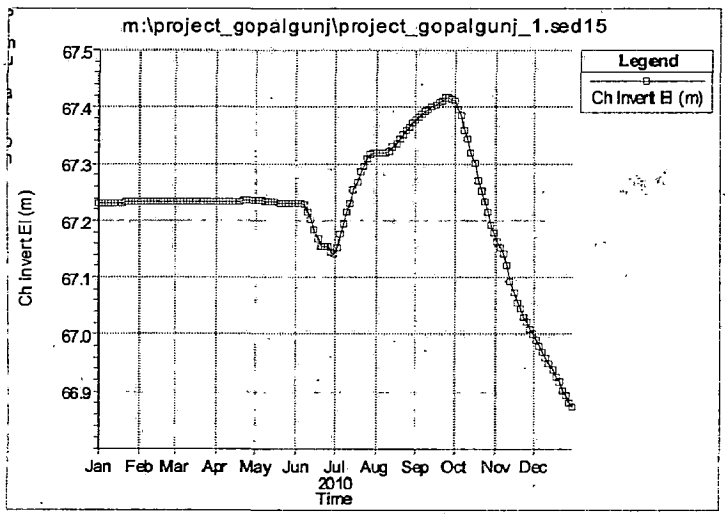

CROSS SECTION 16

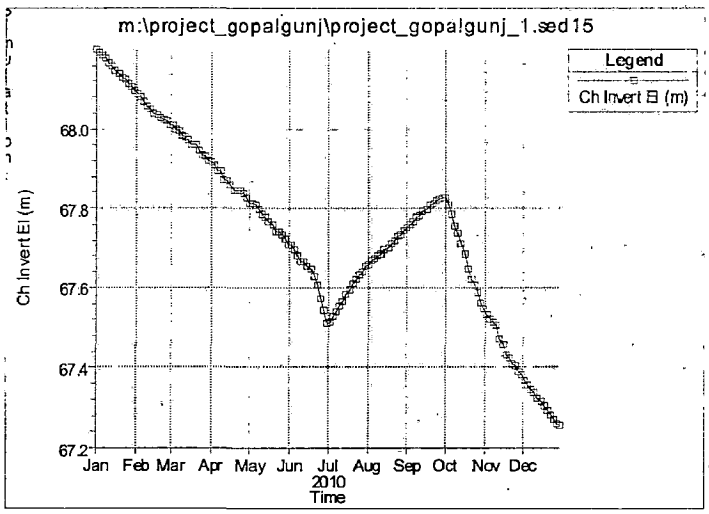

CROSS SECTION 15

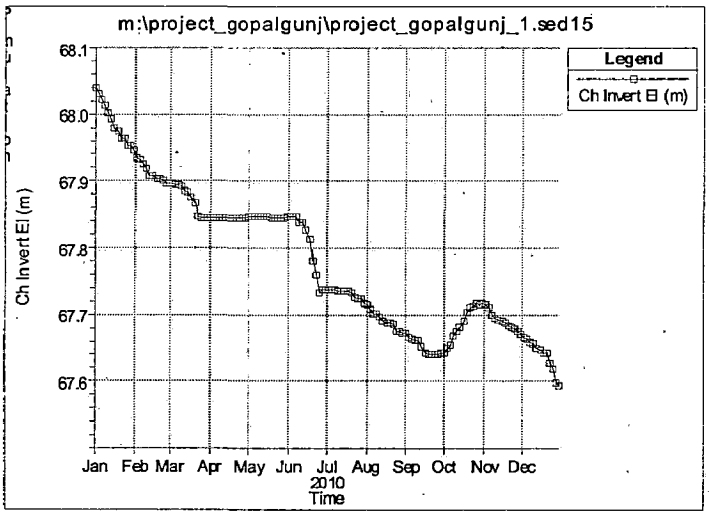

CROSS SECTION 14

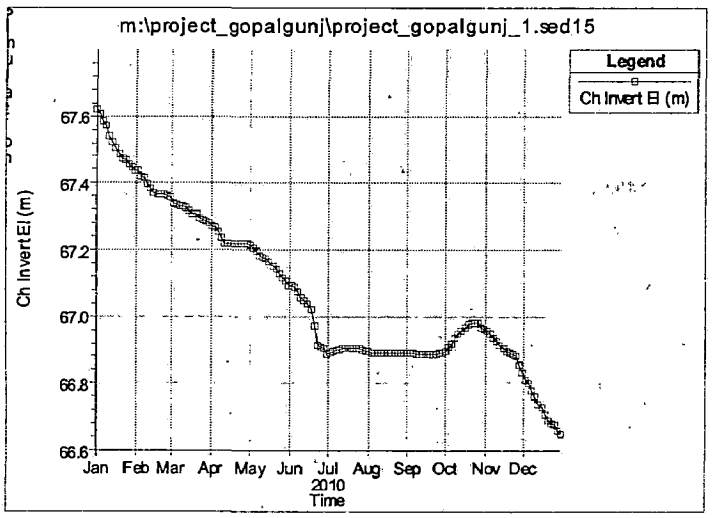

CROSS SECTION 13

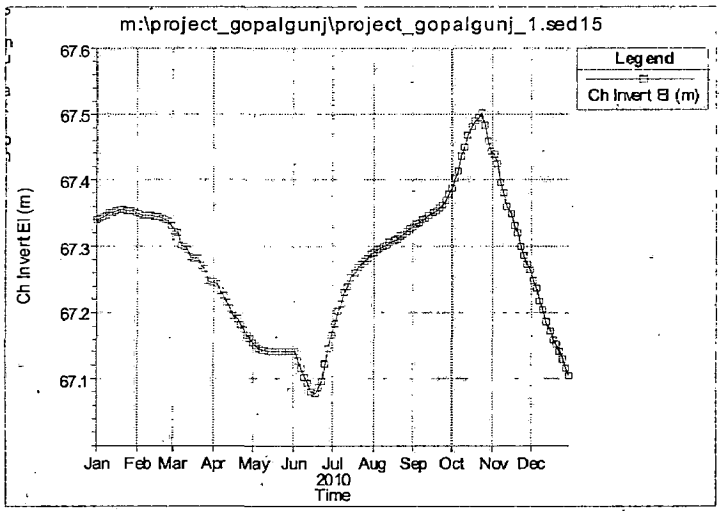

CROSS SECTION 12

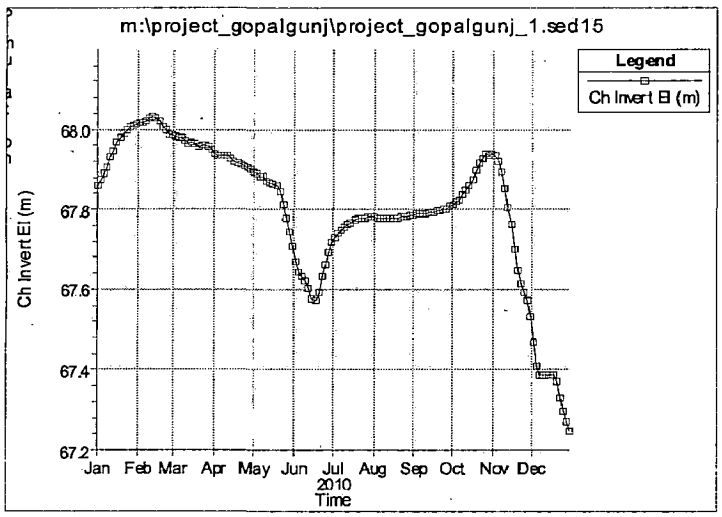

CROSS SECTION 11

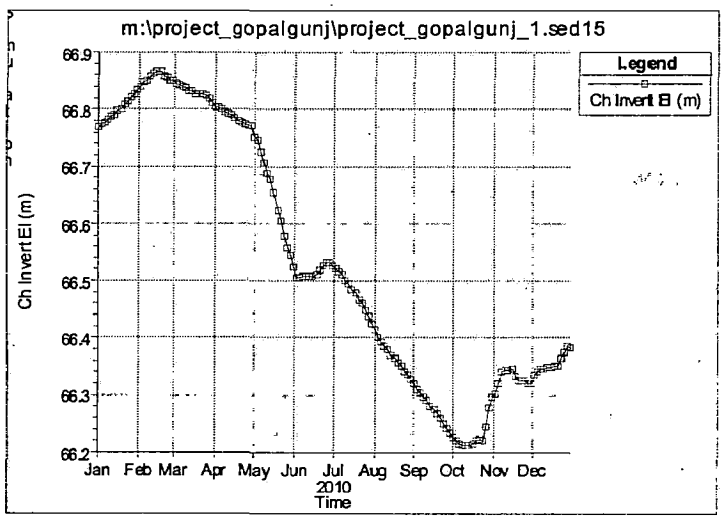

CROSS SECTION 10

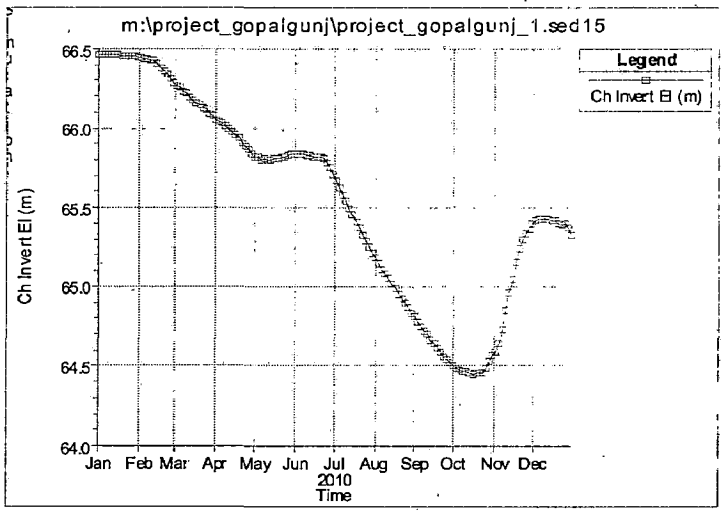

CROSS SECTION 09

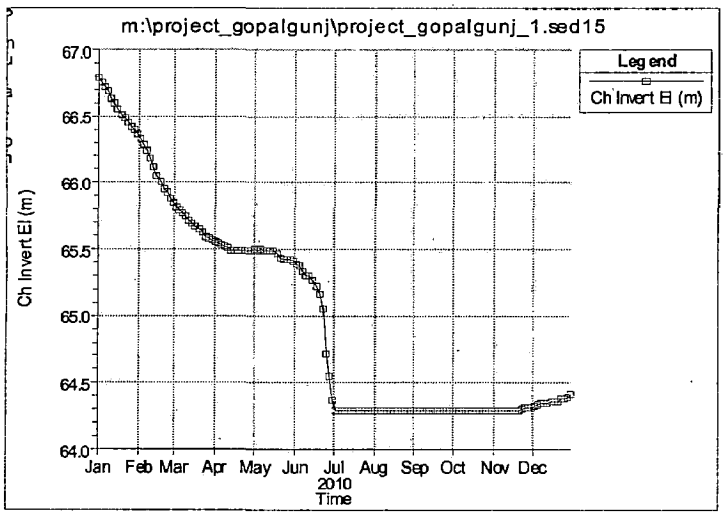

CROSS SECTION 08

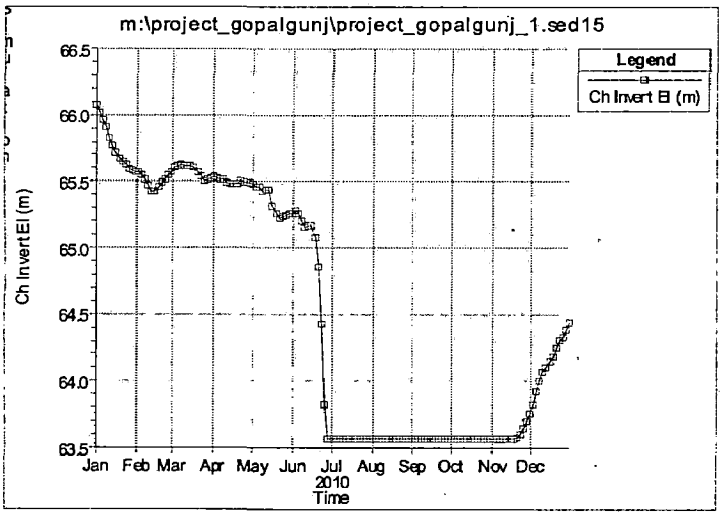

CROSS SECTION 07

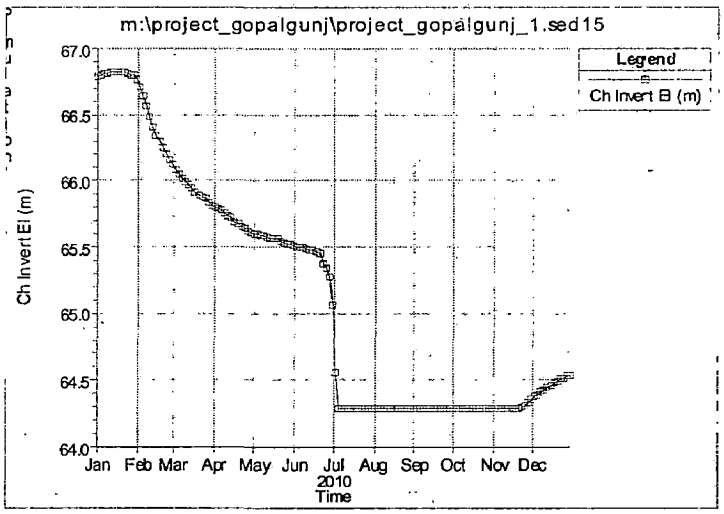

CROSS SECTION 06

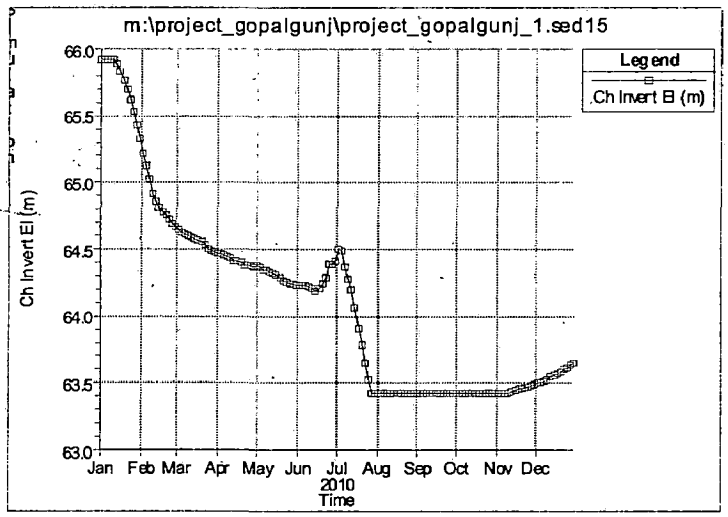

CROSS SECTION 05

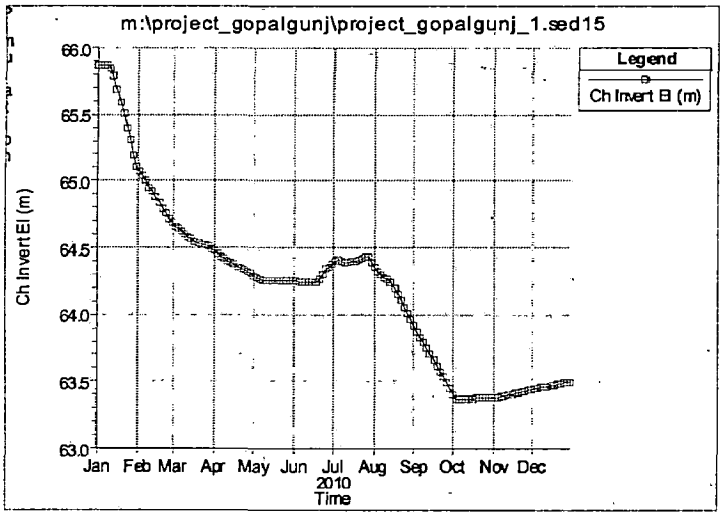

CROSS SECTION 04

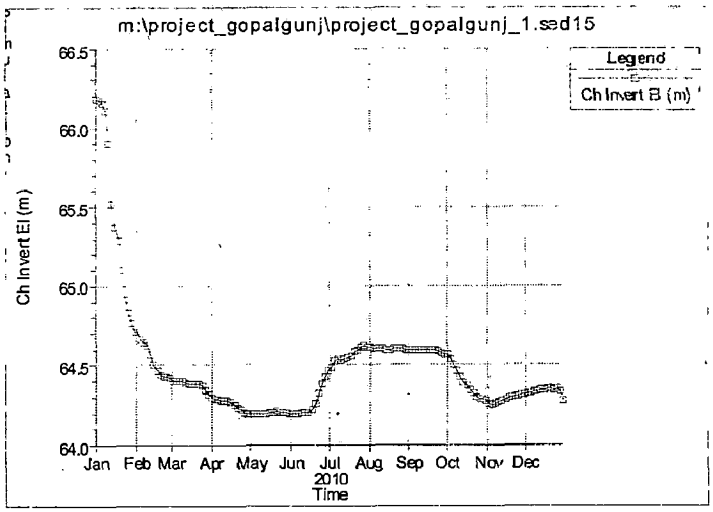

CROSS SECTION 03

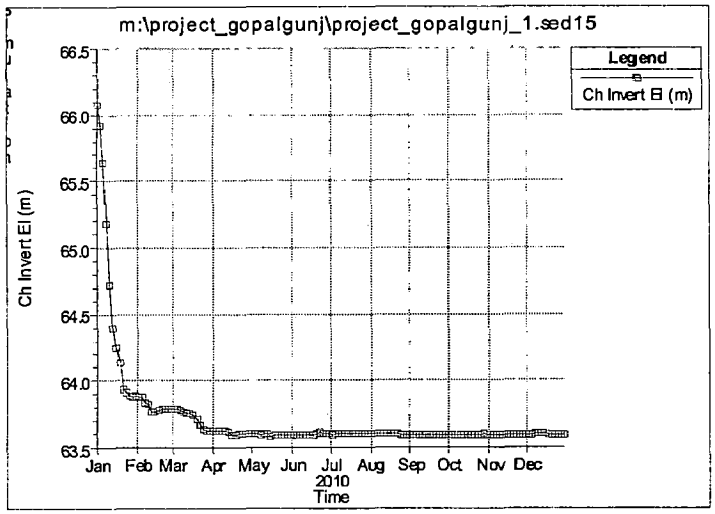

CROSS SECTION 02

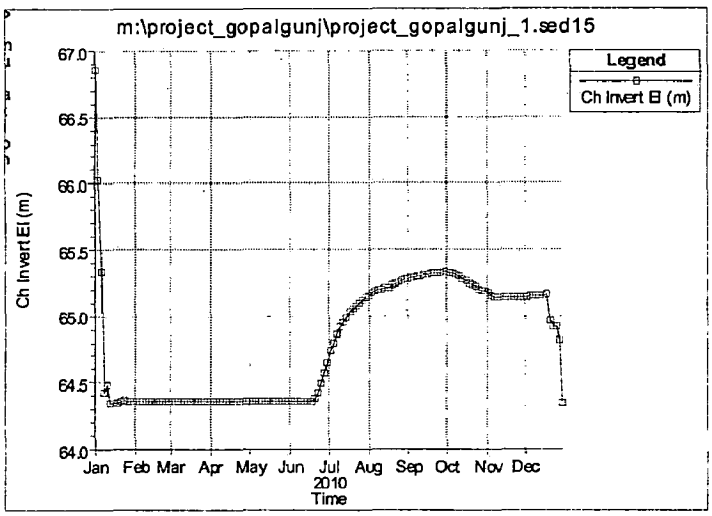

CROSS SECTION 01